

## Optical Biosensors

Sergey M. Borisov, and Otto S. Wolfbeis

*Chem. Rev.*, **2008**, 108 (2), 423-461 • DOI: 10.1021/cr068105t

Downloaded from <http://pubs.acs.org> on December 24, 2008

### More About This Article

---

Additional resources and features associated with this article are available within the HTML version:

- Supporting Information
- Links to the 6 articles that cite this article, as of the time of this article download
- Access to high resolution figures
- Links to articles and content related to this article
- Copyright permission to reproduce figures and/or text from this article

[View the Full Text HTML](#)



**ACS Publications**  
High quality. High impact.

# Optical Biosensors

Sergey M. Borisov<sup>†</sup> and Otto S. Wolfbeis\*

*Institute of Analytical Chemistry, Chemo- and Biosensors, University of Regensburg, D-93040 Regensburg, Germany*

*Received April 2, 2007*

## Contents

1. Introduction and Scope	423	5.2. Receptor-Based Biosensors for Inorganic Ions	447
2. General Remarks	424	5.3. Receptor-Based Biosensors for Gaseous Species	448
2.1. Definition of Biosensors	424	5.4. Receptor-Based Biosensors for Toxins	448
2.2. Classification of Biosensors	424	6. Nucleic Acid Biosensors	449
2.2.1. Catalytic Biosensors	424	6.1. Single DNA Sensors on Solid Supports and on Fiber-Optics	449
2.2.2. Affinity Biosensors	424	6.2. DNA Arrays	450
2.3. General Aspects of Signal Generation, Immobilization of Biomolecules, and Sample Handling	425	6.3. Molecular Beacons in DNA Sensors	451
2.4. Frequently Used Spectroscopies and Internal Referencing	425	6.4. Liposome-Based DNA Assays	451
3. Enzymatic Biosensors	426	6.5. Aptamer-Based DNA Sensing	452
3.1. General Considerations	426	7. Whole-Cell Biosensors	452
3.2. Enzymatic Glucose Biosensors	427	7.1. Catalytic Whole-Cell Biosensors	452
3.3. Other Enzyme-Based Biosensors	430	7.2. External Stimuli-Based Cellular Biosensors	453
4. Immunosensors	436	7.3. Genetically Engineered Whole-Cell Biosensors	453
4.1. General Remarks	436	8. Solid Supports for Use in Optical Biosensors, and Other Methods of Immobilization	454
4.2. Immunosensor Formats	437	9. Outlook	456
4.2.1. Direct Immunosensors	437	10. List of Abbreviations and Acronyms	456
4.2.2. Competitive Immunosensors	437	11. References	457
4.2.3. Sandwich Immunosensors	437		
4.2.4. Displacement Immunosensors	439		
4.2.5. Immunosensors Based on Binding Inhibition	439		
4.2.6. Comparative Study on Immunosensor Formats	439		
4.3. Preferred Optical Readout Formats in Immunosensing	440		
4.3.1. Conventional Readout Formats	440		
4.3.2. Evanescent Wave, Capillary, and Other Readouts	440		
4.4. Immobilization of Antibodies on Sensor Surfaces and Nonspecific Protein Binding	440		
4.5. Specific Examples of Immunosensors	441		
4.5.1. Biosensors for Proteins and Antibodies	441		
4.5.2. Biosensors for Toxins	442		
4.5.3. Biosensors for Drugs	443		
4.5.4. Biosensors for Bacteria Cells	443		
4.5.5. Biosensors for Pesticides	444		
4.5.6. Multianalyte Biosensors	444		
5. Biosensors Based on Ligand–Receptor Interactions	445		
5.1. Receptor-Based Biosensors for Saccharides and Glycoproteins	445		

## 1. Introduction and Scope

Numerous kinds of biosensors do exist, but this chapter is confined to sensors and systems where the information is gathered by the measurement of photons (rather than electrons as in the case of electrodes). More specifically, it relates to sensors based on the measurement of absorbance, reflectance, or fluorescence emissions that occur in the ultraviolet (UV), visible, or near-infrared (NIR). It does not cover sensors based on infrared or Raman spectroscopy, nor those based on surface plasmon resonance. Molecular imprints—while very promising—are not covered either since they do not match the definition of a biosensor (which asks for a biological recognition element to be at work).

Fluorescence is by far the method most often applied and comes in a variety of schemes. Parameters that are being measured in such sensors include intensity, decay time, anisotropy, quenching efficiency, luminescence energy transfer, and the like. Optical layouts include plain sensor foils (stripes) and also waveguide optical systems, capillary sensors, and arrays. Chemical sensors and biosensors do not have separation capabilities unless coupled to respective additional devices that, however, make the system more complex, require larger instrumental effort (and power consumption!), and prevent sensing to be combined with imaging. Hence, specificity can only be based on selective (bio)molecular recognition. To achieve this goal, use is made of more or less specific biorecognition elements such as enzymes, antibodies, oligonucleotides, or even whole cells and tissues. The variety

\* Corresponding author. E-mail: otto.wolfbeis@chemie.uni-r.de. Tel.: (+49) (941) 943-4066. Fax: (+49) (941) 943-4064.

<sup>†</sup> New address: Institute of Analytical Chemistry and Radiochemistry, University of Technology of Graz, Stremayrgasse 16, A-8010 Graz, Austria.



Sergey M. Borisov, born in 1978, at present is a postdoctoral fellow at the Institute of Analytical Chemistry and Radiochemistry at the University of Technology in Graz, Austria. He received a Ph.D. degree in chemistry from the Herzen State Pedagogical University (St. Petersburg, Russia) in 2003 and worked as a postdoctoral fellow at the University of Regensburg before he assumed his present position in Nov. 2006. His research interest is in the chemistry of porphyrins, in the application of fluorescent probes to biosensing schemes, and in the use of (fluorescent) micro- and nanomaterials in bioanalytical methods. He has authored several articles in recent years, mainly in analytical and material science journals.



Otto S. Wolfbeis, born in 1947, is a Full Professor of Analytical and Interface Chemistry at the University of Regensburg, Germany. His research interests are in optical chemical sensing and biosensing, in the design of novel schemes in analytical fluorescence spectroscopy, in fluorescent probes, beads, and labels, in biosensors based on thin gold films and molecular imprints, and in the design of advanced materials for use in (bio)chemical sensing. He has authored numerous papers on optical (fiber) chemical sensors and fluorescent probes, has edited a book on *Fiber Optic Chemical Sensors and Biosensors*, acts as the editor of the Springer Series on *Methods and Applications of Fluorescence*, is the Editor-in-Chief of *Microchimica Acta*, is a member of the board of various journals including *Angewandte Chemie*, and acts as the chairman of the Permanent Steering Committee of the biannual conference on *Methods and Applications of Fluorescence (MAF)* since 1989. For details, see [www.wolfbeis.de](http://www.wolfbeis.de).

of approaches that have been made in the past makes it rather difficult to sort biosensors systematically.

Excellent books and reviews cover the first few decades of research on biosensors,<sup>1–27</sup> but none of those describes the state of the art as comprehensively as the one presented here, since it covers the work from the early stages to the state as of early 2007.

## 2. General Remarks

### 2.1. Definition of Biosensors

Unfortunately, the terminology on biosensors is not systematic. Medical doctors tend to refer to “biosensors” as

solid-phase-based diagnostic devices such as those for glucose, pregnancy markers, or cardiac markers. They are better referred to as test strips. Others (mainly bioorganic chemists) often refer to molecular bioprobes as biosensors. However, true biosensors are solid state, not certain molecules, give a reading after having been contacted with the sample to be analyzed, and do not require the addition of reagent(s). It is noted at this early stage of the review that the world still does not have a fully reversible glucose sensor for *in vivo* use over >1 months, which would be a great relief to the 4–5% of the population suffering from various forms of diabetes and that would enable the construction of an artificial pancreas.

Definitions of biosensors have been given but are diverse.<sup>28–30</sup> However, all include the use of a biological component such as an enzyme, an antibody, a polynucleic acid, or even whole cells or tissue slices. In other words, a pH electrode capable of sensing the pH of blood is not a biosensor by all current definitions, as is xenon gas that can be used to probe the structure and dynamics of a protein.<sup>31</sup> Certain authors confuse the terms sensor and probe; we are referring such authors to the homepage of the world’s largest manufacturer of bioprobes ([www.probes.com](http://www.probes.com)), which never would refer to its many bioprobes as “sensors”.

Over time, this has led to the undesirable situation that electronic searches for literature on biosensors result in two sets of data. The first (still larger one) is on true sensors of all kind (electrochemical, fluorescence, piezo, thermal, surface plasmon resonance (SPR), reflectometric, chemo/bio-luminescent, IR, and the like). The second set of data is on (mainly optical) molecular probes which—in a wrong fashion—are referred to as biosensors.

### 2.2. Classification of Biosensors

The biosensors described in this review can be divided into two kinds of groups, viz. biosensors of the catalytic type and biosensors of the affinity type. Their features are briefly discussed in the following.

#### 2.2.1. Catalytic Biosensors

These make use of biocomponents capable of recognizing (bio)chemical species and transforming them into a product through a chemical reaction. This type of biosensor is represented mostly by enzymatic biosensors, which make use of specific enzymes or their combinations. Many whole-cell biosensors also rely on biocatalytic reactions. More recently, catalytically active polynucleotides (DNAzymes) have been used as well. This type of biosensor also includes biosensors based on measurement of the rate of inhibition of a catalytic reaction by an inhibitor such as a heavy metal ion or a pesticide. Catalytic whole-cell sensors often are employed to sense sum parameters such as toxicity, antibiotic activity, or cell viability.

#### 2.2.2. Affinity Biosensors

These make use of the specific capabilities of an analyte to bind to a biorecognition element. This group can be further divided into immunosensors (which rely on specific interactions between an antibody and an antigen), nucleic acid biosensors (which make use of the affinity between complementary oligonucleotides), and biosensors based on interactions between an analyte (ligand) and a biological receptor.

Some whole-cell biosensors act as recognition elements responding to (trigger) substances by expressing a specific gene.

### 2.3. General Aspects of Signal Generation, Immobilization of Biomolecules, and Sample Handling

The most usual format of a biosensor is that of a biological compound immobilized on the surface of a transducer. The function of the latter is to gather the analytical information when in contact with the sample and to convert it into an electrical signal. Optical transducers respond to an analyte by undergoing a change in their optical properties, such as absorption, reflectance, emission, or a change in an interferometric pattern. Signal changes are recorded by a photodetector and, thus, transformed into an electrical signal. The development of appropriate (and stable) materials probably is more of a challenge in biosensor development than the development of appropriate spectroscopies.

In all kinds of biosensors, recognition is accomplished by a biomolecule. In the overwhelming majority of biosensors, this biomolecule is immobilized on the surface of the sensor. Immobilization serves one or more of the following purposes:

- It enables continuous sensing of analytes in flowing systems such as blood, bioreactor fluids, or water samples.
- The biomolecule is “added” to the sample in well-defined quantity.
- The biosensor becomes reusable or regenerable.

The stability of immobilized biomolecules is a serious issue. It is noted that many articles on biosensors do not consider aspects of long-term stability in a proper way.

Much more often than chemical sensors, biosensors have been combined with (micro)fluidic devices such as (micro)-flow injection analyzers or lab-on-a-chip devices. Optical biosensors are particularly useful in the case of the latter, where voltages of up to several kV are applied that may disturb (or make impossible) electrochemical detection. Valcarcel and Luque de Castro<sup>32</sup> have reviewed the state of flow-through “biosensors”, which, however, often are based on flow-injection and corresponding detectors.

### 2.4. Frequently Used Spectroscopies and Internal Referencing

There are two main types of optical biosensors: The first exploits any changes that can occur in the intrinsic optical property of the biomolecule as a result of its interaction with the target analyte. Such changes can occur in absorbance, emission, polarization, or luminescence decay time of a receptor. Such sensors are not numerous because their sensitivity is usually low, and because many effects occur in the deep UV where spectroscopy has academic merits but is difficult to implement when it comes to analyzing complex (such as environmental or clinical) samples. An additional challenge when using intrinsic biosensors consists of the separation of the shortwave signal from background fluorescence (or absorbance). Enzymes using FAD as a coenzyme are examples of more longwave absorbing receptors that undergo intrinsic spectral changes on binding a ligand (during catalytic conversion), as are some cytochromes and hemoglobin.

The second type of biosensor is making use of optical labels and probes of various kinds. This requires the

biomolecule to be covalently labeled (an extra step) but enables the analytical wavelength(s) to be shifted to almost any desired value. Moreover, luminescence decay times and anisotropy can be adjusted to desired values, and effects such as dynamic or static quenching can be exploited in a more systematic manner. Not surprisingly, luminescent labels are widely used for this purpose. In recent years, the use of luminescent nanoparticles has strongly increased.

Absorptiometry and reflectometry are still the most widely used methods, both in solution assays and in test strips. Absorptiometry is well-established (hardly any lab does not have a photometer) and has the unique merit of being self-referenced (i.e., the intensity of the signal measured is always referenced to the intensity of the incoming light beam in the case of two-path photometers as used in cuvette assays or microtiter plates). Surprisingly enough, fluorescence intensity is by far the most often used analytical parameter when it comes to biosensing. According to Parker,<sup>33</sup> luminescence intensity ( $I$ ) is proportional to the concentration of an analyte present,

$$I = I_0 \epsilon c l \varphi_f k$$

where  $I_0$  is the intensity of the exciting (laser) beam,  $\epsilon$  is the molar absorption coefficient (molar absorbance) of the fluorescent probe or label,  $c$  is its concentration,  $l$  is the length of penetration,  $\varphi_f$  is its quantum yield, and  $k$  is a geometrical factor that accounts for the geometry of the optical system. This linear relationship between measured fluorescence (phosphorescence) intensity and  $I_0$  is valid only for solutions of low molar absorbance.

Fluorescence intensity at a single wavelength is not referenced and obviously depends on numerous variables (and can be compromised by drifts in the photodetection system). Ratiometric (two-wavelength) measurements have, therefore, become quite widespread.<sup>34–40</sup> This either requires addition of an inert reference fluorophore or the application of a FRET system (i.e., a donor dye and an acceptor dye). FRET systems have often been employed in immunosensors,<sup>41–44</sup> nucleic acid sensors,<sup>40,45–47</sup> and those based on ligand–receptor interactions.<sup>48–56</sup>

Another method for self-referencing consists in the measurement of luminescence decay time.<sup>52,57</sup> Since the measurement of decay times in the order of a few nanoseconds (or even picoseconds) so far has required complex and expensive instrumentation (this has changed in recent years, though), labels and indicators were employed with decay times in the order of  $\mu\text{s}$  and ms. Decay time-based sensing is widely employed in optical oxygen sensing and in enzyme sensing based on oxygen transduction.<sup>58–60</sup> Measurement of decay time also was reported for a fluorescent hydrogen peroxide transducer (a europium(III) complex) for use in a glucose biosensor.<sup>61</sup> A final self-referenced method is based on measurement of fluorescence polarization,<sup>62–64</sup> which also is independent of various variables (such as the degree of labeling, photobleaching, quenching, and solvent effects) that make other methods prone to errors. Table 1 summarizes the more important (self-referenced) methods of read-out in luminescence and their respective merits.

Measurement of intensity is most common because they are easily performed, routine instrumentation is available, and one label is required only. Ratiometric ( $2-\lambda$ ) methods are more reliable but require the availability of appropriate probes and labels. Dual-lifetime referencing (DLR) is quite powerful, too, but requires the presence of a reference dye



**Table 1. Fluorescent Schemes and Their Ability to Compensate for Interferences of Various Origin. (++): Well Compensated for; (+) Partially Compensated for; (−) Not Compensated for. These Are General Statements Only That May Be Different in Particular Situations**

interference resulting from	parameter						
	intensity	2- $\lambda^a$	ref dye	FRET	lifetime	anisotropy	DLR
optical components (e.g., filters)	−	−	−	−	++	+	+
instrumental drift (light source, detector)	−	+	+ <sup>b</sup>	+	++	++	++
optical misalignment	−	++	++	− <sup>c</sup>	++	+	++
background fluorescence of sample	−	−	−	−	+ <sup>d</sup>	−	−
light scatter by sensor material/ sample	−	+	+	+	++	−	++
intrinsic color of sample	−	−	−	−	++	++	+
dye leaching/bleaching	−	+	−	−	+	++	−
temperature	−	+ <sup>e</sup>	+	+ <sup>e</sup>	−	−	+ <sup>e</sup>
inhomogeneous dye loading	−	++	−	0	++	++	+

<sup>a</sup> Using a dual-wavelength label or probe. <sup>b</sup> Only compensated for if detected with the same set of optical components. <sup>c</sup> Not used in fiber-optic sensors. <sup>d</sup> Well-compensated only in case of time domain for probes having decay times in the  $\mu$ s or ms range. <sup>e</sup> Assuming both dyes to display the same temperature-dependence of their spectral properties.

with long decay time, so it is more complicated. DLR has not been applied to biosensing so far. The measurement of decay time (“lifetime”) is superior to measurement of intensity in many respects. In the case of affinity sensors, probes are needed whose decay time (that usually is not strongly affected by binding) changes upon biomolecular interactions. It has been demonstrated, for example, that the fluorescence lifetime of certain fluorescent labels (supposed to be inert in terms of changes of decay time) is a useful parameter to detect affinity binding between biotin and streptavidin and between biotinylated bovine serum albumin and streptavidin.<sup>65</sup> Lifetime also can be determined in FRET, preferably if a long-lived donor dye is used.

Refractometry also is self-referenced and has been used in immunosensors.<sup>66–68</sup> Less common spectroscopic techniques such as reflectometric interference spectroscopy,<sup>69</sup> optical waveguide lightmode spectroscopy,<sup>70</sup> supercritical angle fluorescence,<sup>71</sup> and light scattering<sup>72</sup> also shall only be mentioned here.

### 3. Enzymatic Biosensors

#### 3.1. General Considerations

Determination of such analytes as glucose, lactate, urea, ethanol, phenols, pesticides, and many others is of high significance in clinical medicine, food and environmental analysis, and bioprocess monitoring. The lack of indicators that give changes in color or luminescence at room temperature without addition of (aggressive) reagents and at near-neutral pH, in reasonably short time and in a fully reversible way, has made researchers look for alternatives. Enzymes catalyze reactions with a high degree of specificity, and the products of these reactions (or of reactants consumed) are detected directly if colored or luminescent, or by using optical transducers. The steady-state concentration of detectable species is, thus, related to the concentration of the analyte. Some enzymatic reactions require the presence of other specific reactants called coenzymes, e.g., nicotinamide adenine dinucleotide or flavine mononucleotide, which change their optical properties during the reaction.

A cross section of the typical enzymatic biosensor is shown in Figure 1. An indicator layer (often sensitive to oxygen or pH) is spread over a transparent inert support, usually a polyester film. An indicator dye is either directly dissolved in a polymer matrix or, alternatively, covalently immobilized or physically adsorbed on a surface of microbeads, which

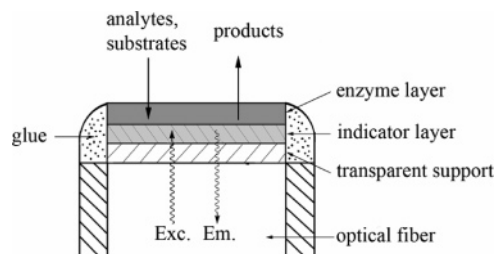


**Figure 1.** Cross section of a fiber-optic enzymatic biosensor. The analyte (substrate) enters the enzyme layer where it is converted into products. The indicator (sensing) layer consists of an indicator dye in a polymer layer and registers the formation of reaction products or the consumption of coreactants such as oxygen. The transparent support is inert and used only to facilitate manufacturing. It may as well be omitted. Exc and Em symbolize the paths of exciting and emitted light, respectively.

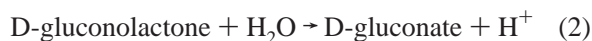
then are dispersed in the matrix polymer. The indicator layer is responsible for sensing of either cosubstrates consumed or of products produced during the enzymatic reaction. Enzyme(s) can be chemically immobilized onto the surface of a polymer membrane (e.g., cellulose, nylon, or inorganic porous glass) or physically entrapped into a polymer network, e.g., sol-gels, hydrogels, or Langmuir–Blodgett films. To avoid leaching of the enzyme, it is often cross-linked to bovine serum albumin via glutaraldehyde linkers. Alternatively, preactivated membranes may be used. When the analyte (the substrate) diffuses into the enzyme layer, it is converted into products. The indicator layer registers the formation of reaction products or the consumption of coreactants such as oxygen. In Figure 1, the sensor “sandwich” is mounted on the tip of an optical fiber that transmits excitation light from a light source to the sensor foil and emitted (reflected) light back to a photodetector. However, the majority of biosensors are not based on fiber-optics.

Optical sensors that exploit chemi- and bioluminescent reactions are usually simpler because no indicator layer is required. The chemical species generated during an enzymatic process are involved in subsequent reactions that result in the production of light. In this case, other substrates (“reagents”) are needed along with the sample solution. Most chemi- and bioluminescent reactions are catalyzed by enzymes that have to be co-immobilized in the enzyme layer. Biosensors that make use of the intrinsic optical properties of the enzyme do not require optical transducers and, thus, usually include an enzyme layer placed

on a planar support or at the tip of an optical fiber, preferably in a hydrogel.

### 3.2. Enzymatic Glucose Biosensors

Not surprisingly, this is by far the most often investigated type of biosensor. Those based on the use of glucose oxidase (GOx) function on the basis of the following reactions:



The concentration of glucose thus can be related to (a) the amount of oxygen consumed,<sup>35,58,59,73–88</sup> (b) the amount of hydrogen peroxide produced,<sup>39,61,89–102</sup> or (c) the decrease in pH due to the conversion of D-gluconolactone to D-gluconic acid.<sup>103–105</sup>

The above equations indicate that the response of such a sensor depends on a number of variables (notwithstanding the effects of temperature and diffusion). The first is pH. If pH transduction is used, the initial pH and the buffer capacity of the sample will govern the shape and the relative signal change. pH also affects enzyme activity. The second is oxygen. Depending on how its concentration is related to that of glucose, different shapes of the response curve and different signal changes will be observed, as can be seen in Figure 2. If the sample is anaerobic (i.e., does not contain any oxygen), no signal change will be detectable. If oxygen is present in large excess, the concentration of oxygen is low, and diffusional processes are fast, hardly any signal changes will be detectable once the steady-state equilibrium is reached. It also needs to be reminded that the shapes are quite different for standing samples, stirred samples, and flowing samples. Finally, the quantity (more precisely, the activity) of immobilized GOx will strongly affect the signal change and the response time.

This is shown in Figure 2 for flowing samples. The sensor is first equilibrated with a buffer solution saturated with air. The flow of buffer is then replaced by a flowing sample at time  $t_1$ . At time  $t_2$ , the sample is replaced by a flow of buffer again. Various curves (A–E) are obtained depending on the levels of oxygen and glucose in the sample:

(A) No oxygen and no glucose in the sample; the shape of the response is mainly determined by the rate of the diffusion of oxygen out of the sensor membrane into the sample flow. The same signal level is reached (even faster) if the sample contains no oxygen but a relatively large concentration of glucose.

(B) Response to a sample where  $[\text{O}_2] \ll [\text{glucose}]$ ; all oxygen in the sensor is quickly consumed as a result of enzymatic oxidation and of diffusion.

(C) Air-saturated sample where  $[\text{O}_2] > [\text{glucose}]$ ; the shape is mainly determined by the rate of the enzyme-catalyzed oxidation of glucose.

(D) Sample where  $[\text{O}_2] \gg [\text{glucose}]$ ; the steady-state signal is smaller than that in (C).

(E) Sample without glucose where the  $p\text{O}_2$  is lower than at air saturation.

These are exemplary plots; the shapes and steady-state intensities also depend on the activity of the enzyme, the flow rates, and the thicknesses of the various layers (and, thus, on the oxygen storage capacity). Note that the shapes for flowing samples are quite different from those obtained

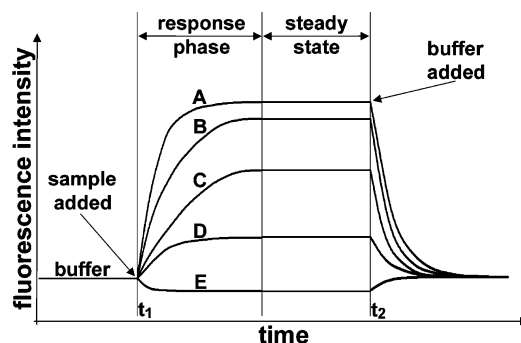


**Figure 2.** Typical signal shapes that can be obtained if a glucose sensor based on immobilized glucose oxidase and using an oxygen sensor as the transducer (in contact with air-saturated buffer) is exposed to flowing samples containing various levels of oxygen and glucose, respectively, and then again to air-saturated buffer. See the text for an explanation of shapes and signal changes.

with standing samples and that even these can differ depending on whether they are stirred or not.

Detection of glucose via the quantity of hydrogen peroxide formed appears to be the most attractive approach since it works at virtually zero background, even though it also is affected by the initial  $p\text{O}_2$  in the sample. Optical continuous sensors for  $\text{H}_2\text{O}_2$  are scarce, however.

The group of Luebbbers<sup>106</sup> probably were the first to describe a glucose sensor based on transduction via oxygen, which acts as a dynamic quencher of the luminescence of certain indicator dyes. The sensors consisted of an oxygen sensor (using pyrenebutyric acid as the oxygen probe) onto which GOx was deposited as a thin layer. The sensor reported glucose in physiological concentrations. The temperature dependence of the biosensor was studied in some detail. Temperature is known to exert an effect on various parameters including the rate of diffusion, the activity of the enzyme, the efficiency of quenching of the indicator by oxygen, and the quantum yield of the fluorophore used. In essence, a reduced analytical range and a steeper slope of the response curve toward glucose is observed.

Diphenylanthracene (DPA) was used as a probe for oxygen in a sol–gel based glucose biosensor. The sensing material was obtained<sup>107</sup> by controlled hydrolytic polycondensation of tetraethoxysilane (TEOS) to give a fairly inert inorganic glassy matrix whose porosity and size of pore network can be varied by polymerization conditions. Both DPA and GOx were entrapped into the sol–gel. Because the material has no absorption in the near UV and visible, it is well-suited for fabrication of optical sensor membranes. Enzymes in sol–gels can be substantially stabilized by addition of polycations.<sup>108</sup>

Other biosensors based on oxygen transduction made use of polyaromatic hydrocarbons such as pyrene, decacyclene, and their derivatives, which were dissolved in silicone.<sup>73–75,77</sup> Following their discovery as probes for oxygen in 1986,<sup>109</sup> ruthenium(II) complexes with ligands such as bipyridyl (Ru-bipy), 1,10-phenanthroline (Ru-phen), and 4,7-diphenyl-1,10-phenanthroline (Ru-dpp) rapidly replaced the polycyclic aromatic hydrocarbons. They possess visible absorption, relatively long decay times (0.6–6  $\mu\text{s}$ ), and good photostability and, therefore, are widely used oxygen probes.<sup>35,76,78,80–88</sup>

The probe Ru-dpp is a preferred indicator because of its good brightness (Bs; defined as the product of quantum yield and the molar absorption coefficient at the excitation wavelength), which is  $10\,500\ \text{M}^{-1}\ \text{cm}^{-1}$  at 465 nm excitation.<sup>110</sup> In being cationic, ruthenium probes can be adsorbed

onto silica gel beads (which are negatively charged at pH 7) and then be dispersed in silicone, which results in an good sensitivity to oxygen. In addition, this material is highly scattering, which increases the efficiency of collection of fluorescence.

Platinum(II) and palladium(II) porphyrins represent another group of viable luminescent oxygen indicators because of their high chemical and photochemical stability, large Stokes' shifts, good brightness, and long luminescence lifetimes. They also are often used in pressure-sensitive paints. Papkovsky<sup>58</sup> used a phosphorescent platinum(II) complex with octaethylporphyrin (PtOEP) dissolved in polystyrene as the oxygen transducer for the glucose sensor. Luminescence intensity and decay times were measured. The sensor was applied to the determination of 0.05–1.2 mM of glucose with a limit of detection of 0.05 mM. Recently, glucose was dually sensed by immobilizing (a) a europium probe acting as a reporter for hydrogen peroxide; (b) the iridium–trisbipyridine complex as a reporter for oxygen; and (c) glucose oxidase in a hydrogel membrane.<sup>111</sup> This sensor measures the hydrogen peroxide formed (without any background) and can compensate for variations in oxygen partial pressure in the sample, which has a strong effect on the shape of the response function (see Figure 2).

Miniaturized glucose sensors are particularly attractive for a number of clinical applications, including measurements of glucose in extremely small volumes or monitoring of localized events where high spatial resolution is desired. Microsensors also are attractive because they produce less injury to patients. Rosenzweig and Kopelman<sup>82,83</sup> designed a fiber-optic glucose microsensor in which a ruthenium oxygen probe and GOx were incorporated into an acrylamide polymer covalently attached to the surface of an optical fiber (of an outer diameter between 2 and 100  $\mu\text{m}$ ). The analytical range of the sensor was rather high (0.7–10 mM), but the detectable quantity of glucose was very small because of the small sample volumes needed. The group of Klimant reported on a fiber-optic flow-through biosensor for online monitoring of glucose.<sup>112</sup> A microdialysis membrane in a Tygon tubing contained a fiber-optic sensor composed of immobilized glucose oxidase and an oxygen transducer layer, and a reference oxygen sensor was used to compensate for interfering effects. The authors have also demonstrated outstanding selectivity of the sensor, which makes use of an oxygen optode as a transducer.<sup>113</sup> No interference was observed from ascorbic acid, acetylsalicylate, uric acid, mannitol, and dopamine in concentrations exceeding physiological levels by several folds. Measurement of glucose in humans via a sensing catheter was demonstrated.

Xu et al.<sup>35</sup> prepared luminescent probes that were encapsulated into nanoparticles to give so-called PEBBLE sensors designed for intracellular glucose imaging. The polyacrylamide nanoparticles of 45 nm diameter incorporate GOx, the oxygen indicator (a sulfonated Ru-dpp derivative), and an oxygen-insensitive fluorescent dye, Oregon Green 488-dextrane, that is used as a reference for the purpose of ratiometric intensity measurements. The small size and inert matrix of these sensors allows them to be inserted into living cells with minimal physical and chemical perturbations of their biological functions.

Because glucose biosensors based on oxygen transducers measure the consumption of oxygen during the enzymatic reaction, the response of such sensors to glucose is actually dependent on concentration of oxygen in the analyzed

medium. This is shown in Figure 2 for the two extremes of ratios of concentrations of glucose and oxygen. To overcome problems associated with variable oxygen supply, oxygen should be present in large excess (compared to the amount consumed) or its concentration should be kept constant (which is not always easy to achieve) or known.

Dual biosensors have, therefore, been developed and represent one possible solution to the above problem.<sup>80,85</sup> Such sensors do contain both an oxygen-sensitive and a glucose-sensitive element located in the proximity, e.g., on a distal end of an imaging fiber.<sup>80</sup> The glucose-sensitive element is prepared by covering the oxygen sensor with an enzyme layer. Wolfbeis et al.<sup>85</sup> tested three different combinations of oxygen transducer and sol–gel immobilized GOx. In the first, GOx was sandwiched between a sol–gel layer doped with Ru-dpp and a second sol–gel layer composed of pure sol–gel. Such configuration provided the highest enzyme activity and the largest dynamic range (0.1–15 mM) but suffered from a distinct decrease in sensitivity upon prolonged use. In the second, which provided the fastest response time ( $t_{90} = 50$  s), a sol–gel layer doped with Ru-dpp was covered with sol–gel-entrapped GOx. In the third sensor type, both the oxygen-sensitive sol–gel powder and the sol–gel powder containing GOx were incorporated into a single sol–gel phase. Such a sensor type provided the best operational lifetime. The authors also have derived equations that describe how the effect of varying oxygen supply can be compensated for by making use of two sensors, one sensitive to oxygen only and the other sensitive to both oxygen and glucose.

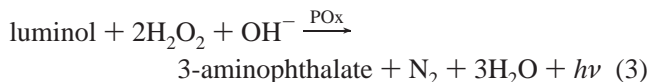
Since both the decay time of the luminescence of oxygen indicators (especially for ruthenium(II) complexes)<sup>114,115</sup> and the quenching by oxygen itself<sup>116</sup> are highly temperature-dependent, the performance of all biosensors based on oxygen transducers also is influenced by temperature. The temperature dependence of such sensors may be compensated for by making use of dual sensors for oxygen and temperature,<sup>116,117</sup> but so far this problem has not been addressed for glucose sensors, which, therefore, need to be thermostated. This option has not been applied to glucose sensors.

The concentration of glucose may also be related to the amount of protons produced in reaction 2; however, only few optical glucose biosensors made use of pH transducers. The fluorescence of the pH probe 8-hydroxypyrene-1,3,6-trisulfonate (having a  $\text{p}K_{\text{a}} \approx 7.3$ ) contained in a proton-permeable hydrogel served as a signal to monitor pH changes during enzymatic reaction.<sup>103</sup> The limit of detection (LOD) for glucose was 0.1 mM. Polyaniline was found to exhibit pH-sensitive spectra and, thus, was used itself as a pH transducer.<sup>105</sup> The enzymatic reaction can be monitored at 550–650 nm (where the absorbance decreases) or at 700–900 nm (where the absorbance increases). The LOD for glucose was 1 mM.

An interesting approach was made by McCurley.<sup>104</sup> A pH-insensitive fluorophore linked to cadaverine was incorporated, along with GOx, into a cross-linked acrylamide-based hydrogel placed at the end of an optical fiber. The amine moiety of cadaverine is responsible for the pH-dependent swelling of the hydrogel. When the volume of the hydrogel increases, a decrease in fluorescent intensity is observed because the total quantity of fluorophore remains constant. The sensor was operative in the range from 0 to 1.6 mM of glucose.



Finally, the amount of hydrogen peroxide produced during the enzymatic reaction can be related to the concentration of glucose. Most “sensors” rely on irreversible chromogenic reactions of hydrogen peroxide. The  $\text{H}_2\text{O}_2$  transducer can be considered a biosensor itself because it makes use of the oxidation of luminol (5-amino-2,3-dihydrophthalazine-1,4-dione) catalyzed by horseradish peroxidase (POx) as shown in eq 3:



The intensity of chemiluminescence (peaking at 430 nm) is proportional to the concentration of hydrogen peroxide and, in the case of the glucose biosensor, to the concentration of glucose. The method was pioneered by Freeman and Seitz,<sup>118</sup> who immobilized POx in a polyacrylamide gel to monitor  $\text{H}_2\text{O}_2$  in concentrations as low as 1  $\mu\text{M}$ . The chemiluminescent reaction was widely used for determination of hydrogen peroxide<sup>93,119–121</sup> and glucose.<sup>39,90,91,93</sup> The sensors typically operate in the flow injection mode where GOx and POx are immobilized in a polymer membrane immersed into a solution containing luminol and sample. The problem to overcome is a mismatch between the optimal pH needed for enzymatic oxidation of glucose (neutral pH) and for enzymatic oxidation of luminol (pH  $\approx$  9). While an intermediate pH may be used, other possible solutions include the use of cetyltrimethylammonium bromide micelles to incorporate luminol and  $\text{HPOx}$ <sup>90</sup> or the use of an internal solution of POx and luminol, located close to a membrane containing immobilized GOx.<sup>93</sup> Similar to the oxidation of luminol, POx also catalyzes the reaction of  $\text{H}_2\text{O}_2$  with other substrates such as homovanillic acid<sup>122</sup> and Amplex Red.<sup>123</sup> The products of oxidation are highly fluorescent species whose intensity can be monitored. Unlike in chemiluminescent “sensors”, the signal is not transient in these cases.

Heo and Crooks<sup>102</sup> used the POx–Amplex Red system for simultaneous determination of glucose and galactose in a microfluidic array biosensor. The enzymes (GOx and POx or galactose oxidase and POx) were entrapped in hydrogel micropatches where they show good storage stability. Amplex Red was added to the analyte solution, which was pumped over the surface of the sensor. The fluorescence of resorufin, the product of the oxidation of Amplex Red, was imaged via a conventional charge-coupled device camera. Glucose was determined in the range of 1–5 mM. By using specific enzymes located in different micropatches, several analytes can be determined simultaneously, as was demonstrated for the sensing of glucose and galactose mixtures. Production of resorufin also was monitored in a biosensor for superoxide ion, which makes use of superoxide dismutase and POx.<sup>124</sup>

Luminol also may be electrochemically oxidized by hydrogen peroxide, a reaction that does not require the enzyme POx and gives strong electrochemiluminescence (ECL). In this case, the polymer membrane containing immobilized GOx is placed on a carbon electrode,<sup>92,94,96</sup> and the intensity of ECL is monitored from the other side. A sol–gel containing the enzyme also was coated on the surface of an electrode,<sup>99</sup> and ECL was measured. Alternatively, the enzyme may be immobilized in a ceramic–carbon composite material.<sup>100</sup> This graphite-containing sol–gel material was placed in a glass tube and served as an electrode to generate the ECL of luminol.

Several other kinds of  $\text{H}_2\text{O}_2$  transducers were reported for use in glucose biosensors. Thus, a mixture of titanium(IV) ion and a pyridylazophenol dye was found to produce a reddish-purple product.<sup>89</sup> Formation of a colored adduct with a dinuclear iron(III) complex was used to quantify  $\text{H}_2\text{O}_2$  and glucose.<sup>95</sup> The colored form of Prussian Blue was formed from the colorless one (Prussian White) upon oxidation by hydrogen peroxide.<sup>97,98</sup>

Wolfbeis et al.<sup>61,101</sup> introduced a novel hydrogen peroxide transducer, which is based on the luminescent europium(III) tetracycline complex (EuTc).<sup>125</sup> The probe is excitable by visible light and responds to  $\text{H}_2\text{O}_2$  by an  $\sim$ 15-fold increase in luminescence intensity. Unlike in previous methods, the determination of  $\text{H}_2\text{O}_2$  does not require the addition of POx, and the reaction is fully reversible although rather slow in both directions ( $\sim$ 10 min). Moreover, the transducer operates at neutral pH. The large Stokes’ shift of  $\sim$ 200 nm and the long-lived emission (with decay times in the microsecond time domain) enable the time-resolved suppression of fluorescent species. The probe immobilized into a hydrogel was successfully used for sensing<sup>101</sup> and time-resolved imaging<sup>61</sup> of glucose.

Trettnak and Wolfbeis<sup>126</sup> exploited the intrinsic fluorescence of GOx, which contains the fluorophore flavine adenine dinucleotide (FAD). FAD displays visible absorption ( $\sim$ 380–450 nm) and weak emission at  $\sim$ 530 nm. The optical properties of the enzyme are slightly different for the reduced form ( $\text{FADH}_2$ ) that is produced during reaction with glucose and, therefore, could be used for analytical purposes. The sensor shows full reversibility ( $\text{FADH}_2$  is back-oxidized by molecular oxygen), but the analytical range is narrow (0.5–0.8 mM). The same authors used the intrinsic fluorescence of lactate mono-oxygenase for determination of lactate.<sup>127</sup> Similarly, Chudobova et al.<sup>128</sup> used the intrinsic absorption of GOx to obtain the sensor with a wider analytical range (1–10 mM) and limit of detection (LOD) of 2 mM. As expected, the LOD was significantly lower (0.5 mM) when the sample was deoxygenated.

Sierra et al. reported on the use of the intrinsic fluorescence of GOx for the determination of glucose in serum.<sup>129</sup> The green fluorescence of FAD is strongly quenched by serum proteins so that high concentrations of enzyme are required. Therefore, the authors suggested to exploit the UV fluorescence of the protein part of GOx, which peaks at 334 nm at  $\lambda_{\text{exc}} = 224$  nm. Even though such a biosensor is suitable, in principle, for the determination of glucose in the range from 0.5 to 20 mM, there are substantial drawbacks that include the lack of affordable (semiconductor-based) excitation light sources for 224 nm and interferences by other luminescent species. De Marcos et al.<sup>130</sup> have investigated sensors based on intrinsic fluorescence of GOx immobilized on different polymer supports and in polymer matrixes, with respect to sensitivity, leaching of the enzyme, and sensor shelf life. The best results were achieved when GOx was immobilized on photopolymerized polyacrylamide. The sensor polymer films had a lifetime of over 2 months and adequate analytical characteristics. The linear range was between 1.67 and 11 mM of glucose.

In an attempt to shift analytical wavelengths into the visible, De Marcos et al.<sup>131</sup> have labeled GOx with fluorescein and found an increase in fluorescence intensity in the presence of glucose, probably a result of an inner filter effect. In fact, the absorption spectrum of GOx-bound FAD (but not of  $\text{FADH}_2$ ) overlaps that of fluorescein. Consequently,



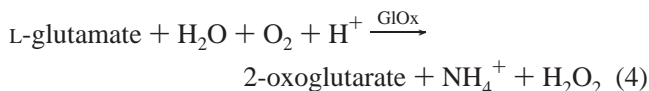
when FAD is reduced to FADH<sub>2</sub> during enzymatic action, fluorescence is enhanced ( $\lambda_{\text{exc}} = 492 \text{ nm}$ ). No such enhancement is observed if GOx is labeled with Cy-5 or Texas Red. For fluorescein-labeled GOx, the linear response is from 0.55 to 5.5 mM of glucose. The labeled GOx was entrapped into polyacrylamide gel, and the sensor was used in the flow injection mode.<sup>132</sup>

Another optical biosensor for glucose makes use of the intrinsic absorption properties of horseradish peroxidase (POx), which undergo spectral changes upon binding of H<sub>2</sub>O<sub>2</sub>.<sup>133</sup> Both GOx and POx were entrapped in a polyacrylamide gel matrix. When glucose is present, H<sub>2</sub>O<sub>2</sub> is produced and reversibly bound by POx. The intermediate species produced during enzymatic activity display different absorption spectra between 400 and 450 nm. The sensor has a linear response between 1.5 and 300  $\mu\text{M}$  of glucose.

The intrinsic optical properties of enzymes also were used for determination of nitrate (absorbance of nitrate reductase)<sup>134</sup> and nitrite ions (absorbance of cytochrome cd1 nitrite reductase)<sup>135</sup> as well as for sensing ethanol,<sup>136</sup> pyruvate,<sup>137</sup> and lactate,<sup>138</sup> using intrinsic fluorescence of alcohol dehydrogenase, lactate dehydrogenase, and lactate oxidase, respectively. The characteristics of various glucose biosensors based on the use of GOx are summarized in Table 2 along with those for other enzyme-based sensors.

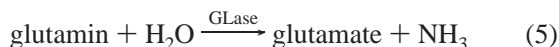
### 3.3. Other Enzyme-Based Biosensors

A number of biosensors were designed by analogy to GOx-based glucose sensors by making use of other oxidases. Enzymatic oxidation of glutamate, for example, can be described by eq 4,



where GLOx stands for glutamate oxidase. Thus, biosensors for glutamate can be based on an oxygen transducer (e.g., decacyclene in silicone)<sup>77</sup> or on detection of H<sub>2</sub>O<sub>2</sub> by chemiluminescence (via the GLOx/POx system).<sup>139,140</sup> It was found that peroxidase from *Arthromyces ramosus* produced a 100 times stronger luminescence signal than the commonly used POx from horseradish. A glutamate biosensor based on an ammonia transducer also was reported.<sup>141</sup>

The enzyme glutaminase (GLase) was used in a glutamine biosensor in which glutamine was converted into glutamate according to eq 5,



Glutamate produced in the first reaction was subsequently oxidized to 2-oxoglutarate (reaction 4). Hydrogen peroxide was detected by the chemiluminescence resulting from the oxidation of luminol that was catalyzed by either hexacyanoferrate(III) ion<sup>142,143</sup> or POx.<sup>139</sup> To avoid interference by glutamate, which can be present in samples along with glutamine, an ion-exchange resin was used<sup>142,143</sup> to remove glutamate, which is an anion at pH 7.

Sensors that make use of an oxidase-type enzyme and an oxygen transducer also were designed for lactate,<sup>142</sup> ethanol and methanol,<sup>145–147</sup> cholesterol,<sup>148–150</sup> sulfite,<sup>151</sup> bilirubin,<sup>152</sup> and phenol.<sup>153</sup> An aspartame biosensor incorporated both  $\alpha$ -chymotrypsin and alcohol oxidase.<sup>154</sup> Aspartame is hydrolyzed by  $\alpha$ -chymotrypsin to produce methanol, which is

oxidized by molecular oxygen. The enzymes were immobilized on an eggshell membrane and showed a remarkable long-term stability there. When stored at room temperature over a period of 6 months, the sensor retained >95% of its initial activity. When the enzymes were immobilized in plasticized poly(vinyl chloride), the sensor lost ~45% of its activity in 5 days. The group of Lübbbers also reported on biosensors for xanthine, lactate, and cholesterol using oxygen transduction. Pyrene butyric acid acted as a fluorescent probe for oxygen and was covered with a layer containing the appropriate oxidase.<sup>155</sup>

Similar to the aspartame biosensor, a dual enzymatic system was used for determination of choline-containing phospholipids (e.g., lecithin).<sup>156</sup> Phospholipids were hydrolyzed by phospholipase D to produce choline, which was subsequently oxidized by oxygen in the presence of choline oxidase. A similar bienzymatic system was used by Kotsira and Clonis,<sup>157</sup> however, in combination with a pH optical transducer. Production of betaine during oxidation of choline results in a change of pH and protonation of the indicator bromothymol blue.

Lactate monooxygenase is more stable than lactate oxidase and was used in a lactate biosensor.<sup>158</sup> Lactate was monitored by measurement of the oxygen consumption via the fluorescence of decacyclene and can be determined with an LOD of 0.3 mM. Its stability in sol–gel matrix can be improved by addition of polycations.<sup>108</sup>

Detection of hydrogen peroxide via chemi- and electrochemiluminescence of luminol was used in biosensors for lactate,<sup>94,96,159</sup> ethanol,<sup>160</sup> choline,<sup>161</sup> lysine,<sup>119,162</sup> sulfite,<sup>163</sup> xanthine and hypoxanthine,<sup>140,164</sup> and choline.<sup>96,165,166</sup> Uric acid and D-amino acids were detected by bienzymatic systems including uricase and POx,<sup>167</sup> and D-amino acid oxidase and POx,<sup>168</sup> respectively. Here, thiamine was oxidized by hydrogen peroxide to give fluorescent thiochrome, whose fluorescence was detected.

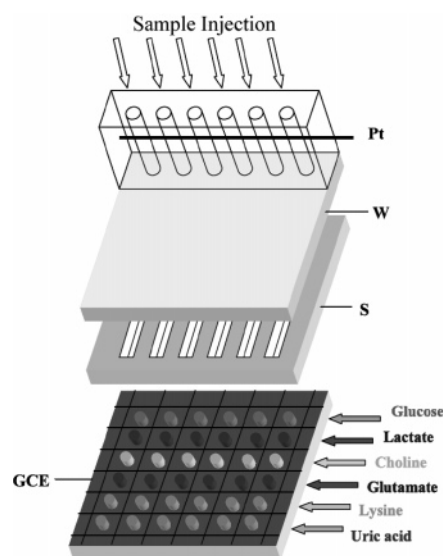


**Figure 3.** Schematic of an electrochemiluminescent multifunctional biosensing chip: GCE, glassy carbon electrode; Pt, platinum pseudo-reference electrode; S, silicone spacer; W, plexiglass window. A solution containing different analytes is injected in each channel, a working potential of +850 mV is then applied, and the emitted light (integrated over 3 min) is detected by a CCD camera. Reprinted with permission from Marquette, C. A.; Degiuli, A.; Blum, L. J. *Biosens. Bioelectron.* **2003**, *19*, 433. Copyright 2003 Elsevier.

**Table 2. Overview of Optical Enzymatic Biosensors: Abs, Absorbance; BL, Bioluminescence Intensity; CL, Chemiluminescence Intensity; EL, Electroluminescence Intensity; LI, Luminescence Intensity; LL, Luminescence Lifetime**

analyte	enzyme	transducer	analytical range	LOD	spectroscopy	indicator or substrate	ref
acetylcholine	AChE	pH	0.5–20 mM	0.5 mM	LI	FITC	206
acetylcholine	AChE	pH	0–20 $\mu$ M	?	ratio of LIs	SNARF	34
acetylcholine	AChE	pH	2–13 mM	1 mM	LI	HPTS	208
acetylcholine	AChE	pH	?	50 $\mu$ M	LI	FITC	207
ATP	f. luciferase		0.1 nM–1 $\mu$ M	0.05 nM	BL		228
ATP	f. luciferase		0.1 nmol–1 $\mu$ M	0.1 nmol	BL		229
ATP	f. luciferase		?	0.1 pmol	BL		234
ATP	f. luciferase		?	10 pmol	BL		235
ADP	hexokinase + pyruvate kinase + glucose 6-P dehydrogenase		0.1–20 $\mu$ M	$\mu$ m	LI	NAD <sup>+</sup> (coenzyme)	236
AMP	adenylate kinase + creatine kinase + luciferase		?	25 pmol	BL		235
L-alanine	L-alanineDH		0.45–4.5 mM	?	LI.	PEG–NAD <sup>+</sup>	223
alcohols	ADH		?	0.9 mM	LI.	NAD <sup>+</sup> (coenzyme)	219
ethanol	ADH + aldehyde-DH		1–100 mM	?	LI.	NAD <sup>+</sup> (coenzyme)	183
ethanol	ADH		10–1000 mM	?	LI.	NAD <sup>+</sup> (coenzyme)	220
ethanol	AOx	oxygen	50–500 mM	10 mM	LI.	Ru-bipy	145
ethanol	AOx	H <sub>2</sub> O <sub>2</sub>	3–750 $\mu$ M	3 $\mu$ M	CL	luminol	160
ethanol	AOx	oxygen	0.5–9 mM	0.5 mM	LI.	a Ru(II) complex	146
ethanol	ADH + OR + b. luciferase		0.4–70 $\mu$ M	0.4 $\mu$ M	BL		233
ethanol	ADH		0.043–1 mM	?	LI.	PEG–NAD <sup>+</sup>	221
ethanol	ADH		0–1.1 mM	?	LI.	PEG–NAD	222
methanol	AOx + HPOx	oxygen	80 $\mu$ M–60 mM	80 $\mu$ M	LI.	Ru-dpp	147
D-amino acid	D-amino acid oxidase + HPOx	H <sub>2</sub> O <sub>2</sub>	0–10 mM	0.3 $\mu$ g/mL	LI.	thiamine	168
aspartame	$\alpha$ -chymotrypsin + AOx	oxygen	0.056–3.07 mM	32 $\mu$ M	LI.	Ru-dpp	154
captan	GST		0–2.0 ppm	?	Abs.	CDNB + GSH	202
Captan + ORP (paraoxon)	GST + AChE		0–2.0 mM	?	Abs.	synthetic substrate	203
bilirubin	bilirubin oxidase	oxygen	0.1–300 $\mu$ M	0.1 $\mu$ M	LI.	Ru-dpp	152
cholesterol	cholesterol oxidase	oxygen	0.2–3 mM	0.2 mM	LI.	decacyclene	148
cholesterol	cholesterol oxidase	oxygen	0.15–3.0 mM	0.15 mM	LI.	Ru-dpp	149
cholesterol	cholesterol oxidase	oxygen	0.07–18 mM	0.05 mM	LI.	Ru-dpp	150
choline	ChOx + HRP	H <sub>2</sub> O <sub>2</sub>	3–150 $\mu$ M	3.0 $\mu$ M	CL	luminol	165
choline	ChOx	H <sub>2</sub> O <sub>2</sub>	10 pmol–30 nmol	10 pM	EL.	luminol	96, 166
choline with phospholipids	phospholipase-D + ChOx	oxygen	0.08–3.00 g/L	0.08 g/L	Lum. I.	Ru-dpp	156
fructose	GFOR		0.278–331 mM	0.278 mM	intrinsic LI.		224
H <sub>2</sub> O <sub>2</sub>	HPOx		?	1 $\mu$ M	CL	luminol	118
H <sub>2</sub> O <sub>2</sub>	HPOx		0.01–1 mM	1 $\mu$ M	CL	luminol	119
H <sub>2</sub> O <sub>2</sub>	HPOx		0.05–1.2 mM	0.025 mM	CL	luminol	93
H <sub>2</sub> O <sub>2</sub>	HPOx		0.1–3 mM	0.67 mM	CL	luminol	120
H <sub>2</sub> O <sub>2</sub>	HPOx		17–117 $\mu$ M	16.7 $\mu$ M	CL	luminol	121
H <sub>2</sub> O <sub>2</sub>	HPOx		1–130 $\mu$ M	1 $\mu$ M	LI.	homovanilic acid	122
H <sub>2</sub> O <sub>2</sub>	HPOx		0.5–250 $\mu$ M	?	LI.	amplex red	123
hypoxanthine	XOx + HPOx	H <sub>2</sub> O <sub>2</sub>	1–320 $\mu$ M	0.55 $\mu$ M	CL	luminol	164
hypoxanthine	XOx + POx	H <sub>2</sub> O <sub>2</sub>	0.5 $\mu$ M–1 mM	?	CL	luminol	140
glucose	GOx		0.5–0.8 mM	0.5 mM	intrinsic LI.		126
glucose	GOx		1.7–11 mM	?	intrinsic LI.		130
glucose	GOx		1–10 mM	0.5–2 mM	intrinsic Abs.		128
glucose	GOx	oxygen	0.1–20 mM	0.05 mM	LI.	decacyclene	73
glucose	GOx	oxygen	0.1–500 mM	0.1 mM	LI.	decacyclene	74
glucose	GOx	oxygen	0.01–2 mM	0.01 mM	LI.	decacyclene	75
glucose	GOx	oxygen	0.06–1 mM	0.06 mM	LI.	Ru-phen	76
glucose	GOx	oxygen	0.05–1 mM	?	LI.	decacyclene	77
glucose	GOx	oxygen	0.03–1.2 mM	0.05 mM	LI.,LL	PtOEP	58, 59
glucose	GOx	oxygen	0.1–8.3 mM	0.1mM	LI.	Ru-dpp	78
glucose	GOx	oxygen	0–2.5 mM	80 $\mu$ M	LI.	Al-feron complex	79
glucose	GOx	oxygen	0–20 mM	0.6 mM	LI.	Ru-ligand complex	80
glucose	GOx	oxygen	0.5–15 mM	?	LI.	Rudpp	81
glucose	GOx	oxygen	0.7–10 mM	0.75 mM	LI.	Ru-phen	82
glucose	GOx	oxygen	0.06–30 mM	6 $\mu$ M	LI.	Ru-dpp	84
glucose	GOx	oxygen	0.1–15 mM	0.1 mM	LI.	Ru-dpp	85
glucose	GOx	oxygen	0.30–2.0 mM	0.3 mM	LI.	Ru-dpp	86
glucose	GOx	oxygen	0.3–5 mM	0.3 mM	ratio of LIs	sulfonated Ru-dpp	35
glucose	GOx	oxygen	9.0–200 $\mu$ M	9.0 $\mu$ M	LI.	a Ru complex	87
glucose	GOx	oxygen	0.1–0.8 mM		LI.	Ru-dpp	88
glucose	GOx	pH	0.1–2 mM	0.1 mM	LI.	HPTS	103
glucose	GOx	pH	0–1.7 mM	?	LI.	Rhodamine (inert)	104
glucose	GOx	pH	1–30 mM	1 mM	Abs.	polyaniline	105
glucose	GOx + HPOx	H <sub>2</sub> O <sub>2</sub>	0.25–250 nmol	0.25 nmol	CL	luminol	91
glucose	GOx + HPOx	H <sub>2</sub> O <sub>2</sub>	0.3–300 $\mu$ M	0.1 $\mu$ M	CL	luminol	90
glucose	GOx + HPOx	H <sub>2</sub> O <sub>2</sub>	1–5 mM	0.43 mM	CL	luminol	93

Table 2 (Continued)

analyte	enzyme	transducer	analytical range	LOD	spectroscopy	indicator or substrate	ref
glucose	GOx + HPOx	H <sub>2</sub> O <sub>2</sub>	0.01–0.8 mM	80 μM	LI.	Amplex Red	39
glucose	GOx + HPOx	H <sub>2</sub> O <sub>2</sub>	1–5 mM	0.8 mM	LI.	Amplex Red	102
glucose	GOx	H <sub>2</sub> O <sub>2</sub>	0–10 mM	0.3 mM	EL.	luminol	92
glucose	GOx	H <sub>2</sub> O <sub>2</sub>	60 pmol–5 μmol	60 pmol	EL.	luminol	94
glucose	GOx	H <sub>2</sub> O <sub>2</sub>	60 pmol–0.6 μmol	60 pmol	EL.	luminol	96
glucose	GOx	H <sub>2</sub> O <sub>2</sub>	50 μM–10 mM	26 μM	EL.	luminol	99
glucose	GOx	H <sub>2</sub> O <sub>2</sub>	0.01–10 mM	8.16 μM	EL.	luminol	100
glucose	GOx	H <sub>2</sub> O <sub>2</sub>	17 μM–15 mM	17 μM	Abs.	Ti(IV) reagent	89
glucose	GOx	H <sub>2</sub> O <sub>2</sub>	30–200 μM	10 μM	Abs.	Fe(III) complex	95
glucose	GOx	H <sub>2</sub> O <sub>2</sub>	0.05–2.0 mM	?	Abs.	Prussian White	97, 98
glucose	GOx	H <sub>2</sub> O <sub>2</sub>	0.1–5 mM	0.2 mM	LI.	EuTc	101
glucose	GOx	H <sub>2</sub> O <sub>2</sub>	0.1–2 mM	0.05 mM	LL.	EuTc	61
glucose	GDH		1.1–11 mM	0.6 mM	LI.	NAD <sup>+</sup> (coenzyme)	213
glucose	GDH		0–0.55 mM	?	LI.	PEG–NAD <sup>+</sup>	222
glucose	GFOR		0.055–55.5 mM	55 μM	intrinsic LI.		224
glutamate	GIOx	NH <sub>3</sub>	1–12 μM	0.1 μM	LI.	carboxyfluorescein	141
glutamate	GIOx + POx	H <sub>2</sub> O <sub>2</sub>	0.1–60 μM	0.1 μM	CL	luminol	139
glutamate	GIOx + POx	H <sub>2</sub> O <sub>2</sub>	1 μM–1 mM	1 μM	CL	luminol	140
glutamate	GIDH + GPT		?	0.13 μM	LI.	NAD <sup>+</sup> (coenzyme)	217
glutamate	GIDH		0–18 μM	0.2 μM	LI.	NAD <sup>+</sup> (coenzyme)	218
glutamine	GAH + GIOx	H <sub>2</sub> O <sub>2</sub>	1–100 μM	1 μM	CL	luminol	142, 143
glutamine	GAH + GIOx + POx	H <sub>2</sub> O <sub>2</sub>	1 μM–2.5 mM	1 μM	CL	luminol	139
lactate	lactate monoxygenase		0.5–1 mM	?	intrinsic, LI.		127
lactate	lactate monoxygenase	oxygen	0.3–6.0 mM	0.3 mM	LI.	decacyclene	158
lactate	LOx	oxygen	0.02–0.5 mM	?	LI.	decacyclene	77, 144
lactate	LOx + HPOx	H <sub>2</sub> O <sub>2</sub>	3–200 μM	3 μM	LI.	homovanillic acid	122
lactate	LOx + HPOx	H <sub>2</sub> O <sub>2</sub>	0.1–1 μmol	?	CL	luminol	159
lactate	LOx	H <sub>2</sub> O <sub>2</sub>	30–300 pmol	30 pmol	EL.	luminol	96
lactate/pyruvate	LDH		2–50 μM	2 μM	LI.	NAD <sup>+</sup> (coenzyme)	214
lactate	LaDH		0.2–1.0 mM	?	Abs. & LI.	NAD <sup>+</sup> (coenzyme)	216
lactate	LDH + GPT		11–150 mg/L	?	LI.	PEG–NAD <sup>+</sup>	221
LDH	OR + b. luciferase		10–250 IU/L	10 IU/l	BL		232
lecitin	phospholipase-D + ChOx	pH	20–120 μM	20 μM	Abs.	BTB	157
lysine	LyOx + HPOx	H <sub>2</sub> O <sub>2</sub>	10 μM–1 mM	10 μM	CL	luminol	162
lysine	LyOx + POx	H <sub>2</sub> O <sub>2</sub>	5 μM–10 mM	5 μM	CL	luminol	119
mannitol	mannitol-DH		0–0.1 g/L	?	LI.	PEG–NAD <sup>+</sup>	222
Hg <sup>2+</sup>	urease	NH <sub>3</sub>	0.04–0.12 μM	0.04 μM	Abs.	Nile Blue	210
Hg <sup>2+</sup>	urease	pH	1 nM–10 μM	1 nM	Refl.	pH ind. strip	211
NADH	OR + b. luciferase		1 nM–3 μM	0.3 nM	BL		225
NADH	OR + b. luciferase		0.3 nM–3 μM	?	BL		226
NADH	OR + b. luciferase		2 pmol–1 nmol	2 pmol	BL		227
NADH	OR + b. luciferase		5.5 nM–1 μM	1 nM	BL		228
NADH	OR + b. luciferase		5–500 nM	5 nM	BL		230, 231
NADH	OR + b. luciferase		1 nM–1 μM	1 nM	BL		229
NADH	OR + b. luciferase		10–500 pmol	?	BL		159
nitrate ion	nitrate reductase		0–1.5 μM	0.125 μM	intrinsic abs.		134
nitrite ion	cytochrome cd1 nitrite reductase		0.07–1.25 μM	0.075 μM	intrinsic abs.		135
<i>p</i> -nitrophenyl phosphate	alkaline phosphatase		10–380 μM	?	Abs.	<i>p</i> -nitrophenyl phosphate	197
<i>p</i> -nitrophenyl phosphate	alkaline phosphatase		0–40 μM	?	LI.	umbelliferyl phosphate	198
ORP (paraoxon)	AChE		0.5–16 μM	0.2 μM	Abs.	AMPT	199
ORP	AChE		?	0.1–58 mg/L	LI.	indoxyl acetate	200
carbamate pesticides	AChE	pH	0.8–3.0 mg/L	25 ng	Refl.	chlorophenol red	204
ORP (paraoxon)	AChE	pH	?	27 ppb	LI.	FITC	206
ORP	AChE		?	2 ppm	Abs.	<i>o</i> -nitrophenol	201
ORP (Carbaryl)	AChE	pH	0.1–8.0 mg/L	108 μg/l	Abs.	bromocresol purple	205
ORP (paraoxon)	OPH		0.01–0.48 mM	2 μM	Abs.	paraoxon	209
ORP (paraoxon)	OPH	pH	0.8–15 μM	0.8 μM	ratio of LI	carboxy SNARF-1	36
ORP (paraoxon)	OPH		20–140 μM	20 μM	ratio of LI	DDAO phosphate	37
ORP (DFP)	OPH	pH	2–400 μM	0.05 μM	ratio of LI	carboxy SNARF-1	38
oxaloacetate	malate DH + OR + b. luciferase		3 nM–2 μM	1 nM	BL		233
penicillin	penicillinase	pH	0–10 mM	?	Abs.	bromocresol green	172
penicillin	penicillinase	pH	0.25–10 mM	75 μM	LI.	acrylofluorescein	175
penicillin	penicillinase	pH	0.1–10 mM	0.1 mM	LI.	FITC	176
penicillin	penicillinase	pH	0.3–10 mM	?	Abs.	azo dye	173
penicillin	penicillinase	pH	0.1–25 mM	0.1 mM	LI.	FITC	177
penicillin	penicillinase	pH	1–10 mM	1 mM	LI.	FITC	178
penicillin	penicillinase	pH	0.5–8 mM	?	Abs. & Refl.	phenol red	174
penicillin	penicillinase	pH	0.25–10 mM	0.25 mM	LI.	acryloylfluorescein	179
phenol	tyrosinase	oxygen	0.08–40 mM	0.08 mM	LI.	Ru-dpp	153



Table 2 (Continued)

analyte	enzyme	transducer	analytical range	LOD	spectroscopy	indicator or substrate	ref
L-phenylalanine	L-phenylalanineDH		0.6–6 mM	?	LI.	PEG–NAD <sup>+</sup>	223
phenylpyruvate	phenylpyruvateDH		0–0.7 mM	?	LI.	PEG–NAD <sup>+</sup>	222
pyruvate	LOx + LDH		0–0.1 mM	8.4 μM	LI.	NAD <sup>+</sup> (coenzyme)	215
sorbitol	sorbitolDH + OR + b. luciferase		20 nM–10 μM	20 nM	BL		233
sulfite	sulfite oxidase	oxygen	0–100 ppm	?	LI.	perylene	151
sulfite	sulfite oxidase + HPOx	H <sub>2</sub> O <sub>2</sub>	1–100 μM	0.5 μM	CL	luminol	163
superoxide radical	superoxide dismutase + HPOx	H <sub>2</sub> O <sub>2</sub>	?	20 nM	LI.	Amplex Red	124
urea	urease	pH	0–40 mM	?	Abs.	BTB	172
urea	urease	pH	0–2 mM	?	Refl.	BTB	180
urea	urease	pH	40–250 μM	?	Refl.	phenol red	181
urea	urease	pH	?	?	LI.	FITC	182
urea	urease	pH	0–1 mM	20 μM	LI.	NBD-PE	186
urea	urease	pH	0–4 mM	?	Refl.	FITC	183
urea	urease	pH	0–100 mM	?	Abs.	PVP	187
urea	urease	pH	0.2–100 mM	0.1 mM	Abs.	Prussian Blue	185
urea	urease	pH	0.06–1 M	0.06 M	Abs.	polypyrrole	184
urea	urease	pH	2.0–12.0 mM	?	Abs.	Prussian Blue	97
urea	urease	pH	0.001–10 mM	2.5 μM	ratio of LI	FITC	39
urea	urease	pH	0–400 μM	?	ratio of LI	SNARF	34
urea	urease	NH <sub>3</sub>	0.05–2.5 mM	?	LI.	CF	188
urea	urease	NH <sub>3</sub>	0.25–8 mM	0.25 mM	Abs.	BTB	189
urea	urease	NH <sub>3</sub>	0.1–5 mM	?	LI.	HPTS	190
urea	urease	NH <sub>3</sub>	0.01–1 mM	0.03 mM	LI.	Nile Blue	191
urea	urease	NH <sub>3</sub>	0.1–100 mM	0.1 mM	Abs.	acridine orange	192
urea	urease	NH <sub>3</sub>	10 μM–100 mM	?	Abs.	ETH 5350	193
urea	urease	NH <sub>3</sub>	0.1–10 mM	?	Abs.	brilliant yellow	194, 195
urea	urease	NH <sub>3</sub>	0.1 mM–0.1 M	0.1 mM	LI.	octadecyl dichlorofluorescein	196
uric acid	uricase + HPOx	H <sub>2</sub> O <sub>2</sub>	3–30 mM	0.9 mM	LI.	thiamine	167
xanthine	XOx + HPOx	H <sub>2</sub> O <sub>2</sub>	3.1–320 μM	2.2 μM	CL	luminol	164

A microarray biochip for simultaneous electrochemiluminescent detection of several analytes was reported<sup>169,170</sup> that contains the following six enzymes: GOx, glutamate oxidase, choline oxidase, lactate oxidase, lysine oxidase, and uricase. They were noncovalently immobilized (along with luminol) on anion-exchanger beads consisting of diethylaminoethyl sepharose, and the resulting beads were dispersed along with the luminol beads into poly(vinyl alcohol) bearing styrylpyridinium groups. This “cocktail” was spotted on the surface of a glassy carbon electrode, giving spots of 0.8 mm in diameter (Figure 3). The spots were allowed to polymerize under UV light. The electrochemiluminescence from the six-channel, six-parameter biosensor was read by a CCD camera. Simultaneous measurements of glucose, glutamate, choline, lactate, lysine, and uric acid could be performed in the ranges 20 μM–2 mM, 1 μM–0.5 mM, 2 μM–0.2 mM, 2 μM–0.2 mM, 1 μM–0.5 mM, and 1 μM–25 μM, respectively. A biosensor for acetate also was developed.<sup>170</sup> Acetate kinase (pre-immobilized on sepharose beads) and pyruvate kinase were immobilized in a layer brought into contact with the sample solution, while pyruvate oxidase was entrapped in a layer placed between the kinase layer and the glassy carbon electrode. Acetate could be measured in the range from 10 μM to 100 mM.

A related microarray biochip of nine screen-printed graphite electrodes was prepared for determination for glucose and lactate.<sup>171</sup> A reproducibility of within 4.4% was found at an optimum luminol oxidation potential of +650 mV. The LODs for simultaneous determination of glucose and lactate were 10 and 3 μM, respectively.

Like in glucose biosensors, pH transducers were also used in biosensors for penicillin and urea. Penicilloate and protons are produced from penicillin in the enzymatic hydrolysis catalyzed by penicillinase. The decrease in pH is monitored by changes of absorption (reflectance)<sup>172–174</sup> or emission

intensity<sup>175–179</sup> of pH indicators. Fluorescein-derived indicators were used almost exclusively in order to monitor pH changes in neutral media. The pH indicator is usually contained in a hydrogel (most often a polyacrylamide gel), which is permeable for protons formed during the enzymatic reaction. A photopolymerization process was used to obtain a pH/penicillin array biosensor with spot diameters of ~27 μm located on the surface of a 350 μm thick optical fiber.<sup>179</sup> Penicillin and pH could be measured simultaneously (via imaging of fluorescence intensity with a CCD camera), and effects of changing pH, which often are large in complex fermentation media, could thus be compensated for. Biosensors based on pH transduction suffer from the fact that pH changes depend on the buffer capacity of the sample medium, which often is unknown and can hardly be compensated for.

Urease-catalyzed hydrolysis of urea leads to formation of ammonium ions (eq 6) but also results in an increase in pH:



Consequently, two types of urea biosensors can be developed. Those based on pH transducers are designed analogously to penicillin optical sensors and make use of absorption-based<sup>172,180,181</sup> or fluorescent<sup>34,39,182,183</sup> pH indicators. In contrast to most optical biosensors that rely on measurements of fluorescence intensity only, the one designed by Tsai and Doong<sup>39</sup> employs a ratiometric scheme of self-referencing. Here, the intensity of the indicator (a fluorescein isothiocyanate–dextrane conjugate) is referenced to the pH-independent intensity of tetramethylrhodamine isothiocyanate–dextrane. Such referencing makes it possible to overcome drawbacks of intensity-based measurements (for example, drifts in the intensity of the light source) but also seems to

increase the sensitivity of measurements (LOD = 2.5  $\mu\text{M}$ , compared to 20–100  $\mu\text{M}$  for other urea biosensors).

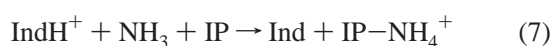
The ratiometric approach also was used by Yadavalli et al.,<sup>34</sup> who prepared sensor arrays composed of poly(ethylene glycol) hydrogel microspots with a diameter of  $\sim 200 \mu\text{m}$  containing urease labeled with a seminaphthofluorescein indicator (SNAFL-1). The ratio of the intensities for the acidic (green emission) and basic (red emission) forms of the indicator was determined using a microscope with two different sets of excitation and emission filters.

Polypyrrole was found to exhibit a pH-dependent intrinsic absorption with a peak at 650 nm. It was used in an urea biosensor where it acts as a support and a pH indicator simultaneously.<sup>184</sup> In other work, Prussian Blue (also having a pH-dependent near-IR absorption) along with the enzyme was chemically incorporated into polypyrrole films.<sup>97,185</sup>

Brennan et al.<sup>186</sup> co-immobilized the fluorescent probe nitrobenzoxadiazole dipalmitoylphosphatidylethanolamine (NBD-PE) and urease on the surface of an optical fiber whose surface was modified with alkylamine monolayers. Alterations of pH during the enzymatic reaction result in a change of physical and electrostatic structure of the membranes, which in turn alters the emission intensity of the NBD-PE. Fluorescence intensity decreases with the degree of ionization of head groups, consistent with an increase in self-quenching. By analogy to the approach made by McCurley,<sup>104</sup> a pH-dependent swelling of a polymer also was used for sensing urea.<sup>187</sup> A layer of poly(vinyl pyrrolidone) cross-linked with sulfonated bisazidostilbenes was coated onto a metal mirror. Protons and certain other ions cause swelling of the material, and the changes in reflectance can be monitored. The analytical range of this fully reversible sensor is from 0 to 100 mM of urea.

A number of urea biosensors are based on the determination of ammonia gas produced during hydrolysis of urea.<sup>188–196</sup> Two types of ammonia transducers were used. In the first, a pH indicator is contained in a buffer solution positioned behind a gas-permeable membrane, in which the enzyme is immobilized. Gaseous ammonia diffuses through the membrane and dissolves in the buffer. This results in an increase of pH of the internal solution and in deprotonation of the indicator. Changes in absorbance or fluorescence intensity of the indicator are related to the ammonia concentration present in the external solution and, thus, to the level of urea. This sensor type was introduced by Rhines and Arnold<sup>188</sup> and often used in later work.<sup>189,190,194,195</sup>

A completely different scheme is utilized in the second type of ammonia transducers. Such transducers contain the  $\text{NH}_4^+$ -selective neutral ionophore nonactin, a proton-selective neutral chromoionophore (a pH indicator), and a lipophilic anionic counterion dissolved in a plasticized poly(vinyl chloride) (PVC) matrix. The sensor layer is covered with a gas-permeable membrane to warrant selectivity for ammonia gas by inhibiting a direct ion-exchange reaction between the sample solution and the sensor membrane. A membrane with immobilized urease is mounted on top of the sensor. Ammonia gas diffuses through the gas-permeable membrane and reaches the PVC layer, where the reaction outlined in eq 7 occurs:



Here, Ind and IP are the neutral chromoionophore and the

neutral ionophore, respectively. Again, both absorption-based<sup>192,193</sup> and fluorescent<sup>191,196</sup> pH indicators came to use. Kawabata et al.<sup>192</sup> manufactured a 140  $\mu\text{M}$  thick urea microsensor based on this principle.

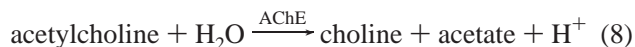
Certain enzymatic reactions do not require optical transduction via a chemical sensor because optically detectable species are generated or consumed during the reaction. Such sensors usually consist of a membrane that contains the immobilized enzyme. Chromogenic or fluorogenic substrates and any cosubstrates are added to the sample into which the sensor is submerged. Because of the absence of a transducer, such biosensors are often referred to as direct optical biosensors. One type of a direct optical biosensor is based on hydrolysis of a substrate catalyzed by a hydrolase-type enzyme. The principle was first demonstrated by Arnold,<sup>197</sup> who used immobilized alkaline phosphatase to catalyze hydrolysis of *p*-nitrophenyl phosphate, which results in the formation of yellow *p*-nitrophenolate. A linear dependence of the change in absorbance on the concentration of the substrate was observed.

The method was further developed by Freeman and Bachas,<sup>198</sup> who introduced a sensor that makes use of a competition between two substrates (4-methylumbelliferyl phosphate and *p*-nitrophenyl phosphate) for the active state of the model enzyme alkaline phosphatase. If the sensor was placed in a solution containing 4-methylumbelliferyl phosphate, the highly fluorescent anion of 4-methylumbelliferone was produced upon hydrolysis. In the presence of the analyte (*p*-nitrophenyl phosphate), the rate of fluorescence change caused by production of 4-methylumbelliferone was decreased. The method also was demonstrated to work for the determination of adenosine monophosphate, another substrate of alkaline phosphatase.

A sensing scheme for determination of organophosphorous pesticides such as paraoxon<sup>199</sup> is based on the inhibitor action of acetylcholine esterase (AChE). The biosensor makes use of a synthetic yellow substrate that is converted into a blue product by AChE. Inhibition of the reaction by pesticides is monitored spectroscopically. The LOD for paraoxon was 200 nM. Although the immobilized enzyme showed a very good long-term stability, that of the synthetic substrate was rather low in that the half-lifetime was  $\sim 2$  weeks only at room temperature. Others<sup>200</sup> have used indoxyl acetate as a substrate for AChE. The fluorescence intensity of indoxyl ( $\lambda_{\text{max}} = 470 \text{ nm}$ ) was related to the concentration of the inhibiting pesticide. Similar to the work of Freeman and Bachas,<sup>198</sup> enzymatic hydrolysis of substrate *o*-nitrophenyl acetate was used also for determination of organophosphates.<sup>201</sup>

Choi et al.<sup>202</sup> developed a biosensor for captans, a group of systemic organophosphorus fungicides and pesticides. The enzyme glutathione-*S*-transferase (GST) converts the substrates, 1-chloro-2,4-dinitrobenzene and glutathione, into yellow *S*-(2,4-dinitrophenyl) glutathione. In the presence of captans, GST is inhibited and the amount of the product is decreased. A dual enzymatic system consisting of GST and AChE was shown to be suitable for simultaneous determination of both paraoxon and captan.<sup>203</sup> The absorbance of *S*-(2,4-dinitrophenyl)glutathione (the product of the reaction catalyzed by GST) and  $\alpha$ -naphthol (the product of the reaction catalyzed by AChE) was detected at 400 and 500 nm, respectively. It was observed that AChE was inhibited by both captan and organophosphorus compounds, while GST was inhibited by captan only. Thus, simultaneous detection of both analytes becomes possible.

Inhibitors of AChE can also be detected using pH optical transducers. The hydrolysis of acetylcholine chloride according to eq 8 results in the formation of acetic acid and, therefore, in a decrease in pH:



Different absorption-based<sup>204,205</sup> and fluorescent<sup>34,206,207</sup> indicators were used for determination of organophosphorous and carbamate pesticides as well as of acetylcholine itself.<sup>208</sup>

All biosensors that make use of the inhibition of AChE show good sensitivity but are severely limited in specificity because AChE is the target of a wide variety of toxic inhibitors. These range from heavy metal ions to chemical warfare agents. Both organophosphate- and carbamate-based pesticides inhibit AChE. Additionally, most sensors using AChE inhibition have lengthy response times because of long incubation periods, inhibition is often irreversible, and subsequent reactivation of AChE sometimes is impossible. More recently, interest has been directed to organophosphorus hydrolase (OPH), which is not susceptible to nonspecific inhibition and offers much better specificity than AChE. OPH hydrolyzes a range of organophosphate esters, including pesticides such as paraoxon and chemical warfare agents such as soman or sarin. Catalytic hydrolysis of these compounds is accompanied by a release of protons, which makes possible determination of organophosphorus pesticides (ORP) using pH transducers.<sup>36,38</sup> Hydrolysis of some ORP also produces detectable chromophoric products.<sup>209</sup>

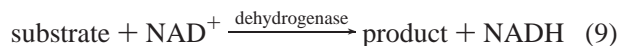
An interesting approach was introduced by Simonian et al.<sup>37</sup> The sensing scheme is far from a conventional enzymatic biosensor but resembles a competitive immunoassay. The enzyme OPH is covalently attached to the surface of a gold nanoparticle. The fluorophore 7-hydroxy-9H-(1,3-dichloro-9,9-dimethylacridin-2-one)phosphate binds weakly to the active site of the enzyme. The fluorescence of the bound fluorophore is enhanced because of the proximity to the gold surface. An inhibitory substrate is added that has a much higher affinity for the active site of OPH and, thus, replaces the fluorophore. When far away from the gold surface, no enhancement of fluorescence is observed any longer.

Biosensors for heavy metal ions have been reported that exploit the inhibition of urease by heavy metal ions.<sup>210,211</sup> Urease is chosen as the enzyme since it is particularly sensitive to ions such as Pb(II), Cd(II), Ag(I), and Hg(II).

In contrast to the catalytic biosensors that monitor inhibition of enzymatic activity, certain biosensors use a different mechanism of signal transduction. Walker and Asher<sup>212</sup> designed an ultrasensitive biosensor for the pesticide parathion. The sensor utilizes an array of colloidal polymer particles (which diffract light in the visible spectral region) emulgated into a polyacrylamide-based hydrogel. AChE is covalently attached to the hydrogel backbone where it irreversibly binds parathion, which in turn results in the formation of a charged product. This induces swelling of the hydrogel network and results in a shift of the wavelength of the diffracted light that is proportional to the concentration of the analyte. The sensor is capable of sensing parathion in the fM to pM concentration range. The LOD is 4.3 fM of parathion, which is several orders of magnitude lower than those for other sensors for organophosphates. As expected, ionic strength severely influences swelling properties and, thus, the performance of the sensor; therefore, 30 min of

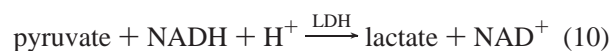
washing with deionized water is necessary after incubation of the sensor with parathion (30 min).

A number of enzymatic redox reactions require the presence of coenzymes. Most systems involve nicotinamide adenine dinucleotide (NAD<sup>+</sup>), to which a hydrogen atom and an electron can be transferred, while the substrate is oxidized according to eq 9:



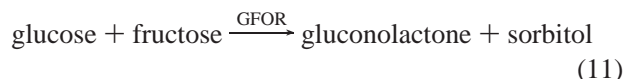
The formation of the reduced form of nicotinamide adenine dinucleotide (NADH) can be monitored via its characteristic absorption at  $\lambda_{\text{max}}$  350 nm and emission peaking at  $\lambda_{\text{max}}$  450 nm, and this enables the optical quantification of substrate concentrations. In early work, the dehydrogenases were immobilized on (or in) a hydrophobic polymer membrane, and the “sensors” were operated in the flow-injection mode, where the analyzed substrate and NAD<sup>+</sup> are passed over the sensor layer. Such sensors were developed for glucose,<sup>213</sup> lactate and pyruvate,<sup>214–216</sup> glutamate,<sup>217,218</sup> and alcohols<sup>183,219</sup> using glucose dehydrogenase, lactate dehydrogenase, glutamate dehydrogenase, and alcohol dehydrogenase, respectively. Enzymatic oxidation of lactate by NAD<sup>+</sup> results in the formation of pyruvate and NADH. The reaction thus was used not only for determination of lactate but also in the reverse direction for pyruvate,<sup>215</sup> with NADH being supplied instead of NAD<sup>+</sup>.

Evidently, the main disadvantage of such sensors relies on the fact that the coenzyme needs to be added to the sample solution. Therefore, some effort was focused on designing a self-contained biosensor, i.e., a sensor that does not require the supply of any additional components. For example, NAD<sup>+</sup> was immobilized together with alcohol dehydrogenase in a sol–gel monolith.<sup>220</sup> However, leaching of the coenzyme into the solution was not completely excluded, and the response of the sensor was rather slow (~30 min). A novel approach was proposed by Scheper and Buckmann,<sup>221–223</sup> who used a poly(ethylene glycol) molecular weight-enlarged NAD<sup>+</sup> (PEG–NAD<sup>+</sup>) instead of NAD<sup>+</sup>. A pair of dehydrogenase-type enzymes (for substrate detection and for regeneration of the coenzyme) and PEG–NAD<sup>+</sup> were enclosed in the sensing compartment between the ultrafiltration membrane and the fiber-optic tip. The analytes and products were allowed to diffuse freely through the ultrafiltration membrane. In contrast to previous sensors (where NAD<sup>+</sup> was supplied in solution), this sensor type allows for the regeneration of PEG–NAD<sup>+</sup> in a subsequent reaction such as the one in eq 10:



The scheme was used for determination of glucose, lactate, ethanol, pyruvate, mannitol, formate, L-alanine, and L-phenylalanine.

The unique enzyme glucose–fructose oxidoreductase (GFOR) is capable of dehydrogenating glucose to gluconolactone and of simultaneously reducing fructose to sorbitol in a ping-pong mechanism according to

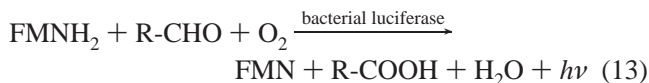
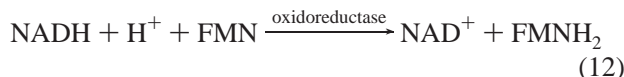


Both the intrinsic absorbance and fluorescence of NADH can be measured and enable optical detection of both substrates. In the GFOR-based biosensor,<sup>224</sup> the enzyme was



cross-linked with glutaraldehyde and placed between an optical fiber and a dialysis membrane. Glucose was sensed via the increase in fluorescence of the enzyme due to formation of NADH, and fructose was sensed via the decrease in fluorescence due to consumption of NADH. The system can be regenerated by passing fructose or glucose solutions, respectively, over it.

Apart from measurements of its intrinsic absorbance or fluorescence, NADH can be detected with much higher sensitivity via reactions 12 and 13, which are catalyzed by bacterial enzymes and result in blue–green bioluminescence:

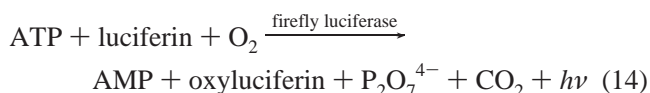


Here, FMN is flavine mononucleotide and R-CHO is a long-chained aldehyde, e.g., decanal. The emission of bioluminescence peaks at 490 nm.

Initially, biosensors for NADH only made use of enzymes immobilized onto a polymer support (a preactivated polyamide membrane), while the cofactor FMN and the long-chained aldehyde were added to the solution to be analyzed.<sup>225–229</sup> Attempts were made to design a self-contained biosensor that would not require the addition of coreactants and, therefore, would operate in a reagentless mode.<sup>230,231</sup> Hence, the flavine cofactor was noncovalently entrapped in a matrix of poly(vinyl alcohol), which allowed its controlled release in the vicinity of the immobilized enzymes. The method works well but the aldehyde needs to be continuously supplied to the reaction medium.

Oxidation of a substrate by a dehydrogenase-type of enzyme coupled to bioluminescent detection of NADH also was used for determination of the activity of lactate dehydrogenase<sup>232</sup> (lactate was supplied together with FMN and the aldehyde) and for analysis of sorbitol, ethanol, and oxaloacetate.<sup>233</sup> Compared to the ethanol biosensors based on direct detection of NADH and those using alcohol oxidase, the biosensor with coupled bioluminescent detection of NADH proved to be 1–2 orders of magnitude more sensitive, with a typical LOD being 0.4  $\mu\text{M}$ . At the same time, such a system is more complicated because it makes use of three enzymes and requires cosubstrates such as FMN and an aldehyde to be added.

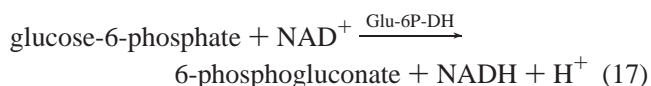
The luciferin/luciferase bioluminescent system with its  $\lambda_{\text{max}}$  of 560 nm was adapted to the determination of adenosine triphosphate (ATP). Oxidation of luciferin is catalyzed by firefly luciferase according to eq 14,



and results in green luminescence. As in the case of bioluminescent determination of NADH, biosensors for ATP are extremely sensitive (LODs are  $<1$  pmol). In earlier systems, luciferin again had to be added to the sample solution.<sup>228,229,234</sup> To overcome this inconvenience, a reagentless biosensor was designed.<sup>235</sup> Here, luciferin was incorporated into acrylic (Eudragit) microspheres entrapped in a film of poly(vinyl alcohol). Such a controlled-release system allowed the determination of ATP via firefly luciferase

entrapped in a collagen membrane, as well as that of adenosine monophosphate (AMP) and adenosine diphosphate (ADP) by entrapping two additional enzymes, adenylate kinase and creatine kinase, responsible for conversion of AMP and ADP into ATP. The sensitivity for ATP was significantly lower and the limit of detection was significantly higher (10 pmol) than for sensors using luciferin in solution.

ADP was also determined via the fluorescence of NADH that is formed in the following sequence of reactions<sup>236</sup> (eqs 15–17) that are catalyzed by the enzymes pyruvate kinase (PyKin), hexokinase (HexKin), and glucose-6-phosphate dehydrogenase (Glu-6P-DH):



ADP could be determined in concentrations as low as 0.1  $\mu\text{M}$ .

It was discovered recently that the europium tetracycline (EuTC) 1:1 complex can act as a luminescent probe for nucleoside phosphates including AMP, ADP, and ATP. The probe can be excited with the 405 nm laser diode and is nonspecific, but the response to the various phosphates is different. It has been applied to the determination of the activity of soluble kinases (which are important in high-throughput screening for new drugs).<sup>237</sup> The same group has used EuTC to monitor the activity of alkaline phosphatase or the efficiency of an inhibitor by determining the amount of phosphate released by the enzyme from phenyl phosphate.<sup>238</sup>

An overview on enzyme-based biosensors is given in Table 2 along with typical data of merit. In conclusion, it can be stated that most enzymatic biosensors (a) are fairly easy to fabricate; (b) do not require labeling but a transducer capable of detecting reaction products or coreactants; (c) are suitable for continuous analyte monitoring; (d) have moderate sensitivity and limits of detection; (e) are prone to poisoning; and (f) are thermally labile (with few exceptions) and frost-sensitive in aqueous solutions.

## 4. Immunosensors

### 4.1. General Remarks

Affinity biosensors make use of specific interactions between an antibody (Ab) and an antigen (Ag) or a hapten. Antibodies are large Y-shaped proteins ( $\sim 150$  kD) used by the immunosystem to identify and neutralize alien objects like bacteria and viruses. The affinity of Ag's to Ab's is very strong ( $K_a$   $10^{12}$ – $10^{14}$ ) but of strictly noncovalent nature. Binding of an antibody to its specific antigen can cause precipitation of the Ab–Ag complex, result in blocking of viral receptors, or mark the Ag for digestion by phagocytes. Smaller molecules such as pesticides or hormones often cause immune response only when attached to a large carrier such as a protein and usually are referred to as haptens. Antibodies to the hapten-carrier adduct produced by the body are able, however, to bind the hapten. It should be stressed that most

components of physiological pathways are not immunogenic, e.g., glucose, citrate, fatty acids, amino acids, and the like. Immunosensors are mainly used for determination of concentration of antigens or haptens or, alternatively, for sensing antibodies because their presence can indicate an infection.

We differentiate between *immunoassays* (performed in solution and not treated here except for certain examples) and *immunosensors* (on solid supports). The latter are treated here but actually are not sensors in their strictest definition because they are not capable of continuously and reversibly recording a parameter. Solid-phase immunoassays make use of a recognition element (Ab or Ag) immobilized on the surface of an inert support which, however, also may act as an optical fiber or a planar waveguide.

Despite the fact that a binding event between an antibody and an antigen is reversible and noncovalent, most immunoreactions are irreversible in practice because of very large association constants and very slow dissociation rates. As a result, practically all immuno“sensors” are suitable for a single measurement only. This makes calibration difficult and requires an enormous reproducibility in manufacturing. Given this, attention has been paid to the regeneration of sensors (e.g., by washing with solutions of high osmolarity, high ionic strength, or low pH), which allows for multiple measurements with a single sensor. However, regeneration procedures do not always result in full recovery of the activity. In recent years, a number of devices were developed that made possible simultaneous detection of several analytes performed automatically.

## 4.2. Immunosensor Formats

The most widely used formats are illustrated in Figure 4, where the upper panel represents the situation before immunobinding has occurred and the lower panel represents the situation after it. A selection of immunosensors for various analytes is presented in Table 3.

### 4.2.1. Direct Immunosensors

These sensors are fairly straightforward but have been reported for a limited number of analytes only.<sup>43,44,66–68,72,239–248</sup> The sensing format is schematically shown in Figure 4. An unlabeled antigen binds to an unlabeled antibody. Interferometric readout is common since it has the advantage of not requiring a label.<sup>66–68</sup> The change of refractive index, however, is much smaller than in a fluorescent or radiolabel sandwich format (Figure 3c) because antigens and particularly haptens possess relatively low molecular mass. The intrinsic fluorescence of benzo[*a*]pyrene tetraol (BTP) was used as analytical information; the anti-BTP antibodies were immobilized onto silica microbeads.<sup>239,240</sup> The optical signal of such single-shot probes is directly proportional to the amount of BTB captured. The LOD is 0.5 nM. Another example is represented by a biosensor for human serum albumin (HSA).<sup>241</sup> When HSA binds to dansyl-labeled antibody attached to the surface of an optical fiber, an increase in fluorescence is observed because the antigen shielded the label from quenching water molecules. Engström et al.<sup>249</sup> observed an enhancement of the intrinsic UV fluorescence of tryptophan of monoclonal mouse antibodies immobilized on the surface of a quartz slide upon binding maltose and panose (a rather rare triglucoside). The low affinity of the antibodies for the saccharides enabled a virtually reversible sensing, with no need for sensor regeneration. The analytical range was from 0 to 8 mM of the

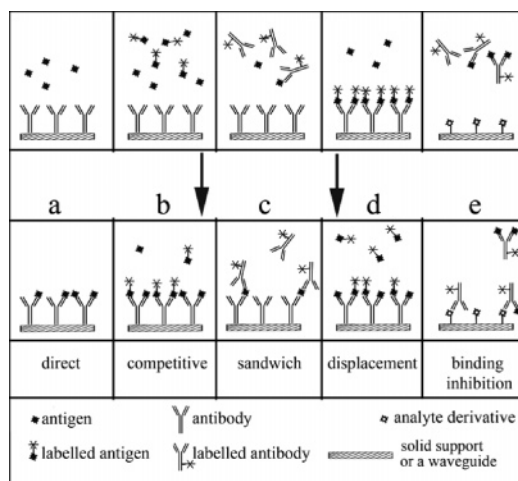


**Figure 4.** Typical formats of heterogeneous optical immunoassay; situations before (upper part) and after equilibration (lower part). The enzyme-linked immunosorbent assay (ELISA) in practically all cases is a modification of the sandwich method as it makes use of an enzyme as a label. Thus, it requires a subsequent enzymatic reaction to produce a colored or fluorescent product whose concentration can be determined, usually in solution and not on the surface of the sensor.

respective saccharides, and the LODs were 5 and 15  $\mu\text{M}$ , respectively, for panose and mannose. Reck et al.<sup>250</sup> reported a homogeneous immunoassay for thyroxine hormone. Quenching of the intrinsic fluorescence of the thyroxine-binding globulin was observed upon binding the thyroxine. Although the initial response was achieved after 5 min of incubation, almost 2 h were needed until the system reached saturation. The main drawback of this approach is its low sensitivity, since the LOD was found to be  $\sim 100$ -fold higher than the concentration of free thyroxine in serum. Other fluorescent immunosensors used in the direct format<sup>242–245</sup> can only serve as model systems, since labeling of the analyte is necessary in the case of the assay, which is difficult (or even impossible) for real samples.

### 4.2.2. Competitive Immunosensors

In this format (see Figure 4b),<sup>41,42,49,246,251–261</sup> an unlabeled antigen (the analyte) and its labeled form compete for a limited number of binding sites of the immobilized antibody. Fluorescence intensity is inversely proportional to the amount of the analyte concentration. The application of the methods requires a labeled antigen to be available. The method can be inverted to enable the detection and assay of antibodies via the competitive binding of labeled and unlabeled antibodies, respectively, to an immobilized antigen.<sup>262</sup>

### 4.2.3. Sandwich Immunosensors

Such assays (Figure 4c)<sup>60,243,261,263–272</sup> are widely used and require relatively large antigens that contain at least two epitopes (the site of a macromolecule that is recognized by an antibody) for the antigen to be bound to the immobilized capture antibody and to the labeled second antibody. Fluorescence intensity is proportional to the concentration of the fluorescently labeled antibody, which, in turn, is related to the concentration of the antigen. Two different protocols are usual. In the “stepwise” protocol, the antigen and fluorescently labeled second antibody are added sequentially to the biosensor. In the “premixed” protocol, the antigen and antibody are premixed before injection into the biosensor. The stepwise protocol is said to give a significantly higher

**Table 3. Overview of Immunosensors (Acronyms Used for Schemes: FI, Fluorescence Intensity; FRET, Fluorescence Resonance Energy Transfer; LL, Luminescence Lifetime; RI, Refractive Index)**

analyte	assay format	analytical range	LOD	scheme	label	material	assay time	ref
human serum albumin (HSA)	direct	0–9 mg/L	?	FI	dansyl/anti-HSA attached to fiber		30 min	241
anti-rabbit IgG	direct	0.011–0.11 g/L	0.011 g/L	FI	FITC/anti-rabbit IgG	rabbit IgG on silica beads	?	244
BTP	direct	1–100 nM	0.5 nM	intrinsic FI		anti-BTP IgG on silica beds (7 μm)	45 min	239, 240
protein A	direct	10–250 nM	20 nM	FI	FITC/protein A	human IgG on an ion exchange waveguide	?	245
anti-goat IgG	direct	0.3–10 mg/L	0.3 mg/L	FI	FITC/anti-rat IgG	goat IgG on a patterned waveguide	30 min	242
IgG	direct	0–5 mg/L	?	FI	Q-dot/protein A on optical fiber		10 min	44
trinitrobenzene	direct	1–8 μg/L	1 μg/L	FI	Cy-5/trinitrobenzol	anti-TNT IgG on a waveguide	5 min	246
PSA	direct	1–100 μg/L	0.5 mg/L	FI	allophycocyanin/anti-PSA antibody		?	247
LDH	direct	0.125–5.0 mg/L	0.03 mg/L	FI	FITC/LDH	anti-LDH IgG on fiber	4 min	243
hemoproteins	direct	10 nM–10 μM	?	FI & FRET	FITC labeled anti-hemoprotein IgG on LB monolayer		30 min	248
<i>Salmonella typhimurium</i>	direct	?	1.03 × 10 <sup>5</sup> cfu/L	ratio of FI	complex of Alexa Fluor 546/anti-Salmonella IgG and Alexa Fluor 594/protein G on optical fiber; FRET		5 min	43
anti-rabbit IgG	competitive	0–150 nM	8 nM	FI	FITC/anti-rabbit IgG	rabbit IgG on fiber	20 min	262
phenytoin	competitive	1–20 μM	1 μM	FI & FRET	Texas red/anti-phenytoin IgG	phycoerythrin-phenytoin; semipermeable membrane	15 min	41
theophylline	competitive homogeneous	0–300 μM	?	FI & FRET	Texas red/anti-theophylline IgG	phycoerythrin–theophylline in a well with semipermeable membrane	15 min	42
inazethapyr	competitive	1 nM–1 mM	1 nM	FI	aminofluorescein /inazethapyr	sheep anti-inazethapyr IgG on fiber	2 min	252, 253
atrazine	competitive	0.5–200 nM	0.5 nM	FI	fluorescein/atrazine	anti-atrazine IgG on fiber	10 min	254
human IgG	competitive	10 <sup>-4</sup> –10 <sup>-1</sup> g/L	?	FI	FITC/rabbit IgG	anti-human IgG on waveguide	15 min	255
cocaine	competitive	0.01–1 μM	5 μg/L	FI	fluorescein and benzoylecgonine	anti- benzoylecgonine IgG on fiber	15 min	256
CCA	competitive	0.1 nM–1 μM	?	FI	fluorescein/CCA	anti-CCA IgG on fiber	20 min	258
TNT	competitive	10–1000 μg/L	10 μg/L	FI	Cy-5-labeled TNT sulfonate	anti-TNB IgG on fiber	4 min	257
TNT	competitive	1–1000 μg/L	5 μg/L	FI	Cy-5/EDTA-TNB	anti-TNT IgG on fiber	5 min	259
TNT	competitive	20–200 μg/L	20 μg/L	FI	Cy-5/trinitrophenyl	anti TNT IgG on waveguide	5 min	246
RDX	competitive	1–100 μg/L	2.5 μg/l	FI	Cy-5/EDTA-RDX	anti-RDX IgG on fiber	5 min	259
TCPB	competitive	50 μg/L–10 mg/L	10 ppb	FI	fluorescein/TCPB	anti- polychlorinated biphenyls IgG on fiber	20 min	260
theophylline	competitive	1–50 mg/L	?	FI	Cy-5/theophylline	anti-theophylline IgG on waveguide	5 min	261
hCG	sandwich	0–50 nM	?	FI	FITC/anti-hCG IgG	anti-hCG IgG on waveguide	2 min	263
<i>Clostr. botulinium</i> toxin A	sandwich	0.03–1.2 nM	30 pM	FI	TRITC/ anti-botulinium toxin A IgG	anti-botulinium toxin A IgG on fiber	2 min	264, 265
ASF protein	sandwich	1.5–200 mg/L	2 mg/L	FI	FITC/anti-AFS IgG	anti-AFS IgG on Immobilon membrane	40 min	266
human IgG	sandwich	10–100 μg/L	?	FI	NIR dye1/goat anti-human IgG	goat anti-human IgG on PMMA droplet on fiber	30 min	267
mouse IgG	sandwich	40–300 ng/L	40 ng/L	FI	Cy-5/anti-mouse IgG	anti-mouse IgG on capillary	20 min	271
LDH	sandwich	0.1–10 mg/L	0.03 mg/L	FI	FITC/anti-LDH IgG	anti-LDH IgG on fiber	4 min	243
<i>Salmonellax typhimurium</i>	sandwich	3 × 10 <sup>7</sup> –3 × 10 <sup>11</sup> cfu/L	10 <sup>7</sup> cfu/L	FI	Cy-5/anti-Salmonella IgG	anti-Salmonella IgG on fiber	60 min	268
ricin	sandwich	0.1–250 μg/L	100 ng/L	FI	Cy-5/anti-ricin IgG	anti-ricin IgG on fiber	15 min	269
SEB	sandwich	0–1 mg/L	10 μg/L	FI	Cy-5/anti-SEB IgG	anti-SEB IgG on PS waveguide	10 min	270
SEB	sandwich	30–400 ng/L	30 ng/L	FI	Cy-5/sheep anti-SEB IgG	sheep anti-SEB IgG on a capillary surface	20 min	271
hCG	sandwich	1–1000 μg/L	1 μg/L	FI	Cy-5/anti-hCG IgG	anti-hCG IgG on waveguide	5 min	261
TNT	sandwich	5–30 μg/L	5 μg/L	FI	Cy-5/anti-TNT IgG	anti-TNT IgG on waveguide	15 min	246
mouse IgG	sandwich	0.5–25 μg/l	0.5 μg/L	LL	GOx/anti-mouse IgG	mouse IgG on PtOEPK/PS layer	1 h	60
LDH	sandwich	2.5–10 μg/L	2.5 μg/L	LL	GOx/anti-LDH	LDH on PtOEPK/PS layer	1 h	60
TNT	displacement	10–50 μg/L	10 μg/L	FI	Cy-5/trinitrophenyl	anti-TNT IgG on waveguide	5 min	246



Table 3 (Continued)

analyte	assay format	analytical range	LOD	scheme	label	material	assay time	ref
pacitaxel	displacement	1–100 $\mu\text{g/L}$	1 $\mu\text{g/L}$	FI	Rhodamine/pacitaxel	anti-pacitaxel on a capillary	2 min	273
terbutryn	binding inhibition	0–10 $\text{mg/L}$	0.1 $\text{mg/L}$	FI	FITC/anti-triazine IgG	aminohexyltriazine on fiber	1 h	274
terbutryn	binding inhibition	20–200 $\text{mg/L}$	15 $\text{mg/L}$	RI	anti-triazine IgG	aminohexyltriazine on fiber	30 min	275
atrazine	binding inhibition	0.1–1 $\text{mg/L}$	0.25 ppb	RI	mouse anti-atrazine IgG	atrazine on the interference layer	10 min	69
atrazine	binding inhibition	0.1–1000 $\mu\text{g/L}$	?	FI	Cy-5.5/anti-atrazine IgG	atrazine derivative on waveguide	20 min	276
atrazine	binding inhibition	0.35–1.47 $\mu\text{g/L}$	0.16 $\mu\text{g/L}$	FI	Cy-5.5/anti-atrazine IgG	atrazine derivative on waveguide	15 min	277
isoprotruron	binding inhibition	0.11–2.83 $\mu\text{g/L}$	0.05 $\mu\text{g/L}$	FI	Cy-5.5/anti-isoprotruron IgG	isoprotruron derivative on waveguide	15 min	277
estron	binding inhibition	0.17–10.7 $\mu\text{g/L}$	0.08 $\mu\text{g/L}$	FI	Cy-5.5/anti-estron IgG	estron derivative on waveguide	15 min	277
2,4-D	binding inhibition	0.3–10 $\mu\text{M}$	?	FI	Cy-5/anti-2,4-D	2,4-D on fiber	15 min	279
2,4-D	binding inhibition	0.07–1.8 $\mu\text{g/L}$	0.03 $\mu\text{g/L}$	FI	Cy-5/anti-2,4-D	dichloroanilineglutaric acid on waveguide	15 min	280
paraquat	binding inhibition	0.01–100 $\mu\text{g/L}$	10 $\text{ng/L}$	FI	Cy-5.5/anti-paraquat IgG	paraquat derivative on waveguide	15 min	281
testosteron	binding inhibition	0.2 $\text{ng/L}$ –100 $\mu\text{g/L}$	0.2 $\text{ng/L}$	FI	Cy-5.5/anti-testosterone IgG	testosterone derivative on waveguide	12 min	282

response than the premix protocol. Typical examples of fluorescent sandwich assays are listed in Table 3.

Gold nanoparticles may be used to enhance the fluorescence signal of a labeled antibody. Hong et al.<sup>272</sup> have designed a biosensor operating in a sandwich format by immobilizing protein C antibody, protein C, and secondary antibodies that were labeled with Cy-5 and Alexa Fluor 647. Their signal was typically enhanced by 10–200% when gold nanobeads were added. Self-assembled nanolayers (SAMs) can be used to control the distance between the nanobeads and the labeled antibodies. Maximal enhancement of the signal was achieved with SAM thicknesses of 2 nm. It was also found that using ethanol instead of water resulted in an up to 10-fold enhancement of fluorescence intensity.

#### 4.2.4. Displacement Immunosensors

This less common format (Figure 4d)<sup>246,273</sup> requires an initial saturation of all the antibody binding sites with a fluorescently labeled antigen. Upon introduction of the unlabeled antigen, displacement of the labeled antigen occurs and is measured in this sensor as a decrease in the fluorescence intensity. It needs to be kept in mind that the “sensor” only works if the reaction rates of displacement are adequately fast. In fact, such sensors usually are quite slow.

#### 4.2.5. Immunosensors Based on Binding Inhibition

In contrast to other formats, such sensors (Figure 4e)<sup>69,70,274–282</sup> require immobilization of an unlabeled analyte derivative on the surface of a waveguide. In the absence of the antigen, the labeled antibody can bind to the surface. Binding is inhibited, however, in the presence of the analyte because it blocks the binding sites (paratopes) of the antibody. For the binding inhibition assay to be quantitative, the number of high-affinity binding sites on the surface has to be much higher than the number of labeled antibodies in the bulk solution. If an antigen or an antibody is immobilized on a solid surface, the flexibility of the system becomes limited. More flexible sensors can be prepared by immobilization of an arbitrarily chosen ligand (antigen) on the surface.<sup>276</sup> Different analyte derivatives that are conjugated to an antibody can be then attached to the ligand for assay operation in the binding-inhibition format.

#### 4.2.6. Comparative Study on Immunosensor Formats

Snapsford et al.<sup>246</sup> compared the performance of four immunoassay formats (direct, competitive, sandwich, and displacement) that can be used for determination of 2,4,6-trinitrotoluene (TNT). Anti-TNT was attached to waveguide surface via avidin–biotin linkage. Cy-5-labeled trinitrobenzene was used in direct, competitive, and displacement assay formats, and Cy-5-labeled antibody was used in a sandwich format. While TNT itself is unsuitable for detection using the sandwich assay format, it was conjugated to ovalbumin (OVA), so that the OVA–TNT complex can be bound not only to the antibody attached to the waveguide but also to the tracer antibody. Each assay format resulted in different LODs and dynamic ranges. The LOD was the lowest in the direct assay (1  $\mu\text{g/L}$ ); however, it also had the narrowest dynamic range (1–8  $\mu\text{g/L}$ ). On the other hand, the dynamic range was the widest in the competitive assay (20–200  $\mu\text{g/L}$ ), but it had the highest LOD (20  $\mu\text{g/L}$ ). The LODs in the displacement and sandwich assay formats were 10 and 5  $\mu\text{g/L}$ , respectively. While 15 min was required to perform the

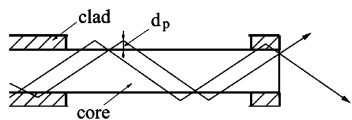


**Figure 5.** Principle of the total internal reflection fluorescence in an optical fiber waveguide. On reflection at dielectric interface, light penetrates into the second phase that has a lower refractive index than that of the core. Intensity decreases exponentially over the penetration depth  $d_p$  (which typically is about as long as the wavelength of the light employed). Any labeled antibodies located in the declad zone within  $d_p$  are excited to produce fluorescence, while those located outside this distance will not.

two-step sandwich assay, the other assays required only 5 min. It was also shown that complete regeneration of the sensor was possible within 2 min by passing a regeneration buffer containing 50% ethanol over the sensor layer. No loss of activity was observed after 10 regeneration cycles.

### 4.3. Preferred Optical Readout Formats in Immunosensing

#### 4.3.1. Conventional Readout Formats

In the most simple version, immunosensor spots on glass, metal, or plastic supports are read out by either absorption, fluorescence, interferometry, various methods of polarization spectroscopy, or surface plasmon resonance (treated elsewhere).<sup>283</sup> They can be combined with methods of optical spectroscopy. Fluorescence intensity serves as the analytical parameter in most immunosensors (see Table 3) and is mostly read at a single wavelength, but this may cause difficulties in measuring reproducible data. According to Parker's law (see section 2.4), luminescence intensity depends not only on the concentration of the fluorophore but also on other variables such as the intensity of the exciting light and the geometry of the experimental arrangement. Self-referenced methods, where the latter parameters are being referenced out, are, therefore, preferred.

Measurement of intensity at two wavelengths (e.g., after addition of a reference dye or by making use of fluorescence resonance energy transfer from a donor fluorophore to an acceptor fluorophore) is one common self-referenced method. Solution immunoassays often are performed by measuring polarization, but less often in solid-state devices for obvious reasons. The measurement of fluorescence decay time represents another, albeit less common, self-referenced method.

#### 4.3.2. Evanescent Wave, Capillary, and Other Readouts

It was recognized rather early that the solid supports required in biosensors also may act as optical components. Evanescent wave spectroscopy (EWS) has become particularly useful and is often applied in immunosensors (which contrasts the situation in the case of enzymatic biosensors). EWS can be performed in various ways, but total internal reflection fluorescence (TIRF) is, by far, the most often applied. A schematic of how TIRF works is shown in Figure 5. Light transported by a waveguide (here, an optical fiber) excites the fluorescence of a label on its surface only within the evanescent field. This has several advantages: (a) the unbound labeled species in solution remain unexcited and, thus, do not form a background signal; (b) measurements can be performed in absorbing or turbid media such as most biological solutions; and (c) background fluorescence of the serum can also be largely reduced.

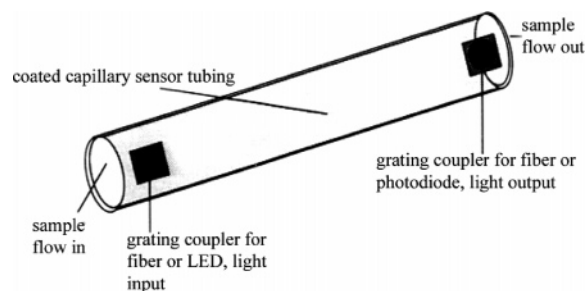


**Figure 6.** Capillary flow sensor. The capillary acts (a) as a sample compartment (or flow-through cell); (b) as an optical waveguide; and (c) as the solid support for immobilized antibodies. Light is coupled into and out of the capillary through grating couplers. Antibodies are deposited on the inner surface of the capillary. The fluorescence of labeled antibodies or antigens is interrogated by the evanescent wave mode. Reprinted with permission from Weigl, B. H.; Wolfbeis, O. S. *Anal. Chem.* **1994**, *66*, 332. Copyright 1994 American Chemical Society.

In contrast to surface plasmon resonance and interferometric sensors, the response of TIRF immunosensors does not depend on the mass of an analyte, which makes possible detection of even small haptens. If planar waveguides are used, the fluorescence is typically collected perpendicularly to the surface of the waveguide. In most fiber-optic biosensors, the emission is, however, collected at the distal end of the optical waveguide, as shown in Figure 5.

The use of capillaries<sup>284,285</sup> for optical immunosensing is very attractive because a capillary can not only guide fluid but also light in its wall (see Figure 6). Usually, the excitation light is introduced at the end of the capillary and propagates on the inner surface as an evanescent wave. When the evanescent excitation generates a signal from an antigen–antibody–fluorophore complex, the emitted light is coupled into and propagates along the capillary. At the distal end, a grating can be used to couple the light out of the waveguide into a photodetector. When the active surface area is increased inside the capillaries, the fluorescence signal integrates over their length, but the electronic background noise remains constant. Sensitivity of the sensor, thus, is significantly improved.

The group of Seeger<sup>71</sup> has designed an immunosensor that exploits changes in the supercritical angle of the fluorescence (SAF) of molecules bound to a glass surface. Because the detection volume in the aqueous sample is significantly reduced in this technique, bulk (i.e., background) fluorescence from solution is strongly suppressed. The SAF signal can be captured by a parabolic glass lens, thus leading to high spatial collection efficiency and detection sensitivity. As little as 2 pM concentrations of labeled rabbit IgG could be detected in a direct immunoassay format. The sensitivity could be further improved by using tight focusing and smaller excitation spots. In this case, however, rapid photobleaching is a serious limitation. On the other side, spot diameters of 60  $\mu\text{m}$  allow for up to 200 measurements with photodegradation not exceeding 1%. This is more than adequate to obtain a smooth response plot. The group also reported on a confocal reader for biochip screening and fluorescence microscopy.<sup>286</sup>

### 4.4. Immobilization of Antibodies on Sensor Surfaces, and Nonspecific Protein Binding

There are several widely used methods for immobilization of large proteins such as antibodies on solid support. One is

based on the creation of a covalent linkage between the support and the protein, often via a spacer group. The surface of a support is rendered reactive with groups such as  $-\text{COOH}$ , maleinimide,  $-\text{NH}_2$ , or, less often, iodoacetamide groups, isothiocyanate groups, or boronic acid. These can be reacted with amino groups, thiol groups, carboxy groups, or saccharide groups of antibodies to form covalent chemical bonds. Glass surfaces and metal oxide nanoparticles are often derivatized using silyl reagents (aminopropyltrimethoxysilane being a typical example), while gold surfaces are derivatized with thiolated reagents of the type  $\text{HS}-(\text{CH}_2)_n-\text{X}$ , where X is one of the reactive groups given before. Such thiols readily bind to gold to form self-assembled monolayers on its surface. Quantum dots based on metal (Zn, Cd) sulfides and selenides also are surface-modified first by making use of an appropriate thiol chemistry. Plastic materials are more difficult to derivatize unless they contain intrinsic chemical groups such as in the poly(acrylonitrile-co-acrylic acid) copolymers.<sup>287</sup>

Another important method is based on the strong affinity of biotin to (strept)avidin.<sup>67, 68, 246, 270, 288</sup> Neutravidin also has been used recently.<sup>289–291</sup> They all have four binding sites for biotin. Typically, the surface of a biosensor is modified (as described in the previous paragraph) by introducing biotin groups, in the overwhelming majority by using di- or tri-(ethylene glycol)-modified biotin of the chemical structure



(where  $n = 2$  or  $3$ ). Any protein that has been modified with (strept)avidin will strongly bind to such a surface. The affinity (binding) constants of the resulting noncovalently linked conjugates are in the order of  $10^{12}$  to  $10^{14}$  depending on the protein and the surface (or particle) used. One may wonder why the rather affordable avidin (a glycoprotein) is used so much less often than the rather expensive streptavidin (not a glycoprotein). On the other side, streptavidin has an isoelectric point (pI) of 5 and is less prone to nonspecific binding as compared to avidin with its pI of 10.5.

Proteins also can be immobilized via a polyhistidine tag. The method is based on an amino acid motif in proteins that consists of at least six histidine (His) residues. It also is known as hexahistidine tagging, or 6xHis-tag, or by the tradename His-tag. The polyhistidine tag can be used for the immobilization of proteins on a nickel- or cobalt-coated microtiter plate, on glass, or on another protein. The most simple way to add a poly-His unit to a protein is to insert a protein DNA in a vector encoding a His-tag so that it will be automatically attached to one of its ends. The other technique is to perform a PCR with primers that have repetitive histidine codons next to the start or stop codon in addition to several (16 or more) bases encoding specifically to the protein to be tagged.

Another widely used method (with particular applicability to the immobilization of antibodies) is based on the use of protein A. This is a 40–60 kD surface protein that strongly binds to immunoglobulins from many mammalian species. Specifically, it binds to the Fc region through interaction with the heavy chain and, thus, does not strongly compromise its affinity to the respective antibody.

Shriver-Lake et al.<sup>292</sup> investigated different heterobifunctional cross-linkers for covalent attachment of antibodies through thiol-terminated silanes onto glass, silica, silicone, and other surfaces. A variety of cross-linkers were found to be suitable for effective immobilization of antibodies. The

use of carbohydrate-reactive cross-linkers resulted in immobilized antibodies having higher activities than when using reactive succinimide residue but required a more complex procedure, which implied the risk of denaturation of some antibodies.

Preininger et al.<sup>293</sup> have investigated three different types of polymer supports used for immobilization of antigens and antibodies with respect to specific binding and nonspecific binding (NSB, better referred to as nonspecific adsorption) and regeneration of the sensor. Interaction of rhodamine-labeled anti-human IgG with immobilized human IgG was used in a direct assay format for investigation of specific binding. The degree of NSB was determined using anti-human IgG and was found to be quite high ( $\sim 80\%$  of the level of specific binding) for human IgG immobilized onto a sol-gel support. Carboxylated poly(vinyl chloride) (PVC) support showed  $\sim 50\%$  of nonspecific absorption, while the NSB to polystyrene was negligible. However, only 35% of initial signal was regenerated when polystyrene support was used, while the regeneration level of 50% was possible for carboxy-modified PVC.

Liu et al.<sup>294</sup> have shown that, when using polystyrene fibers, the extent of NSB can be significantly reduced by introducing a spacer between the polystyrene surface and the photoimmobilized antibody. Poly(ethylene glycol) cross-linkers with five ethylene glycol units decrease the degree of NSB dramatically, and additional treatment of the surface with BSA eliminates it completely. The authors also showed that the “stepwise” protocol of sandwich assay formats resulted in a much higher sensitivity than when using the more convenient “premix” protocol.

NSB also can be significantly reduced by using a dextrane linker.<sup>295</sup> Carboxymethylated dextrane was attached to the surface of a fiber-optic waveguide whose surface was treated with aminopropyltriethoxysilane; this was followed by carboxamide formation using activation with EDC and formation of a reactive NHS ester.

The same method was applied to covalently immobilize an antibody to dextrane. The amount of NSB was shown to be only 2% of the level obtained for the untreated glass chip. Different immobilization techniques for glass fibers were investigated by Tedeschi et al.<sup>296</sup> Immobilization of antibodies via glycidyoxypropyl-trimethoxysilane-dextrane resulted in the highest density of active sites.

The Langmuir-Blodgett (LB) technique represents an alternative for immobilization of antibodies.<sup>255</sup> Protein A has a specific affinity for a specific section of IgG and can be prepared as a stable monolayer by the LB film technique. Such a monolayer was immobilized on an alkylsilanized hydrophobic synthetic quartz plate. Anti-human IgG antibody was self-assembled on the protein A film. Rabbit IgG labeled with fluorescein isothiocyanate was used in a competitive assay for determination of human IgG over the analytical range from  $10^{-4}$  to  $10^{-1}$  g/L. Anderson et al.<sup>297</sup> showed that the sensitivity of fluorescent immunoassays for determination of antigens was similar when the antibody was covalently attached to the support or via protein A.

## 4.5. Specific Examples of Immunosensors

### 4.5.1. Biosensors for Proteins and Antibodies

Barnard and Walt<sup>251</sup> developed a kind of reversible immunosensor for continuous measurements of IgG over a prolonged period of time using a controlled-release system. The fluorescein-labeled antibody and the Texas Red-labeled



antigen were separately incorporated into an poly(ethylene-co-vinyl acetate) matrix, allowing for controlled release of the components. The analyzed IgG from the media and the two released biocomponents diffuse into the reaction chamber, where the competitive immunoreaction occurs. FRET is observed in the absence of IgG but is suppressed once the complex between fluorescein-labeled antibody and unlabeled IgG has been formed. Fluorescence intensity is monitored with the help of an optical fiber located above the reaction chamber. The steady-state rate of release is achieved after 2 days, allowing continuous monitoring of 0–500 mg/L of IgG over a period of 1 month. The approach, thus, can be applied to situations where continuous monitoring of analyte is required over prolonged periods of time and where rapid response (limited here by the diffusion of the analyte from the bulk solution or the release rate) is not an issue.

Lepesheva et al.<sup>248</sup> developed a FRET assay for hemoproteins in the analytical range from 10 nM to 10  $\mu$ M. In the direct biosensor, fluorescein-labeled anti-hemoprotein IgG was absorbed onto a LB monolayer contained on a quartz support. Fluorescence intensity decreased in the presence of hemoprotein as the result of the quenching of the fluorescence of the label by heme.

Luminescent quantum dots are viable optical markers<sup>44</sup> and have been used in a direct assay for IgG. Protein A was labeled with CdSe/Zn Q-dots with a fluorescence  $\lambda_{\max}$  of 655 nm and then was immobilized at the tip of an optical fiber. Once the immunoreaction with IgG occurs, a decrease in fluorescence intensity is observed as a result of FRET from the Q-dot to the bound protein.

Enzyme-linked immunosorbent assays employ enzymes as labels. Several attempts were made to design biosensors based on the use of enzyme labels. Papkovsky et al.<sup>60</sup> demonstrated the feasibility of an enzyme-linked biosensor with the IgG–anti-IgG model system. Mouse IgG antigen was absorbed onto a surface of a glass fiber membrane combined with an optical oxygen transducer (a phosphorescent metalloporphyrin contained in polystyrene). Mouse IgG was detected in a sandwich ELISA using anti-mouse IgG antibodies labeled with glucose oxidase (GOx) as the secondary antibody. The amount of the antigen was quantified by measurement of the consumption of oxygen that results from the enzymatic reaction in the presence of glucose. The (rather long) luminescence decay time of the oxygen probe was monitored. This is in contrast to immunosensors based on the measurement of fluorescence intensity. A glass cover was used to limit oxygen access, and this significantly improved sensitivity, the LOD being 0.5  $\mu$ g/L. Lactate dehydrogenase (LDH) was detected analogously using anti-LDH antibodies labeled with GOx. As little as 2.5  $\mu$ g/L (=10 pM) of LDH could be sensed. The assay time was 1 h.

Kim et al.<sup>298</sup> made use of microbeads (made from a modified acrylamide) of  $\sim$ 1  $\mu$ m diameter that were assembled onto an amino-functionalized glass surface. A network of biotin and anti-biotin couples was attached to the beads (that also act as microlenses) via photopolymerization with aminobenzophenone. In the absence of the analyte, the immobilized antigens and antibodies interact with each other, which results in microspheres that are in the “on”-state (Figure 7). The interactions between the attached antigens and antibodies are disrupted when a sample containing antigen (biocytin) is introduced. The microlenses are transformed from the “on”-state to the “off”-state as a result

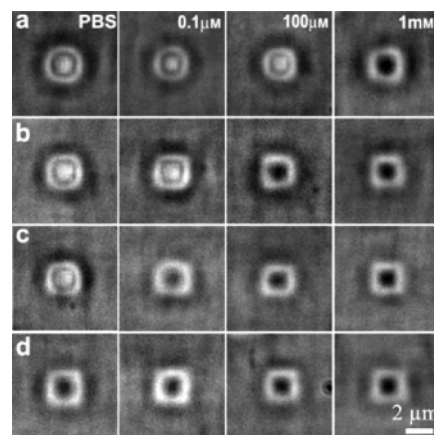


**Figure 7.** Microscope images of a microlens-based optical immunosensor array. Its sensitivity can be tuned by changing the concentration of the antibody used in the cross-linking stage. The concentrations of antibody were (a) 6.7  $\mu$ M, (b) 2  $\mu$ M, (c) 1  $\mu$ M, and (d) 0.6  $\mu$ M. With decreasing concentrations of antibody, the microlenses are inverted at lower concentration of biocytin. Reprinted with permission from Kim, J.; Singh, N.; Lyon, L. A. *Angew. Chem., Int. Ed.* **2006**, *45*, 1446. Copyright 2006 Wiley.

of gel swelling once the concentration of the analyte exceeds a certain critical value. The changes can be monitored microscopically.

The sensitivity can be tuned by changing the concentration of the antibody used in the photochemical cross-linking stage. When the hydrogel microlenses are prepared with an excess of binding pairs above the critical point, they swell only after a suitably large number of displacement events have occurred. However, if the number of cross-linked units is just slightly above this critical point, only a few displacement events will result in gel swelling. The system was demonstrated to be fully reversible as the microlenses return to the initial “on” state when the antigen is removed by washing the sensor with phosphate-buffered saline.

#### 4.5.2. Biosensors for Toxins

In the integrating capillary biosensor described by the group of Ligler et al.,<sup>271</sup> antibodies (anti-mouse IgG or sheep anti-staphylococcal enterotoxin B (SEB) were coated onto the entire inner surface of the capillary. Immunosensing of mouse IgG and SEB was accomplished in a sandwich format using antibodies labeled with Cy-5. Compared to conventional fiber-optic biosensors and planar waveguide-based about  $\sim$ 2 orders of magnitude (40 and 30 ng/L for IgG and SEB, respectively). The analytical range of the sensor is from 40 to 300 and from 30 to 400 ng/L of IgG and SEB, respectively. Moreover, multianalyte detection can be attained by passing the sample through multiple capillaries, each coated with a different antibody, either sequentially or in parallel, depending on the amount of sample available.

An ELISA type of biosensor for antibodies against cholera toxin B (CTB) was developed by Konry et al.<sup>299</sup> An electroconductive surface was created on a fiber-optic waveguide by coating it with indium tin oxide to allow surface electropolymerization of biotin–pyrrole monomers. Biotin-conjugated CTB was attached to the surface using avidin. Anti-CTB was quantified via a competitive assay format in which the sensor was incubated first with the analyzed antibodies and then with goat anti-rabbit IgG labeled with horseradish peroxidase. Fibers were then immersed into a solution of luminol and oxidizing agent (a standard kit), and chemiluminescence was monitored. The

LOD of the sensor is said to be  $1 \times 10^6$  "titers". The total assay time was 65 min. In another biosensor for anti-CTB, the antigen was attached to the surface of the optical fiber via a photoreactive benzophenone derivative,<sup>300</sup> and the same LOD was achieved. An analogous system was developed for detection of antibodies against anti-West Nile virus IgG,<sup>301</sup> and the LOD was similar. A 2-fold increase in sensitivity was observed compared to a chemiluminescent ELISA, presumably because light emission occurs near the optical fiber, which enhances the efficiency of light collection.

#### 4.5.3. Biosensors for Drugs

A capillary displacement-type immunosensor for the drug paclitaxel was designed by Sheikh and Mulchandani.<sup>273</sup> The anti-paclitaxel antibodies were attached via protein A to the silanized inner walls of a glass capillary, and the binding sites were saturated with rhodamine-labeled paclitaxel. Although fluorescence intensity of the displaced labeled antibodies was monitored in another chamber, thus taking no advantage of the light-guiding properties of the capillary itself, the sensor still proved to be very sensitive. In fact, the detection limits were 1 and 4 ng/mL at flow rates 0.1 and 1 mL/min, respectively. The assay time ranged from 2 min at 1 mL/min to 8 min at 0.1 mL/min. Moreover, the regeneration of the capillary column was possible without affecting the performance of the biosensor.

Anderson and Miller<sup>41</sup> developed a homogeneous immunoassay for the anticonvulsant drug phenytoin where B-phycoerythrin-labeled phenytoin and Texas Red-labeled antibody were contained in a 200  $\mu\text{m}$  cellulose dialysis tube connected to the distal end of an optical fiber (see Figure 8). The two species form a complex in which fluorescence resonance energy transfer (FRET) occurs from phycoerythrin to Texas Red. The interaction thus results in the quenching of the fluorescence of phycoerythrin. Phenytoin is small enough to diffuse through the dialysis membrane, where it displaces some of the phycoerythrin–phenytoin conjugates in the complex. The increase in the fluorescence of phycoerythrin is, thus, proportional to the concentration of phenytoin. This biosensor, notably operating in a fully reversible way(!), was suitable for determination of phenytoin with an LOD of 5  $\mu\text{M}$  and a measurement time of 15 min. Later, the system was optimized to detect phenytoin in concentrations as low as 1  $\mu\text{M}$ .<sup>49</sup> A similar system was used for determination of theophylline.<sup>42</sup> This biosensor design is of wider interest because full reversibility is achieved. However, the system is applicable only to antibodies having high reverse rate constants, which is not usually the case (see Figure 8).

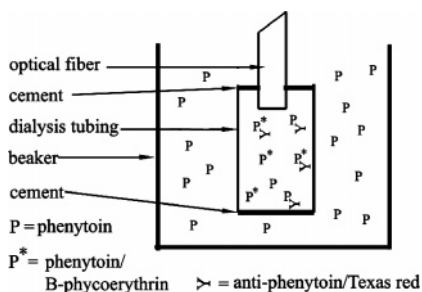


**Figure 8.** Schematic representation of the reversible competitive immunosensor for phenytoin. Phenytoin and the phycoerythrin–phenytoin conjugates competitively bind to the antiphenytoin-TR complex. Redrawn with permission from Anderson, F. P.; Miller, W. G. *Clin. Chem.* **1988**, *34*, 1417. Copyright 1988 American Association for Clinical Chemistry.

#### 4.5.4. Biosensors for Bacteria Cells

Ko and Grant developed a FRET-based immunosensor for determination of *Salmonella typhimurium*.<sup>43</sup> *S. typhimurium* antibody was labeled with a donor dye, while protein G was labeled with an acceptor. Both were immobilized on the surface of an optical fiber. In the absence of the antigen, very little fluorescence is observed from the acceptor. FRET occurs as a result of conformational changes when the antigen binds to the antibody. The ratio of the fluorescences of donor and acceptor serves as the analytical information. Concentrations of the bacterium as low as  $1 \times 10^5$  cfu/L can be detected in 5 min.

Antimicrobial peptides (AMPs) were recently shown to be suitable as recognition elements for microbial cells. AMPs are produced by many organisms for protection against invasion of harmful microbes. AMPs recognize microbes by interacting with their membranes, which then are destroyed. Several immunosensors reported recently<sup>302,303</sup> rely on this recognition ability of AMPs. A direct immunosensor<sup>302</sup> for *Escherichia coli* and *Salmonella typhimurium* was demonstrated to work with the AMP magainin I, which was either covalently attached to the patterned microscope slide surface or immobilized via biotin–avidin chemistry. Cy-5-labeled cells could be detected with detection limits comparable to analogous antibody-based assays. The LODs for *E. coli* and *S. typhimurium* were  $1.6 \times 10^5$  and  $6.5 \times 10^4$  cfu/mL, respectively, in the case of covalently immobilized magainin, and  $6.8 \times 10^5$  and  $5.6 \times 10^5$  cfu/mL, respectively, for the AMP immobilized via biotin–avidin. The assay time was 70 min.

AMPs also were applied in the more-practical sandwich types of assays.<sup>303</sup> Here, the immobilized AMPs were used to capture the unlabeled targets, while detection of bound cells was accomplished using fluorescently labeled antibodies. A significant degree of nonspecific binding was found in the case of tracer antibodies labeled with Cy-5 and Alexa Fluor 647 dyes. Replacement of the marker to Cy-3 was found to significantly reduce the amount of nonspecific binding. It was also found that high peptide density was necessary for optimal results. Limits of detection for *E. coli* and *S. typhimurium* were  $5 \times 10^4$  and  $1 \times 10^5$  cfu/mL, respectively, when magainin I was used, and 2–10-fold higher with other peptides.

Martinez et al.<sup>304</sup> reported on a biosensor for the protective antigen (PA) and for cellular components of *Bacillus anthracis* using SiON<sub>x</sub> waveguides. The sensor can detect 83  $\mu\text{g/L}$  (i.e., 1 picomolar concentrations) of PA in a complex fluid within 10 min when operated in a sandwich assay format, but it possibly can become even more sensitive if interferences by background fluorescence and nonspecific binding can be further reduced.

When whole cells are monitored immunologically by optical methods, the use of ultrasonic standing waves significantly improves the sensitivity of a biosensor. Zourob et al.<sup>72</sup> showed that ultrasonication for 3 min enhanced sensitivity of detection of *Bacillus subtilis* cells by 2 orders of magnitude because the diffusion-limited capture rate is replaced by much faster cell movement. Rabbit anti-*B. subtilis* antibodies were immobilized on the surface of a metal-clad leaky waveguide. Evanescent light-induced scattering was detected by a CCD camera. Obviously, fluorescent labeling was not required, and the analytical range of the sensor operated in the direct assay format was from  $1 \times 10^6$  to  $1 \times 10^{12}$  cfu/L.

#### 4.5.5. Biosensors for Pesticides

A biosensor for the pesticide atrazine made use of polystyrene nanobeads dyed with a luminescent europium(III) chelate.<sup>278</sup> Beads containing carboxy groups were covalently coupled to atrazine antibodies, which, in turn, were used in a binding inhibition assay format. An indium tin oxide (ITO) waveguide was used for immobilization of the capture analyte derivative to minimize nonspecific binding of the beads. Particles with diameters of 107, 304, and 396 nm were investigated in some detail. A decrease in their size resulted in faster binding but did not increase the assay sensitivity, which was comparable with the sensitivity of a known ELISA for atrazine. The use of such labels (having decay times of 0.1–1 ms) enables an almost complete elimination of background fluorescence by applying time-resolved measurements on the ITO waveguide.

#### 4.5.6. Multianalyte Biosensors

Lately, significant effort was devoted to the development of automated biosensor devices capable of simultaneous immunosensing of several analytes of importance in environmental monitoring but, in particular, for the determination of (bio)chemical warfare agents and explosives. A compact, portable, multichannel fiber-optic instrument named MANTIS (of 5.5 kg weight)<sup>270</sup> was reported to be capable of automatically transporting sample, buffer, and labeled antibodies to fibers and to perform fluorescence measurements. It enables four fluorescence immunoassays to be performed simultaneously on the surface of miniaturized polystyrene fiber-optic probes. The device was demonstrated to work for determination of staphylococcal enterotoxin B (SEB). Antibodies to SEB were immobilized on the surface of a polystyrene waveguide through avidin–biotin bridging. Cy-5-labeled SEB antibodies were used in the sandwich assay format. The analytical range of the biosensor was from 10  $\mu\text{g/L}$  to 1 mg/L, and the time required was 10 min. The improved version of the MANTIS device (termed RAPTOR) was shown to be able to determine  $10^5$  cfu/mL of *Bacillus globigii*,  $10^7$  cfu/mL of *Erwinia herbicola*, and  $10^9$  pfu/mL of MS2 coli phages simultaneously.<sup>305</sup> Analogously, the RAPTOR system can determine staphylococcal enterotoxin B, ricin, *Francisella tularensis*, and *Bacillus globigii* simultaneously.<sup>305</sup>

In other work,<sup>306</sup> plastic capillaries with immobilized antibodies were used for simultaneous determination of hormones prolactin, follitropin, and human chorionic gonadotropin (hCG). Fluorescein-labeled antibodies were used in a sandwich assay format. The detection limits were 1.3  $\mu\text{g/L}$ , 2.3 IU/L, and 3.6 IU/L for prolactin, follitropin, and hCG, respectively.

Feldstein and others at the Naval Research Laboratory<sup>307</sup> developed an automated array biosensor for determination of biological warfare agents. The central element of the sensor is a planar optical waveguide (Figure 9) used for direct excitation of antibodies that are bound to the waveguide surface within the penetration depth of the evanescent field. A physically isolated patterning method has been developed to manufacture an array of recognition elements (each  $\sim 1$  mm<sup>2</sup> in size). In this technique, the multichannel patterning cell is placed on the prefunctionalized surface of the waveguide. Then, the recognition species (e.g., antibodies) are introduced into appropriate channels and are patterned on the waveguide surface during incubation, after which the cells are removed. The sensor is then used in a sandwich format.

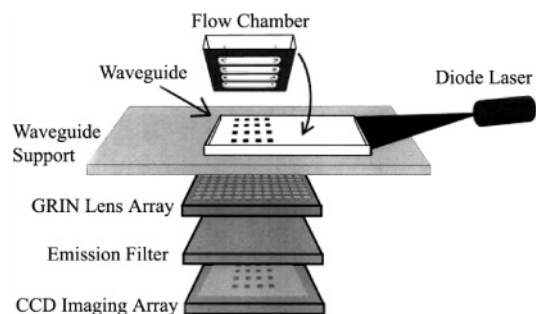


**Figure 9.** Optical system of an array biosensor. Light from a diode laser is coupled into the waveguide. Fluorescence from the waveguide surface is focused by a graded index lens array (GRIN) through optical filters onto a Peltier-cooled CCD imaging array. Reprinted with permission from Feldstein, M. J.; Golden, J. P.; Rowe, C. A.; MacCraith, B. D.; Ligler, F. S. *J. Biomed. Microdev.* **1999**, *1*, 139. Copyright 1999 Springer Science and Business Media.

Simultaneous determination of the explosives 2,4,6-trinitrotoluene (TNT) and hexahydro-1,3,5-trinitro-1,3,5-triazine (RDX) was performed by a system named “Analyte 2000” developed at the Naval Research Laboratory.<sup>259</sup> Two probes for determination of TNT were coupled with two probes for RDX. Cy-5-labeled analyte derivatives were used in a competitive immunoassay format to determine as low as 5  $\mu\text{g/L}$  of TNT and 2.5  $\mu\text{g/L}$  of RDX. Only a minimal cross-reactivity for the two haptens was observed in the multianalyte immunosensor, which was, therefore, capable of analyzing samples containing mixtures of the two compounds.

The same array biosensor<sup>307</sup> was used (a) for simultaneous screening of human serum for antibodies against bacterial and viral antigens including *Staphylococcus aureus* enterotoxin B, tetanus toxin, diphtheria toxin, and hepatitis B, with detection limits from 0.2 to 3  $\mu\text{g/mL}$  and an LOD as low as  $\sim 100$  fg;<sup>308</sup> (b) for the mycotoxin deoxynivalenol (LOD = 0.2 ng/mL in buffer);<sup>309</sup> (c) for simultaneous determination of large food pathogens such as *Campylobacter jejuni* (LOD = 500 cfu/mL) and of small toxins such as aflatoxin B<sub>1</sub> (LOD = 0.3 ng/mL);<sup>310</sup> (d) for staphylococcal enterotoxin B and botulinum toxin A (with LODs of 0.1 and 20 ng/mL, respectively);<sup>311</sup> (e) for ochratoxin A in cereals and beverages (LODs ranging from 4 to 100 ng/g);<sup>312</sup> (f) for *Salmonella typhimurium* (LOD =  $8 \times 10^4$  cfu/mL within 15 min and  $8 \times 10^4$  cfu/mL within 1 h);<sup>313</sup> (g) for the aggressive *Escherichia coli* species O157/H7 in food samples (with LOD of  $5 \times 10^3$  cfu/mL in buffer and  $1\text{--}5 \times 10^4$  cfu/mL in spiked food matrixes, and an assay time of 30 min only);<sup>314</sup> and (h) for *Campylobacter* and *Shigella* species in food (LOD =  $9.7 \times 10^2$  and  $4.9 \times 10^4$  cfu/mL, respectively).<sup>315</sup> These articles reveal that the standard  $6 \times 6$  array sensor can be used to analyze six samples for up to six different analytes. Tait et al. showed<sup>316</sup> that the same format is suitable for analyzing a single sample for 36 different analytes by using complementary mixtures of capture and tracer antibodies. Mixtures were optimized to allow detection of closely related species without significant cross-sensitivity. The approach was demonstrated to work when analyzing a sample for 9 targets with a simple  $3 \times 3$  array. The only limitation of the approach is that the quantity of reagents needed increases significantly.

Several other array biosensors suitable for simultaneous immunosensing were developed. The RIANA (river analyzer)<sup>280</sup> array biosensor is based on a TIRF arrangement that was combined with a flow injection technique for



automated and reproducible fluid handling. Herbicides can be detected by a heterogeneous binding inhibition immunoassay. Analyte derivatives were attached via an amino-dextrane linkage to defined detection spots ( $\varnothing$  3 mm) located on a glass waveguide, with a 2.5 mm distance between the spots. Analyte-specific antibodies labeled with a fluorescent marker were preincubated with analyte present in the sample, and the remaining (nonblocked) antibodies were then selectively attached to the spots. Each test cycle includes regeneration with hydrochloric acid of pH 1.9 and washing with an acetonitrile/water/propionic acid (49/50/1) mixture and is finished within 15 min. Because the glass surface included three sensitive spots, simultaneous detection of three analytes was possible. The following pesticides were detected: atrazine, simazine, isoproturon, alachlor, 2,4-dinitrophenoxyacetic acid, and pentachlorophenol. The respective LODs were 0.03, 0.03, 0.11, 0.07, 0.07, and 4.23 mg/L.

In related work,<sup>277</sup> the pollutants atrazine and isoproturon and the hormone and endocrine disruptor estrone were determined simultaneously with LODs of 0.155, 0.046, and 0.084  $\mu\text{g/L}$  using the binding inhibition assay format. No interference in the analysis of target compounds was observed upon simultaneous quantification. It was shown later<sup>317</sup> that much lower concentrations of the pollutants can be detected by the RIANA biosensor. The highest standard deviation observed at very low analyte concentration results from the inaccuracy of the dilution procedures that require up to 11 steps. Much lower standard deviations were observed when stock solutions were used for each concentration. The errors resulting from dilutions can be compensated for by using a statistical method. The LODs for atrazine, estrone, and isoproturon were 0.002, 0.019, and 0.016  $\mu\text{g/L}$ , which is  $\sim 1$  order of magnitude lower than if the statistical method was not applied.

The RIANA array biosensor also was employed for monitoring testosterone in water samples (LOD 0.2 ng/L),<sup>282</sup> progesterone in water (LOD 0.37 ng/L<sup>318</sup> and 0.2 ng/L<sup>319</sup>), progesterone in milk (LOD 45 ng/L),<sup>319</sup> the pesticide propanil in aqueous samples (LOD 0.6 ng/L),<sup>320</sup> and other antibiotics, hormones, and endocrine-disrupting chemicals with similar LODs.<sup>321</sup>

A completely different approach toward array immunosensors was developed by Rissin and Walt.<sup>322</sup> The underlying scheme of this type of microsensor is similar to the one used in DNA array sensors that were developed by the same group. In a typical example, antibodies to lactoferrin and IgA were covalently immobilized on the surface of 3  $\mu\text{m}$  sized poly(methylstyrene) microspheres. These, in turn, were positioned onto the array of  $\sim 50\,000$  individual optical fibers. A luminescent europium(III) chelate in two different concentrations was applied for encoding purpose, i.e., to establish the position of the two types of microbeads. Lactoferrin and IgA were determined in a sandwich assay format, with the secondary antibodies being labeled with Alexa Fluor 546. IgA can be determined in concentrations between 700 pM and 100 nM, while for lactoferrin the range is between 385 pM and 10 nM. While simultaneous determination of only two analytes was demonstrated, the approach is likely to be suitable for multianalyte sensing.

In conclusion, it can be stated that immunosensors (a) are versatile because they enable the determination of highly different species that range from haptens to viruses and cells; (b) display excellent sensitivity and have very low limits of detection; (c) are highly specific; (d) act irreversibly and,

therefore, are not suitable for continuous sensing in most cases; (e) are less prone to poisoning than enzyme-based biosensors; (f) are thermally labile and frost-sensitive in aqueous solutions; and (g) can be multiplexed.

## 5. Biosensors Based on Ligand–Receptor Interactions

This type of affinity biosensor makes use of specific interactions between a biological receptor and an analyte. Reports on receptor-based biosensors are less numerous than those on immunosensors for the following reasons. This is mainly due to the fact that working with receptors is limited by the facts that (a) their isolation often is tedious and—unlike the production of antibodies—requires individual protocols for each receptor; (b) they need the natural (cellular) environment to function best; (c) they are not stable over time; and (d) their molecular diversity requires an individual labeling protocol for each single species.

### 5.1. Receptor-Based Biosensors for Saccharides and Glycoproteins

The first optical receptor-based biosensors were developed for sensing glucose and made use of its specific interaction with the glucose-binding protein concanavalin A (ConA).<sup>323–325</sup> The approach (see Figure 8 for a closely related scheme) is similar to competitive immunoassays, with the notable exception that it acts reversibly. ConA is immobilized on the inner wall of a mm-sized hollow dialysis chamber via a 1,6-hexanediamine glutaraldehyde spacer. The chamber is placed at the distal end of an optical fiber. Fluorescein-labeled dextrane is contained in the solution filling the chamber. In the absence of glucose, it binds to ConA. Unlike the large ConA, glucose can freely diffuse through the membrane and bind to ConA, and this results in the displacement of dextrane. The released fluorescein-labeled dextrane is distributed within the chamber and “seen” by the fiber if located in the cone determined by the numerical aperture. Because the walls of the chamber are located out of the aperture of the fiber, no fluorescence is registered in the absence of glucose. The sensor operates in the 0–50 mM glucose range and has a response time of  $\sim 7$  min.

A FRET sensor based on the same principle was designed later.<sup>48</sup> Here, the interaction of fluorescein-labeled dextrane with rhodamine B-labeled ConA resulted in a decrease in fluorescence intensity because of the more efficient FRET. Aggregation of ConA is prevented by chemical modification of the protein with succinic anhydride followed by labeling with the rhodamine and results in more stable calibration plots.<sup>326</sup> Concentrations of glucose as high as 0.08 M could be analyzed.

Russell et al.<sup>327</sup> provided another solution for the FRET system. Concanavalin A was labeled with the FRET acceptor dye tetramethylrhodamine isothiocyanate (to give TRITC-ConA) and covalently immobilized in photopolymerized poly(ethylene glycol) hydrogel spheres with an average diameter of  $\sim 2$   $\mu\text{m}$ . The FRET donor dye fluorescein isothiocyanate dextrane (FITC dextrane) was physically entrapped in the hydrogel. It can bind TRITC-Con A in the absence of glucose, while in its presence, FITC-dextrane is liberated. An increase in its fluorescence is observed as a result. The dynamic range of the sensor was from 0 to 44 mM of glucose, and the response time is 10 min for a glucose concentration step from 0 to 11 mM.

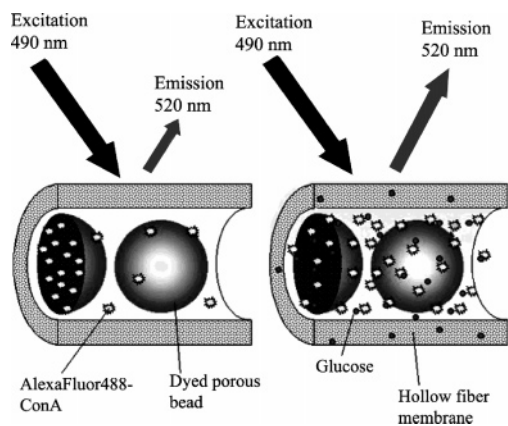


**Figure 10.** Schematic of an affinity glucose sensor (redrawn with permission from Ballerstadt, R.; Schultz, J. S. *Anal. Chem.* **2000**, *72*, 4185; Copyright 2000 American Chemical Society). (Left) The Alexa-488–ConA conjugate is bound to dextrane and, therefore, confined in the porous microbeads, which do not allow the excitation light to penetrate. (Right) As glucose diffuses through the dialysis membrane, it liberates Alexa-488–ConA conjugate so that fluorescence is enhanced a result of better exposure to the exciting light beam and because fluorescence emission is no longer screened off.

Ballerstadt and Schultz<sup>328</sup> have further developed the ConA-based system, thereby providing a most elegant solution. The system is based on an inner filter effect. Highly porous Sephadex beads were colored with two red dyes (safranin and *para*-rosaniline), which were selected to block the excitation and emission spectra of the fluorescent Alexa 488–ConA conjugate (see Figure 10). The latter is bound to dextrane inside the beads but is liberated when glucose is present. Once located outside the beads, the conjugate is fully exposed to the excitation light and fluorescence intensity, therefore, increases. The sensor has a dynamic range from 0.2 to 30 mM of glucose, and the total signal change was much higher than that for the FRET-based system.<sup>327</sup> Moreover, faster response times were accomplished (4–5 min). In other work,<sup>329</sup> the IR-dye Alexa-647 was conjugated to ConA in order to make the sensor work in the IR, which is less prone to spectral interferences by the intrinsic fluorescence of serum samples. The authors also carefully investigated the long-term stability of the biosensors by monitoring their performance over a 4 month period. The sensors displayed an initial increase in fluorescence over the first 3–4 weeks, which later on gradually decreased with an approximately linear drop of 25% per month. The decrease in fluorescence was not due to denaturation of the ConA but rather due to leakage of the fluorescently labeled ConA through the interface between the outer sealant and the membrane. If this problem can be coped with, the sensors potentially are suitable for continuous usage for up to 1 year.

The main drawback of all sensors based on the use of ConA is their poor selectivity because they also respond to many other carbohydrates. For example, binding of fructose is ~3 times stronger than that of glucose. This is in distinct contrast to the high specificity of enzymatic glucose sensors. On the other side, they have lower limits of detection.

Other schemes for affinity sensing of glucose make use of the *E. coli* glucose-binding protein (GBP) that can be gene engineered. In contrast to ConA, GBP binds glucose with very high selectivity. In fact, the affinity to other saccharides is 100–1000-fold weaker than that for glucose or galactose. These proteins are rather stable and can be stored several months without degradation of activity.<sup>330</sup> Since GBP

undergoes significant conformational changes upon binding of glucose, a polarity-sensitive fluorescent indicator introduced at specific positions can act as an optical transducer. The proof of principle for the case of glucose was demonstrated by Marvin and Hellinga,<sup>331</sup> who used GBP labeled with acrylodan. A homogeneous assay for glucose was developed that operates in the micromolar concentration range (0–2  $\mu$ M). However, it was much earlier shown that a similar scheme could be applicable to sensing of maltose using a fluorescently labeled maltose-binding protein.<sup>332</sup> A 60–180% increase of fluorescence intensity was observed in the presence of maltose. Concentrations of maltose from 0 to 200  $\mu$ M could be determined.

Ge et al.<sup>330</sup> showed that the sensitivity of such assays strongly depends on the brightness ( $B_s$ ) of the label used ( $B_s = \epsilon \cdot QY$ ). In fact, GBP labeled with the thiol label 2-(4'-iodoacetamidoanilino)naphthalene-6-sulfonate resulted in a working range from 0.3 to 10  $\mu$ M of glucose. For comparison, the assay based on the glutamine binding protein (GlnBP) labeled with a much brighter acrylodan was performed in the analytical range from 0.03 to 3.2  $\mu$ M. The response of the proteins is very fast in solution (<1 min) but, however, much slower in dialysis cassettes (5–12 min). The recovery in the dialysis cassettes (which have a volume of 1 mL) was unacceptably slow in taking several hours, but this can be possibly accelerated by using smaller volumes. A ratiometric assay also was reported<sup>333</sup> where GBP was labeled with both an environmentally sensitive fluorophore acrylodan and a reference luminophore, a ruthenium(II) polypyridyl complex. Sensing of glutamine using GlnBP was also demonstrated by Dattelbaum and Lakowicz.<sup>63</sup> The *E. coli* GlnBP was covalently modified with acrylodan and other environmentally sensitive probes and used in a homogeneous assay format to detect glutamine from 0.05 to 6.4 mM. Time-resolved and polarization-based sensing of glutamine also was demonstrated. No interference by glutamate was demonstrated, which is a common drawback of the enzymatic glutamine biosensors based on the enzyme glutaminase.

Ye and Schultz<sup>53</sup> engineered a novel glucose indicator protein (GIP) that makes use of FRET from the donor (green fluorescent protein, GFP) to the acceptor (yellow fluorescent protein, YFP). In the absence of glucose, the two fluorescent proteins are in close proximity so that FRET occurs. When excited at 395 nm (corresponding to the absorbance maximum of GFP), the emission from the YFP (peaking at 527 nm) is observed. The spatial separation between the two moieties increases when GIP binds glucose, and FRET is reduced. In the biosensor, a solution of GIP was brought into a hollow cellulose dialysis fiber ( $\varnothing$  190  $\mu$ m), which was placed into a microcuvette, and fluorescence intensity was monitored at two wavelengths and the ratio was determined. The sensor responded reversibly to glucose with response and recovery times of ~100 s, although some drift in the baseline occurred. Glucose could be determined in concentrations between 0 and 10  $\mu$ M.

Chinnayelka and McShane<sup>54</sup> have used an inactive form of glucose oxidase as a selective glucose-binding protein. The apoenzyme labeled with tetramethylrhodamine isothiocyanate was placed inside nanoengineered polymeric microcapsules together with fluorescein-labeled dextrane. The FRET that was observed in the absence of glucose was reduced when glucose diffused into the microcapsules and replaced labeled dextrane in a competitive way. The ratio of fluorescence intensities of the two labels was used as the

analytical information. The sensor reversibly responded to glucose concentrations in the range from 0 to 40 mM, was fast (1–2 min), and was rather selective (a 5–10-fold higher sensitivity for glucose compared to other saccharides). The sensitivity of the system can be easily tuned by varying the concentration of the GOx–dextrane complex.

Ogasawa et al.<sup>334</sup> designed an affinity sensor for the riboflavin-binding protein (RBP). It exploits the intrinsic green fluorescence of riboflavin. Hydrophobic 3-octylriboflavin is adsorbed on an optical fiber whose surface was made lipophilic by modification with octadecyl groups. On exposure to a solution of RBP, it binds to the surface-immobilized octylriboflavine. The sensor can be renewed with good reproducibility by removing the RBP–riboflavine complex and loading the surface again with octylriboflavine. In fact, 15 individual sensors for RBP were prepared on a single optical fiber, which varied in performance by <5%. When RBP binds to the immobilized riboflavin, quenching of fluorescence is observed. As little as 0.73  $\mu\text{M}$  of the RBP can be detected in 5 min.

Medintz et al.<sup>55</sup> prepared two kinds of biosensors for maltose, which make use of quantum dots (QDs) and a maltose-binding protein (MBP) from *E. coli*. The first type of the sugar-sensing nanoassemblies consisted of 560-nm donor QDs conjugated to 10 molecules of MBP (in average). The displaceable dextrane was labeled with a fluorescent acceptor dye. No FRET was observed when maltose replaced dextrane in the sugar-binding site. The second maltose biosensor consists of 530-nm donor QDs loaded with 10 cyanine-labeled MBP molecules. The protein-bound label served as a bridging acceptor/donor for ultimate energy transfer to maltose-displaceable labeled dextrane. Both sensors respond to maltose concentrations from 10 nM to 1 mM.

Another nanobiosensor for maltose<sup>56</sup> was reported that is based on the use of thiolhexanoate-capped CdSe nanoparticles ( $\varnothing$  3.0–3.5 nm) conjugated to the MBP, which was labeled with a luminescent ruthenium(II) complex. Little fluorescence is detectable in the absence of maltose because of the electron transfer from the ruthenium complex to the nanobead. Fluorescence is enhanced as a result of conformational changes that occur upon binding of maltose. Glucose and lactose were shown not to interfere, while maltose could be sensed from 10 nM to 10  $\mu\text{M}$ .

An unusual approach toward receptor-based sensing of glucose in blood was proposed by Sanz et al.<sup>335</sup> It is based on the fact that oxidation of hemoglobin (Hb, contained in the sample) by  $\text{H}_2\text{O}_2$  (generated after addition of glucose oxidase GOx according to eq 1) results in distinct changes in the absorption spectrum of Hb. To make the assay operative, blood samples prepared without pretreatment and reactions of  $\text{H}_2\text{O}_2$  with other blood components such as catalase need to be blocked (which is achieved by addition of azide). The activity of GOx should be high enough for the “chemistry” to work, given the fact that the activity of GOx is inhibited by azide by  $\sim 30\%$ , and low enough to avoid its interaction with hemoglobin. The linear response range of the system was from 0.1 to 30 mM of glucose.

## 5.2. Receptor-Based Biosensors for Inorganic Ions

Biosensors for cations exploit the need of enzymes for certain ions in order to function. This results in two kinds of sensing schemes. The first is the effect of the catalytic ion on the *activity* of the enzyme (which is treated in section

3). The second is the effect of the catalytic ion on the *conformation* of the enzyme (regardless of its activity). Respective sensors are treated in this section. In such sensors, an enzyme serves as a kind of chelator for certain metal ions, but with much higher selectivity than classical chelators such as EDTA. The ions usually are required as enzyme cofactors. For example, Thompson and Jones<sup>336</sup> reported a highly sensitive zinc(II) biosensor, which makes use of the enzyme carbonic anhydrase (CA). The  $\text{Zn}^{2+}$  ion is its natural cofactor and is bound by CA with excellent selectivity. The apoenzyme prepared by dialysis was contained in a chamber together with the fluorescent probe dansylamide. The ion-permeable chamber was attached to an optical fiber. The probe does not bind to the apoenzyme and, thus, remains weakly fluorescent in water. However, when (practically irreversibly) bound to CA in the presence of  $\text{Zn}^{2+}$ , the fluorescence intensity increases significantly. The analytical range of the sensor was from 40 to 1000 nM. The main drawback of the system is its moderate brightness and the limited applicability to real samples because UV excitation is required at  $\sim 330$  nm where background fluorescence of most samples is very strong.

A more flexible system for detection of  $\text{Zn}^{2+}$  is based on fluorescence quenching.<sup>52</sup> In the presence of the metal cation, the active site of CA labeled with the fluorescent donor fluorescein permits binding of the colored quencher azosulfamide. The fluorescence decay time (measured by phase fluorometry) was shown to decrease with increasing concentrations of zinc cation, which could be determined in the concentration range from 1 to 100  $\mu\text{M}$ .

A cobalt biosensor was reported<sup>51</sup> that is based on the finding that the d–d absorption of  $\text{Co}^{2+}$  coordinated to CA labeled with a cyanine dye promoted radiationless FRET since the absorption of the  $\text{Co}^{2+}$  ion overlaps the emission of the label. The labeled apoenzyme was entrapped in a polyacrylamide gel positioned at the distal end of an optical fiber. The sensor was capable of sensing  $\text{Co}^{2+}$  in the concentration range from 0 to 20  $\mu\text{M}$  with response times of a few minutes.

The fact that certain variants of CA exhibit different selectivity to metal ions was used by Zeng et al.<sup>57</sup> to design a sensor for  $\text{Cu}^{2+}$ . Two variants of human CA II were labeled (with Oregon Green and Alexa Fluor 660, respectively) and immobilized at the distal end of an optical fiber. An  $\sim 85\%$  drop in fluorescence intensity and decay time (as measured by phase fluorometry) was observed upon binding of  $\text{Cu}^{2+}$ . The analytical range of the system was from 0.1 to 100 pM. Ions such as  $\text{Co}^{2+}$  and  $\text{Ni}^{2+}$ , and even  $\text{Zn}^{2+}$ , were shown to interfere only if present in much higher concentration, because the affinity of the CAs to these ions is much lower than that for  $\text{Cu}^{2+}$ . It was demonstrated that the sensor was suitable for real-time analysis of  $\text{Cu}^{2+}$  in seawater.

The phosphate-binding protein isolated from *Escherichia coli* and labeled with the fluorophore acrylodan is potentially suitable for biosensing purposes<sup>337</sup> by showing a 50% increase of fluorescence intensity in the presence of micromolar concentrations of phosphate. In another detection scheme for phosphate,<sup>338</sup> two cysteine mutations were introduced into the phosphate-binding protein, allowing it to be labeled with two rhodamine fluorophores. When close to each other (in the absence of phosphate), the rhodamine molecules form a noncovalent and nonfluorescent dimer. A linear correlation between fluorescence intensity and the concentration of phosphate was observed in the range from 0 to 6  $\mu\text{M}$  of the analyte. At saturation (concentrations of



phosphate of 6  $\mu\text{M}$  or higher), an 18-fold increase (at average) in fluorescence intensity was observed for the mutants investigated.

A homogeneous assay for sulfate was reported that is based on fluorescently labeled sulfate binding protein.<sup>339</sup> The fluorescence of the labels was quenched upon binding sulfate. The LODs varied from 30 to 200 nM depending on the label used.

Sumner et al.<sup>340</sup> have discovered that the wild form of red fluorescent protein (RFP) can reversibly bind  $\text{Cu}^+$  and  $\text{Cu}^{2+}$  ions with high selectivity and sensitivity. In fact, the quenching of fluorescence of the RFP by the heavy metal ions occurred even at 10 nM concentrations of the analytes. The RFP was found to be  $\sim 10^7$ -fold more selective for copper over  $\text{Mg}^{2+}$  and  $\text{Ca}^{2+}$ , with its fluorescence being virtually unaffected even by high concentrations of those. Fluorescence was recovered on addition of EDTA, albeit not to the initial level. A nanobiosensor for  $\text{Cu}^{2+}$  also was designed on the basis of RFP.<sup>341</sup> The protein was immobilized in 80-nm polyacrylamide nanobeads together with an inert reference dye. The ratio of the intensities under 488-nm excitation served as the analytical parameter. The signal change caused by  $\text{Cu}^{2+}$  returned to 95% of its original value within 3 min when EDTA was added, thus showing an almost complete reversibility of the sensor. As in the case of the homogeneous assay in solution, no interference by other metal ions was observed. The sensitivity to  $\text{Cu}^{2+}$  was independent of pH in the range from 6 to 8.5. However, the nanobiosensor was found to be much less responsive to  $\text{Cu}^{2+}$  at low pH. The analytical range for  $\text{Cu}^{2+}$  is from 0.2 to 50  $\mu\text{M}$ , but sensitivity can be fine-tuned by varying the concentration of the nanobeads, thus generating a larger signal change per nanoparticle at the same concentration of the analyte.

### 5.3. Receptor-Based Biosensors for Gaseous Species

A number of optical affinity biosensors make use of heme proteins, natural compounds that can weakly bind gases such as oxygen and carbon dioxide, and much more strongly bind carbon monoxide and nitrogen monoxide. Blyth et al.<sup>342</sup> showed that the heme proteins cytochrome *c*, myoglobin, and hemoglobin (Hb) enable semiquantitative detection of CO and NO in aqueous medium. The heme proteins immobilized into a sol-gel matrix exhibited a distinct change of their absorption spectra upon coordination of NO and CO. Although the effect was reversible, desorption of gases took up to 2 h. However, fast regeneration was accomplished by using other reagents. For example, cytochrome *c* could be regenerated from its complex with NO by reduction with sodium dithionite, washing with buffer, and addition of potassium ferricyanide. Cytochrome *c* embedded in a sol-gel was demonstrated to sense NO in a gas phase, with a response time of 200 s and full recovery within 300 s.<sup>343</sup> The sensor operated in the dynamic range from 1 to 25 ppm of NO.

Reversible and fast micro- and nanosensors for NO were developed by Barker et al.<sup>344</sup> Cytochrome *c'* was immobilized on gold nanobeads ( $\varnothing$  50 nm). Two ways of optical interrogation were reported. The first is to measure the intrinsic fluorescence of cytochrome *c'*, which changes in the presence of NO. The second is to measure the increase in the efficiency of FRET from the label (Oregon Green) to cytochrome (which is enhanced when the latter binds NO because of better spectral overlap between the emission spectrum of Oregon Green and the excitation spectrum of cytochrome). The response to NO is linear in the concentra-

tion range from 20  $\mu\text{M}$  to 1 mM. The sensors operate in a fully reversible way and have response and recovery times of  $<1$  s. Although the LOD of the sensor was relatively high (20  $\mu\text{M}$ ), the limits of quantification are very low because only small volumes are required. Cytochrome *c'* also was entrapped in polyacrylamide; however, binding of NO was found to be irreversible.

The performance of such microsensors was further improved by using a reference fluorescent indicator and employing ratiometric measurements.<sup>345</sup> The microsensor incorporated labeled with Oregon Green cytochrome *c'* along with polystyrene nanobeads ( $\varnothing$  40 nm) labeled with a fluorescent reference dye whose red emission ( $\lambda_{\text{max}} = 685$  nm) allowed for ratiometric (two-wavelength) measurements. Compared to the previous work,<sup>344</sup> the LOD of the sensor was improved to as low as 8  $\mu\text{M}$ . Immobilization of the reference spheres was, however, not reproducible, and the ratio of fluorescence intensities and calibration plots, therefore, varied from sensor to sensor. The ratiometric sensors were employed to measure extracellular NO released by macrophages.

Blyth et al.<sup>346</sup> observed that cytochrome *c'*, when immobilized into a sol-gel, undergoes irreversible conformational changes (in 2–4 days), which lowers binding affinity of the metalloprotein. However, after these changes have occurred, the protein remains selective for NO and the calibration plots are well-reproducible.

Analogous biosensors were prepared with the heme domain of soluble guanylate cyclase, the only protein receptor known for signal transduction involving in vivo produced NO and having many similarities to cytochrome *c'*, including a very low affinity for oxygen and a high affinity for nitric oxide.<sup>347</sup> The LOD of the sensor was 1  $\mu\text{M}$ .

Reversible binding of oxygen to hemoglobin (Hb) was exploited by Zhujun and Seitz<sup>348</sup> to design an oxygen biosensor. They showed that Hb immobilized on a Sephadex ion-exchange resin can sense oxygen in the dynamic range from 0 to 160 Torr. The shelf life of this reflectance-based biosensor is very short due to fast irreversible degradation of the immobilized Hb (within 2 days at room temperature or within 7 days at 4 °C). The sensor is, thus, hardly an alternative to conventional optical oxygen sensors, which are based on stable quenchable luminescent indicators.

### 5.4. Receptor-Based Biosensors for Toxins

An evanescent-wave biosensor for  $\alpha$ -bungarotoxin was designed by immobilizing the nicotinic acetylcholine receptor on an optical fiber.<sup>349</sup> Fluorescein-labeled  $\alpha$ -bungarotoxin was used in the competitive assay format. As little as 1 nM of the toxin could be detected within 5 min. Although the nonspecific binding was totally eliminated by addition of bovine serum albumin, the sensor was inhibited by agonists such as acetylcholine, nicotine, and carbamylcholine and by antagonists such as pancuronium and D-tubocurarine. No regeneration of the biosensor was possible.

Song and Swanson<sup>50</sup> developed biosensors for cholera toxin (CT). The bioreceptor ganglioside GM1 was incorporated into a biomimetic membrane surface (composed, e.g., of 9-octadecenoyl phosphatidylcholine), which, in turn, was spread onto glass microbeads. The labeled receptor molecules are homogeneously distributed in the lipid bilayer but aggregate in the presence of CT, which has five binding sites for GM1. As a result, fluorescence self-quenching is observed. Alternatively, the receptor molecules are labeled

with a fluorescent donor, and a fluorescent acceptor dye, FRET, is observed in the presence of CT. Generally, the sensors respond to the concentration of toxin from 0 to 10 nM. Sensitivity and dynamic range can be tuned by varying the total concentration of the labeled GM1 in the membrane. Limits of detection as low as 0.05 nM and small dynamic range are associated with samples having low concentration of the receptor, while lower sensitivity and large dynamic range are found for samples with high concentration of the receptor. Boradipyrroles also were found to be viable labels in both types of the biosensor. No interference by albumin was observed in this case, whereas a significant nonspecific drop in fluorescence was observed for GM1 labeled with fluorescein.

Many bacterial toxins, viruses, and bacteria target carbohydrate moieties on the surface of a cell so as to attach and gain entry into the cell. Ngundi et al.<sup>350</sup> designed a monosaccharide-based array biosensor for detection of protein toxins. Arrays of *N*-acetyl galactosamine (GalNAc) and *N*-acetylneuraminic acid (Neu5Ac) derivatives were immobilized on the surface of a planar waveguide (similar to ref 307) and were used as receptors for protein toxins. These arrays were probed with fluorescently labeled bacterial cells and protein toxins. While *Salmonella typhimurium*, *Listeria monocytogenes*, *Escherichia coli*, and staphylococcal enterotoxin B did not bind to either of the monosaccharides, both cholera toxin and tetanus toxin bound to GalNAc and Neu5Ac and could be detected at concentrations down to 100 ng/mL.

In conclusion, it can be stated that biosensors based on ligand–receptor interactions are (a) often highly specific; (b) sensitive in giving rather low limits of detection; (c) characterized by virtually irreversible response; (d) sensitive to environmental effects; (e) prone to poisoning; and (f) tedious to fabricate, in particular in terms of genetic modification and isolation of proteinic receptors.

## 6. Nucleic Acid Biosensors

Such sensors (also referred to as DNA biosensors) represent an attractive alternative approach to immunological sensing of species such as bacteria. They take advantage of the exceptional long-term stability of nucleic acids and the high selectivity of the interaction of complementary chains of polynucleotides. Nucleotides and their polymers also can be synthesized easily. Typical examples of DNA biosensors are described in the following (see Figure 11).

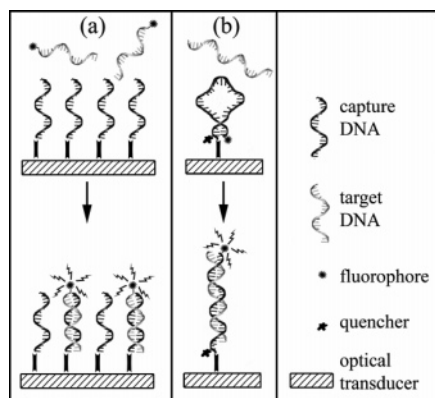


**Figure 11.** Two fundamental forms of nucleic acid-based sensors: (a) conventional DNA sensor using a fluorescently labeled counter strand or a fluorogenic intercalator; (b) molecular beacon DNA sensor.

### 6.1. Single DNA Sensors on Solid Supports and on Fiber-Optics

The feasibility of optical nucleic acid biosensing was demonstrated by Graham et al.<sup>351</sup> 16- and 20-base oligonucleotides, but also long (204-base) oligonucleotide chains, were attached to the surface of an optical fiber as shown schematically in Figure 11a. Fluorescein-labeled complementary chains were shown to interact with complementary chains within  $\sim 1$  min as determined by TIRF spectroscopy (see section 4.3.2). Regeneration of the biosensor was accomplished by raising the temperature from 65 to 80 °C, resulting in complete dissociation of the bound duplex within 10–15 min. The analytical range of the sensor was from 0 to 200 nM of nucleotides.

Piunno et al.<sup>352,353</sup> immobilized a DNA sequence on an optical fiber by first activating the surface with a long-chain aliphatic spacer arm terminated with a nucleoside to which a longer chain was attached through automated step-by-step DNA synthesis. Detection of hybridized DNA at the fiber surface was achieved by treating it with a solution of the intercalator ethidium bromide. The sensor was regenerated by exposing it to a 85 °C hybridization buffer for 5 min. Total analysis time was  $< 1$  h, and the LOD was 86 ng/mL. The sensor showed reproducible results within 3 months of storage.

Watts et al.<sup>354</sup> immobilized biotinylated oligonucleotide sequences on a solid surface via streptavidin and used a resonant mirror technique (see section 4.3.2) for direct and rapid detection of hybridization. The lowest detectable concentration of the target 40-base nucleotide was 9.2 nM. Hybridization at the sensor surface was followed for 15 min, although a positive response was obvious within 30–60 s.

Abel et al.<sup>355</sup> compared the performances of DNA biosensors operating in the direct and competitive assay formats, respectively. A biotinylated capture probe was immobilized on a glass surface via avidin or streptavidin. A complementary fluorescein-labeled 16-base oligonucleotide could then be determined with an LOD of 0.2 pM. A competitive assay (using labeled and unlabeled nucleotides) resulted in a much higher LOD (1.1 nM). The use of poly(acrylic acid) sodium salt and Tween 20 reduced the nonspecific binding to 1–2% of the amount of specific binding. The signal loss during long-time measurements, i.e., after consecutive hybridization assays, can be described by a single-exponential function and, thus, compensated for. After 200 cycles, the net signal had decreased by 50%, corresponding to a signal variation of only 2.4% after correction for this signal loss. By using a 50% (w/w) aqueous urea solution for regeneration of the biosensor, the duration of an assay cycle was reduced to 3 min.

Pilevar et al.<sup>356</sup> used a near-IR cyanine dye ( $\lambda_{\text{exc}} = 787$  nm,  $\lambda_{\text{em}} = 807$  nm) as a label for an oligonucleotide sequence in order to make measurements outside the background fluorescence from natural compounds, which is substantial when using fluorescein labels. The feasibility of detecting bacterial cells using rRNA as the target was demonstrated in a solid-phase sandwich-type of assay where *Helicobacter pylori* rRNA was used along with IR dye-labeled detector oligonucleotide probe. The result indicates that this biosensor is capable of detecting *H. pylori* RNA at picomolar concentrations.

A biosensor for detection of L-adenosine was developed by Kleinjung et al.<sup>357</sup> An L-adenosine specific RNA was attached to an optical fiber via an avidin–biotin link.

Fluorescein-labeled L-adenosine was used in a competitive assay format. The sensor responds to concentrations from 1 nM to 100  $\mu$ M.

Bagby et al.<sup>358</sup> found that an intercalating thiazole orange derivative (TOMEHE) gives a 10-fold larger signal change over the commonly used ethidium bromide, thus providing higher sensitivity for hybridization events. TOMEHE, however, also showed a significant response to single-stranded DNA and concentration-dependent phenomena at high loading with the dye. This limits the dynamic range over which TOMEHE can be used.

A capillary sensor (see section 4.3.2.) for DNA also was reported.<sup>359</sup> A capture DNA was attached to the inner walls of a capillary via biotin–streptavidin chemistry. The complementary DNA sequence labeled with Alexa Fluor 532 can be sensed with a detection limit of 30 pg/mL.

## 6.2. DNA Arrays

Ferguson et al.<sup>360</sup> created a fiber array biosensor capable of simultaneous measurements of 7 DNA sequences. The optical fibers (each 200  $\mu$ m in  $\varnothing$ ) carrying the immobilized oligonucleotide probes were bundled to form a multiplex DNA sensor. The fluorescence intensity of all the fibers was imaged with a CCD camera. Up to 7 DNA sequences could be detected within 10 min with an LOD of 10 nM. As in the case of individual sensors, the array can be stored for prolonged periods (months) without loss of activity.

Walt and co-workers demonstrated later<sup>361</sup> that the actual detection limits of the array microsensors can be much smaller if microspheres are being used. Small sample volumes (10  $\mu$ L for a 500  $\mu$ m array) and higher local concentrations of the DNA enable further amplification. Fewer sensor numbers in the array also increase the signal because more target molecules hybridize per microsphere. By examining multiple identical sensors simultaneously, the signal-to-noise ratio can be improved by allowing incoherent noise to be signal averaged. The authors demonstrated that as few as 600 target DNA molecules ( $10^{-21}$  mol) can be detected. Although DNA at higher concentration can be assayed within 10–30 min, 17 h were necessary to complete hybridization and to achieve the lowest detection limits.

The same group developed a method for encoding a set of randomly ordered functionalized microbeads (each bearing alkaline phosphatase, avidin, or biotin) using luminescent dyes.<sup>362</sup> This method formed the basis for a smart array system suitable for simultaneous detection of numerous DNA sequences.<sup>363</sup> Polymer microbeads ( $\varnothing$  3.1  $\mu$ m) were dyed with various fluorophores such as Cy-5 and europium(III) complexes and functionalized with different oligonucleotide probes. Because microbeads with different concentrations of a single fluorophore are optically distinguishable, a total of 100 different beads could be prepared. A mixture of the beads was distributed over a distal end of a fiber bundle ( $\varnothing$  500  $\mu$ m, 6 000 individual fibers) so that each microbead occupied a single well (Figure 12). The position of the recognition elements was decoded by imaging with a CCD chip because each type of the beads has a characteristic emission wavelength and luminescence intensity. The signal was monitored after hybridization to fluorescein-labeled complementary oligonucleotides. Only 10 min are needed to determine 100 pM of oligonucleotides, but up to 17 h are needed for the lowest concentration (10 fM).

In continuation of this methodology, Walt and co-workers have designed array biosensors for simultaneous determi-

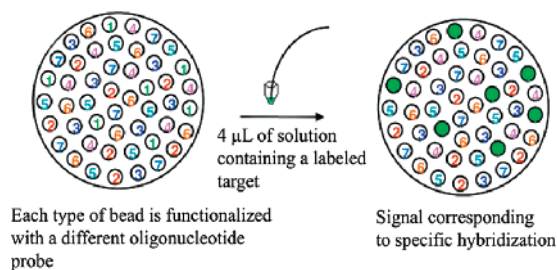


**Figure 12.** Overview of a fiber-optic array system. The functionalized beads occupy the micrometer-sized wells (1 bead/well) located on the tip of the optical fiber. The position of the beads is decoded by imaging its color. When immersed into a sample solution containing labeled DNA, a signal is observed only on the beads bearing the DNA probe complementary to the target in solution. Reproduced with permission from Ferguson, J. A.; Steemers, F. J.; Walt, D. R. *Anal. Chem.* **2000**, *72*, 5618. Copyright 2000 American Chemical Society.

nation of *Bacillus anthracis*, *Yersinia pestis*, *Francisella tularensis*, *Brucella melitensis*, *Clostridium botulinum*, *Vaccinia virus*, and a biological warfare agent simulant named *Bacillus thuringiensis kurstaki*.<sup>364</sup> The replacement of the 20-mer probes by 50-mer probes allowed for a high specificity of the array. The authors report LODs of “10 fM” (10 femtomolar concentrations) for *B. anthracis*, *Y. pestis*, *Vaccinia virus*, and *B. thuringiensis kurstaki*, and of 100 fM for *B. melitensis* and *C. botulinum*. This is difficult to interpret since a bacillus does not have a molecular weight. It was also found that overlapping target sequences are partially complementary to the probe sequences. This can result in a nonspecific response, unfortunately. The use of multiple probes (at least two for each analyte) minimizes the potential possibility of false identification. The assay time was 30 min.

The above DNA optical fiber array subsequently was coupled to a microfluidic system<sup>365</sup> operated at a flow rate of 1  $\mu$ L/min. This resulted in faster hybridization (15 min, compared to 30 min required for static measurements) and in  $\sim$ 100-fold lower LODs (10 aM, compared to 1 pM as achieved in static measurements), which makes this approach highly advantageous. The systems described in refs 360–367 are quite successful in commercial terms.

The target rRNA of an algal bloom species can be determined with a microarray biosensor operating in a kind of “sandwich” assay format.<sup>366</sup> The RNA to be analyzed interacts with a long capture probe, and the labeled tracer oligonucleotides then interact with the residual free end. Fluorescently labeled oligonucleotides (acting as tracers that can capture nucleotide sequences) were coupled to the surface of microbeads positioned in the wells at the tips of optical fibers in an array. As few as 5 cells could be detected within 45 min, and the LOD of the rRNA is  $4 \times 10^4$  molecules. In similar work,<sup>367</sup> the microarray biosensor was used for detection of different *Salmonella* strains with LODs of  $10^3$ – $10^4$  cfu/mL in pure samples and of  $10^4$ – $10^5$  cfu/mL in the presence of interfering organisms. All investigated *Salmonella* strains were detectable, albeit with different sensitivities. Other common food pathogens were shown not to interfere at concentrations of  $10^8$  cfu/mL. The assay time was 1 h.

Another approach of addressing and specifically depositing DNA was demonstrated by Swanson et al.,<sup>368</sup> who designed a semiconductor biochip containing a microelectrode array. In order to immobilize a specific capture DNA probe at a



certain location, an electric field was applied that causes the attraction of DNA fragments and their deposition at predetermined electrodes. The target DNA may be guided to the specific locations as well. The assay is performed in a sandwich format by exposing the array to the tracer DNA bearing a fluorescent label. If coupled to an integrated fluidic system, the following steps of the DNA analysis of *E. coli* can be automatically performed:<sup>369</sup> (a) di-electrophoretic collection of bacteria; (b) DNA amplification and electronic DNA hybridization; and (c) fluorescence readout with the help of a CCD camera. The whole assay can be performed in 2.5 h.

Rissin and Walt have demonstrated recently<sup>370</sup> that the sensitivity of array biosensors can be significantly improved by employing an enzymatic amplification step similar to that known from ELISAs. To prove its feasibility, a biotinylated femtoliter array was incubated with a solution of streptavidin- $\beta$ -galactosidase ( $S\beta G$ ) conjugate, and then with a solution of the enzyme substrate, which generated fluorescent resorufin upon hydrolysis. Since the volume of the wells is very small, the limit of quantification for  $S\beta G$  was found to be 2.6 amol. No signal was measured in control experiments, in which the enzyme was bearing no streptavidin, or, alternatively, the surface of the fiber was not biotinylated.

### 6.3. Molecular Beacons in DNA Sensors

Described first by Tyagi and Kramer,<sup>45</sup> molecular beacons (MBs) have become an important tool for studies in genetics, disease mechanisms, and molecular interactions. MBs represent single-stranded types of oligonucleotide probes that possess a stem-and-loop structure (see Figure 11b). The stem is formed by the two ends of an MB containing complementary nucleotides. A fluorophore attached to one end of the stem and a quencher attached to the other are in close proximity, and little or no fluorescence is observed. The loop portion of the molecule is responsible for reporting the specific complimentary oligonucleotide. Hybridization of a matching oligonucleotide to the loop portion results in conformational reorganization that brings the stem apart so that fluorescence is enhanced. This smart technique has the advantage that no labeling of other species is required (compared to, e.g., the competitive assay format).

Following the work of Tyagi and Kramer,<sup>45</sup> who used MBs in homogeneous solution, Fang et al.<sup>46</sup> immobilized an MB onto the surface of a silica plate via avidin linkage to design a solid-state biosensor. A biotinylated MB was prepared that had a total of 28 bases, including 18 bases complementary to the sequence of interest and 5 base pairs for the stem. Tetramethyl rhodamine was selected as a fluorophore, and a modified azobenzene Dabcyl was selected as a quencher. A significant increase in fluorescence was observed upon addition of the complementary DNA both for the MB contained in homogeneous solution and in the immobilized form. In the control experiment, no effect was observed on addition of the noncomplementary DNA. The results indicated that the immobilized MB could be used to detect target DNA molecules in the subnanomolar range.

Liu and Tan<sup>47</sup> have investigated DNA sensing in more detail using a similar MB (also labeled with TMR and Dabcyl). The biotinylated MB was immobilized onto the surface of an optical fiber via a streptavidin bridge. A spacer group between the MB and the fiber substantially reduces steric hindrance and increases its mobility. A strong increase in fluorescence intensity was observed only upon hybridiza-

tion with a complementary DNA, while the increase was much lower for the oligonucleotide strand having a single mismatch. The MB could be regenerated by immersing it into 90% formamide plus 10% tris/EDTA buffer mixture for 1 min. While a single regeneration cycle completely recovered the sensing properties of the MB, a few repeated regeneration cycles resulted in a significant drift. A 50% aqueous urea solution can be used for regeneration of DNA sensors as well.<sup>371</sup> The authors also showed that higher ionic strength (IS) favored hybridization by decreasing electrostatic repulsion between the loop chain of an MB and the target DNA. Moreover, the initial reaction rate in the presence of divalent cations was  $\sim 20$  times higher than in the presence of monovalent ones at the same IS. The best results were obtained by using a high IS created by the divalent cation Mg(II). Under these conditions, 1–100 nM of DNA could be sensed in 10 min.

Ueberfeld and Walt<sup>40</sup> have designed an MB capable of virtually reversible binding of the target nucleotide. This can be achieved if the free energy of the duplex formation is of the same magnitude as the free energy of the stem formation. To do so, 6 oligonucleotides in the fully complementary 20-mer loop were replaced by adenine moieties. The reversibility was indeed achieved, but only when working at a carefully adjusted temperature (38.8 °C), while working at 34 °C resulted in irreversible binding, and working at 43.8 °C resulted in the melting of the loop-target hybrid. In order to measure the efficiency of FRET, the stem of the MB was labeled with a fluorescent donor, while the acceptor dye was positioned between the stem and the loop sequence where it neither hinders stem formation nor inhibits target-loop hybridization. A two-wavelength ratiometric approach was made use of. This has the advantage that the ratio of the fluorescence intensities of the donor and the acceptor, respectively, is independent of the concentration of the labels.

Du et al.<sup>372,373</sup> attached a fluorescently labeled oligonucleotide to a thin gold surface to create an MB that requires no quencher on the second stem. In the absence of a complementary DNA, the label is in close proximity to the gold surface and its fluorescence is quenched. The intensity increased about 100-fold upon hybridization with a complementary DNA, which was detectable at concentrations from 0.2 to 3  $\mu\text{M}$ . An 8-fold lower sensitivity was observed for a singly mismatched target. The sensor was, however, not suitable for multiple measurements in showing an  $\sim 40\%$  degradation of fluorescence intensity after each regeneration cycle.

### 6.4. Liposome-Based DNA Assays

Some biosensors for nucleic acids make use of liposomes containing thousands of dye molecules and thus generating strong signal for even low nucleic acid concentrations so that quantitative reflectance (or even qualitative visual) measurements are possible. A typical biosensor of this type includes a capture oligonucleotide attached to the surface of a liposome. Biotin-streptavidin binding is employed to attach a reporter oligonucleotide to a liposome loaded with sulforhodamine B. In the presence of the target sequence, a sandwich is formed and the detection zone becomes colored. RNA from *B. anthracis* spores in concentrations from 0.1 pg/L to 1 ng/L could be detected in 90 min.<sup>374</sup> As little as one *B. anthracis* spore is detected in 12 h.

Bäumner et al.<sup>375</sup> used a similar system for detection of RNA sequences from *B. anthracis*, *C. parvum*, and *E. coli*,

but with the difference that the fluorescein-labeled capture oligonucleotides were immobilized on a polyethersulfone membrane via anti-fluorescein antibodies. Quantification of the RNA was possible between 10 nM and 1  $\mu$ M by simultaneously incubating the RNA with streptavidin-labeled liposomes, biotinylated capture oligonucleotide, and the membrane containing a target sequence. The assay time was 20–30 min. An analogous RNA biosensor was used for detection of Dengue virus in blood samples.<sup>376</sup>

## 6.5. Aptamer-Based DNA Sensing

Aptamers are nucleic acid species that have been evolutionary engineered through in vitro selection to bind various molecular targets such as haptens, proteins, nucleic acids, and even cells, tissues, and organisms. Lee and Walt<sup>377</sup> have designed an aptamer biosensor for thrombin. The aptamer was immobilized onto nanoporous silica beads that were placed on the distal end of a fiber array. Fluorescein-labeled thrombin was used in a competitive assay format. Although fluorescence signals from the individual aptamer beads showed significant variability, the average signals of 100 beads provided much more precise values. The fiber-optic microarray system had a detection limit of 1 nM for nonlabeled thrombin, and each test could be performed in  $\sim$ 15 min including the regeneration time.

Rupcich et al.<sup>378</sup> reported on the immobilization of an aptamer-based system in a sol–gel matrix. Fluorescein was covalently attached to the aptamer, and the quencher (dabcyl) was attached to the complementary oligonucleotide and, thus, was in close proximity of the fluorescein upon hybridization. Binding of the target molecule (ATP) to the aptamer results in a conformational change in the aptamer and formation of a stem-and-loop structure. The quencher-labeled oligonucleotide (QDNA) strand is displaced, and a large increase in fluorescence is observed. A tripartite aptamer complex also was prepared, where the fluorophore was attached to an oligonucleotide sequence complimentary to the stem part of the aptamer. The aptamer was attached to streptavidin to provide a larger molecular mass so to reduce leaching from the sol–gel matrix. Aminopropyltriethoxysilane was added to the sol–gel to promote electrostatic retention of the DNA because it introduces amino groups into the sol–gel, which are positively charged at pH's below 8. The leaching rate was  $\sim$ 12%/h. The authors also showed that a QDNA composed of 11 nucleotides is the best compromise between sensitivity and response time. The analytical range of the sensor was from 0.01 to 3 mM ATP. The sensor retained full signaling capability for 1 month but showed no response after a 3 month storage in buffer solution, presumably because of irreversible aging of the sol–gel matrix.

To summarize this chapter, one can state that DNA sensors (a) have exceptional stability; (b) possess very low limits of detection; (c) are highly specific; (d) can be easily produced using automated procedures; (e) are self-contained in case of using molecular beacon; (f) are relatively tolerant to heat and frost; (g) are rather sensitive to effects of ionic strength; and (h) have very wide applicability and large potential in the case of aptamer DNA or DNAzyme sensors, thus allowing sensing even of haptens and proteins.

## 7. Whole-Cell Biosensors

This type of biosensor makes use of living cells such as individual microorganisms or tissue, rather than relying on

using specific biomolecules such as enzymes, proteins, or DNA. Whole-cell biosensors generally exhibit longer shelf lifetimes compared to, e.g., enzymatic biosensors because the active components are contained and produced in the “natural” environment and not in a polymer matrix on the surface of a sensor, which has limited biocompatibility. Whole-cell biosensors often are less costly than the corresponding enzymatic biosensors because some microorganisms can be cultivated and isolated rather easily, which is not the case for many enzymes. On the other side, they often lack specificity for the respective analytes. Whole-cell biosensors mostly are self-contained, do not require the addition of cofactors, and are the biorecognition elements of choice when the total amount of hazardous substances or pollutants is to be determined. Biosensors for determination of biological oxygen demand (BOD) represent a typical example. In contrast to such biosensors, those making use of genetically modified microorganisms can be highly specific. Another disadvantage of whole-cell biosensors is the relatively slow response (tens of minutes to hours) because the analytes need to diffuse through a cell membrane. Such response times are, however, adequate in certain cases. The standard BOD<sub>5</sub> test, for example, requires 5 days.

### 7.1. Catalytic Whole-Cell Biosensors

Biosensors for determination of biochemical oxygen demand (BOD) make use of oxygen transducers. As in the case of many enzymatic biosensors, the consumption of oxygen is monitored optically over time or at the endpoint. *Trichosporon cutaneum*<sup>379</sup> and *Bacillus subtilis*<sup>380</sup> bacteria were immobilized into poly(vinyl alcohol) (PVA) and sol–gel PVA–PVP [(poly(4-vinylpyridine))] networks. A combination of *Bacillus licheniformis* with *Dietzia maris* and *Marinobacter marinus* contained in a sol–gel–PVA matrix<sup>381</sup> was used to obtain even lower selectivity and, thus, monitor much more possible pollutants. Compared to the sensor that makes use of *B. Licheniformis* only, a decrease in LOD from 0.9 to 0.2 mg/L and in response time from 30 to 3.2 min was observed for the multibacteria sensor. In all BOD sensors, the microorganism layer was placed on an oxygen-sensitive layer of various layouts and materials. These include a quenchable ruthenium(II) complex contained in plasticized PVC,<sup>379</sup> in ormosil,<sup>381</sup> or in silicone.<sup>380</sup> Analytical ranges of the sensors were reported to be from 0 to 110,<sup>379</sup> 0 to 25,<sup>380</sup> and 0.2 to 40 mg/L,<sup>381</sup> respectively (expressed as equivalents of a glucose/glutamate BOD standard solution). The first sensor<sup>379</sup> possessed moderate stability, and a 30% drop in sensor response was observed after 1 month of storage. The shelf life of the sensors reported later was much higher (a 12% decrease in activity in 1 month for the *B. subtilis* biosensor<sup>380</sup> and only a 5% decrease in 6 months for the multibacteria sensor).<sup>381</sup>

A biosensor for the organophosphorous pesticide methyl parathion<sup>382</sup> was prepared by analogy to the enzyme-type biosensors that made use of organophosphorous hydrolase (OPH). Whole cells of *Flavobacterium sp.* containing OPH were immobilized on a glass fiber filter. Hydrolysis of methyl parathion (catalyzed by OHP) results in the formation of *p*-nitrophenol, which is readily detected by absorbance. The LOD (0.3  $\mu$ M) and analytical range (4–80  $\mu$ M) are comparable to the properties of OPH-based enzymatic biosensors.

Recombinant *E. coli* cells immobilized in agarose were placed on a nylon membrane and used for determination of

organophosphorous pesticides.<sup>383</sup> These cells are capable of expressing OPH directly on the cell surface, which improves response times because of the low resistance to mass transport of the analytes and products across the cell membrane. The sensor detected as little as 3  $\mu\text{M}$  of paraoxon and 5  $\mu\text{M}$  of coumaphos and could be stored >1 month without a decrease in activity. Evidently, the main advantage of the whole-cell biosensors for pesticides over the enzymatic ones is that no isolation of the enzyme OPH is necessary. This reduces the costs significantly and improves the long-term stability.

Araïn et al.<sup>410</sup> have studied the inhibitory effect of toxic metal ions on the cellular activity of *E. coli* and *P. putida*. Microtiter plates were prepared with integrated, fluorescence-based sensors for pH and oxygen, and bacterial respirational activity was monitored via the decrease in oxygen partial pressure of the closed system and also via the decrease in pH value. Other applications of such biosensors include respirometry and general toxicity assays.

## 7.2. External Stimuli-Based Cellular Biosensors

Whole-cell biosensors were developed for the determination of various toxicants. For example, Bains<sup>384</sup> immobilized *Escherichia coli* into an agarose membrane and monitored its UV absorbance at the unusual wavelength of 200 nm. In the presence of toxicants (e.g., sodium azide), the cells were stressed so that their metabolism was reduced and a drop in optical density was observed within 15 s. The sensitivity of the system was, however, poor with respect to the requirements of environmental monitoring.

Frense et al.<sup>385</sup> used algae cells (*Scenedesmus subspicatus*) for the determination of environmentally harmful impurities in water. These chlorophyll-containing cells were immobilized on a filter paper that was covered with a thin alginate layer. Pollutants such as atrazine, endrine, and many other pesticides inhibit the electron-transport occurring during photosynthesis. This results in the increase of fluorescence of chlorophyll. The increase of fluorescence is well-related to the concentration of the pesticides, which can be measured at levels of several parts/billion (ppb). The sensor showed comparatively fast response ( $\sim 10$  min) and good long-term stability in that storage at 4 °C within 6 months did not alter the sensor properties significantly.

A similar approach was used by Naessens et al.<sup>386</sup> who used algal cells from *Chlorella vulgaris* (immobilized on a glass microfiber) for determination of atrazine, simazine, diuron, and other pesticides with high sensitivity (e.g., as little as 5 nM of atrazine when using the sensor in a flow mode). The biosensor showed good storage stability only for a limited period of time (7 days), and significant loss of activity was observed during longer storage. Different bacteria and mutants were found to respond to different pesticide classes<sup>387</sup> because they can selectively modify the activity of photosystem II. The microorganisms were immobilized in a BSA–glutaraldehyde network deposited on a porous septum filter that was placed in a flow-through cell. Several flow-through cells were combined as an array to enable simultaneous sensing of several pesticides. The selectivity of the individual sensors, however, remained low enough, because each type of bacteria was sensitive to several classes of pesticides. The long-term stability of the biosensor was rather poor (half-life from 12 to 54 h).

## 7.3. Genetically Engineered Whole-Cell Biosensors

Progress in genetic engineering made possible the creation of a new type of microbial biosensor. It relies on the ability of a cell to respond to an environmentally harmful toxin by expressing specific genes. As a result, the toxin is transported out of the cell. To monitor the process, a reporter gene is fused to the induced gene. In the presence of the toxin, both genes are activated and expressed. A reporter gene usually is responsible for production of species that could be monitored optically, e.g., the green fluorescent protein. In a certain sense, all genetically engineered biosensors are external stimuli biosensors.

A variety of biosensors makes use of the *lux* gene coding for the enzyme luciferase. In contrast to enzymatic bioluminescent sensors, the whole-cell biosensors often are self-contained because luciferase and other reagents such as the cofactor, flavine mononucleotide, and substrate (a long-chain aldehyde) are produced in vivo. Typical examples of such biosensors are described below.

Virta et al.<sup>388</sup> developed a mercury biosensor that makes use of *Escherichia coli* containing the *lux* gene fused to the *mer* operon. The latter encodes for resistance to mercury, which is a nonessential and toxic metal for bacteria. The bioluminescence was triggered in the presence of  $\text{Hg}^{2+}$ . Concentrations as low as 0.1 fM are detectable. A linear dependence is observed up to 0.1  $\mu\text{M}$  of  $\text{Hg}^{2+}$ . At higher concentrations, the luminescence rapidly drops to zero because of the toxicity of  $\text{Hg}^{2+}$  ions. The assay exhibits high selectivity, and no interference by other metals ions (except  $\text{Cd}^{2+}$ ) is observed. Sensitivity to  $\text{Cd}^{2+}$  is, however,  $\sim 10^7$ -fold lower than that to  $\text{Hg}^{2+}$  and, therefore, does not really compromise the performance of the assay.

Another metal ion biosensor<sup>389</sup> makes use of *Escherichia coli* containing the *znt A* gene fused to the reporter *lac Z* gene. While the first is responsible for transporting heavy metal ions out of the cell, the second produces the enzyme  $\beta$ -galactosidase, which cleaves the added substrate fluorescein di- $\beta$ -D-galactopyranoside. Hence, fluorescence is increased in the presence of heavy metal ions. Individual cells of *E. coli* were immobilized on an array of 50 000 fibers ( $\varnothing$  of 2.5  $\mu\text{m}$ ) so that each bacterium occupied one individual fiber. Averaging the response from multiple identical sensors improved the signal-to-noise ratio. The LOD for  $\text{Hg}^{2+}$  was 100 nM. Unfortunately, no information is given about conceivable interferences by other heavy metal ions.

Leth et al.<sup>390</sup> have developed a biosensor for copper(II) ion based on a genetically engineered strain of *Alcaligenes eutrophus* into which was inserted a *lux* operon from *Vibrio fischeri* under the control of a copper-induced promoter. As a result, copper ions induce bioluminescence whose intensity is proportional to the concentration of the triggering ion. The cells were immobilized into calcium alginate and agarose gels, which were positioned in a home-made flow-cell, and luminescence intensity was monitored by means of a photodetector. The biosensors based on the two gels showed similar performance, which was highly influenced by the growth medium used. In fact, the analytical range of the sensor for both alginate and agarose was from 0 to 250  $\mu\text{M}$  of  $\text{Cu}^{2+}$  when using the Luria-Broth (LODs of 50 and 25  $\mu\text{M}$ , respectively). The use of a modified mineral reconstruction medium resulted in an LOD of 1  $\mu\text{M}$  and an analytical range from 0 to 25  $\mu\text{M}$  for alginate. The authors also showed



that the performance of the biosensor is influenced by the concentration of riboflavin, suggesting the necessity of using a standard composition of nutrient medium. Unfortunately, the activity of the immobilized species was shown to decrease dramatically with time. In fact, a 2 week storage resulted in the complete loss of the activity of the bacteria for both alginate and agarose biogels. After the first 6 days of storage, the activity was, however, almost unchanged for alginate, while it dropped by 7-fold in agarose.

Aromatic hydrocarbons are widespread and harmful pollutants that can be successfully detected by whole-cell biosensors. Here, the content of individual hydrocarbons is of less significance than the determination of overall toxicity. For example, Heitzer et al.<sup>391</sup> used *Pseudomonas fluorescens*, which carried the *nah G* gene fused to a *lux* reporter gene to design a naphthalene biosensor. The bacteria were physically immobilized in alginate gel that was hardened at elevated temperature in the presence of SrCl<sub>2</sub>. Exposure of this sensor layer to both naphthalene and its degradation intermediate, salicylate, results in an increase of gene expression and, consequently, an enhancement of bioluminescence. The sensor demonstrated complete reversibility for at least 20 h, but the lowest detectable concentration of naphthalene was 0.12 mM, which is rather high.

Ikariyama et al.<sup>392</sup> used *Pseudomonas putida* bearing a *xyl R* gene (which recognizes benzene and its derivatives) fused to the reporter *lux* gene from firefly. Because firefly luciferase catalyzes a different bioluminescent reaction than bacterial luciferase, addition of the substrate luciferin was necessary. The luminescent signal had a good linear relationship to the concentration of xylenes, which ranged from 0.05 to 1 mM. The response of the biosensor (where *P. putida* was immobilized onto a polycarbonate membrane) was shown to be much slower than the respective assay in solution and required hours of incubation time to achieve an adequate intensity of bioluminescence.

In contrast to the sensors described above, biosensors for toxic chemicals are based on measurement of the reduction of intensity of the bioluminescent reaction when cells experience toxic or lethal conditions. Gil et al.<sup>393</sup> immobilized a recombinant *E. coli* species bearing a *lux* reporter gene in a solid agar gel located in proximity of the distal end of an optical fiber. The biosensor was used for detection of toxic gases and vapors. As little as 48 ppm of benzene vapor could be detected. The sensor had a response time of ~10 min and could be stored up to 20 days without degradation of activity. The sensitivity can be improved by increasing the surface that is exposed to vapors and by enhancing the diffusion of vapors, which can be accomplished by addition of glass beads.<sup>394</sup> The sensitivity of other strains of bacteria bearing a *lux* reporter gene also was investigated.<sup>395</sup>

Shetty et al.<sup>396</sup> developed a bioassay for determination of L-arabinose. The binding of the monosaccharide to the *ara C* regulatory protein was linked to the production of green fluorescent protein (GFP) by the reporter gene in an *E. coli* strain. The amount of GFP expressed is, thus, directly related to the concentration of L-arabinose. The dynamic range of the assay is from 0.5  $\mu$ M to 5 mM. The sensitivity to other monosaccharides was ~10 times lower than to arabinose. A biosensor also was developed where the bacteria were entrapped behind a membrane at the tip of a bifurcated fiber bundle. Although operated similarly to the bioassay, an ~10-fold increase in the LOD was reported.

Recently, several bioassays were developed for detection of endocrine-disrupting chemicals (EDCs), compounds that affect human health by irregularly modulating endocrine functions. Michelini et al.<sup>397</sup> used recombinant *Saccharomyces cerevisiae* cells that were modified to express the human androgen receptor together with *Photinus pyralis* luciferase. The assay responds to testosterone in the concentration range from 50 pM to 1  $\mu$ M. Luciferin needs to be added to the assay solution. Compared to other available methods, the assay is rather fast (150 min of incubation needed for optimal performance against 24 h for other methods). A biosensor also was developed for estrogenic EDCs.<sup>398</sup> Genetically modified *Saccharomyces cerevisiae* cells containing the estrogen receptor were entrapped in hydrogel matrices based on calcium alginate or poly(vinyl alcohol). The LODs for the two EDCs investigated were 0.08 and 0.64  $\mu$ g/L. The immobilized cells retained their activity for 1 month, however only if stored at -80 °C.

A lactate biosensor was reported<sup>399</sup> that utilizes a bacterial cytoplasmic membrane isolated from *E. coli*, which was genetically modified to express its lactate-oxidizing activity. The sensor properties can be tuned by varying the conditions of cultivation. The cytoplasmic membranes were adsorbed on a cellulose disk placed above an oxygen transducer—a ruthenium(II)-derived luminescent probe in a silicone matrix. The sensing scheme is based on the consumption of oxygen during oxidation of lactate and is the same as that used in the enzyme based on the use of lactate oxidase. The analytical range of the biosensor is from 0.05 to 5 mM of lactate.

In some optical biosensors, even whole tissues have been used as recognition elements. For example, Lundström et al.<sup>400</sup> used fish scales from *Labrus ossifagus* containing melanophores. Their cells contain pigment granules that are either dispersed or aggregated. Aggregation of the granules is promoted by noradrenaline, which can be monitored optically via the increase in the transmittance of the scale. Addition of the noradrenaline antagonist yohimbine recovers the initial signal. Nanomol quantities of noradrenaline could be measured, and the response time of the sensor was ~10 min.

In summary, it can be stated that cellular biosensors (a) are relatively easy to manufacture; (b) are rather unspecific in the case of catalytic biosensors but fairly specific in the case of external-stimuli biosensors and gene-modified biosensors; (c) possess rather slow response; (d) are self-contained; (e) are more stable, in general, than enzymatic biosensors but are sensitive to heat and, less so, to frost; and (f) vary over a wide range in terms of sensitivity.

## 8. Solid Supports for Use in Optical Biosensors, and Other Methods of Immobilization

The success of (bio)sensor research and development depends—more often than anticipated—on the availability of adequate materials. One may differentiate between materials for mechanical sensor supports and materials for use as matrices or membranes that contain the biologically active species, or indicators in the case of catalytic biosensors. These shall be discussed here briefly in addition to the specific examples of immobilization given in section 4.4. There are three kinds of “supports” for optical biosensors.

The first one is of the completely inert type. Its only purpose is to serve as a mechanical support to facilitate the handling of planar sensors. The second is of the optical waveguide type and, thus, can serve as an essential compo-

ment in the process of optical interrogation of the sensor material. The third (and most recent) group of supports are the “active” supports such as fluorescent nanoparticles (Q-dots), metal films, beads of noble metals, or inorganic or organic micro- and nanoparticles. These can act as micro-light sources or quenchers, for example, and thus can actively take part in the spectroscopic scheme. Any of these supports can be preactivated (i.e., made bioreactive) form to enable covalent immobilization of the biocomponent or of other species.

Inert supports come in various forms and include films of poly(ethylene terephthalate), which is readily available at low costs and also easy to handle. Other supports include poly(methyl methacrylates) and polycarbonates, with their excellent optical transparency, and polystyrene, which is widely used in microtiterplates (MTPs). In most cases, the chemically responsive material (the sensor “cocktail”) is deposited, or printed, or stamped on such a support, in a groove of this material, or in the wells of a (plastic) MTP. The material, after having been deposited as a thin film on the support, is punched into sensor spots, and these are being placed in disposable sensor devices. The sensor layer is then interrogated by guiding the light beam onto the sensor layer, and reflectivity or fluorescence is measured or interference is measured. It is obvious that the mechanical supports are expected to create no background signal.

The support also may act as a waveguide material. Planar waveguides, fiber-optics, and, less often, capillaries have been applied. There are two ways to guide the exciting light to the sensor material. The first is by direct illumination and by collecting luminescence via the waveguide. The second is to use the waveguide for both the exciting beam and for collection of emitted luminescence. Both geometries have their merits (see section 4.3). Waveguide-based sensors are most elegant and, therefore, have found widespread application.

Among the third kind of supports, the nanobeads exploit the fact that, because of their intrinsic luminescence, they can act as a donor in FRET assays.<sup>55</sup> Metal particles and films, in turn, can act as quenchers or enhancers of luminescence (depending inter alia on the spatial distance between metal and fluorophore and on the kind of metal).

A most interesting class of micro- and nanoparticles is represented by the so-called upconverting phosphors (UCPs). They are capable of converting near-infrared light (from low-cost diode lasers) into visible light with fair to high efficiency. Upconversion is not related to 2-photon excitation, which occurs at strong light intensities only. UCPs (mostly oxides, sulfides, and—preferably—fluorides of trivalent lanthanide ions) enable complete elimination of autofluorescence, which commonly impairs the performance of fluorescence-based assays. UCPs are ideal donors for fluorescence resonance energy transfer (FRET)-based assays. UCP-based FRETs have been applied in immunoassays<sup>401,402</sup> and in nucleic acid hybridization assays.<sup>403,404</sup> Arguably, these methods are at the borderline between solid-phase-based biosensors of the conventional type and of classical solution assays.

With respect to materials for use as a bulk matrix for sensors, it is important to remind that the design of such sensors depends on the size of the analyte. Enzyme-based sensors usually digest or metabolize substrates of low or medium molecular weight. Hydrogel matrices, for example, are useful in the case of low-molecular-weight analytes only,

since these can penetrate the bulk matrix, where, in the case of enzyme sensors or whole-cell sensors, metabolism can occur. Immunosensors almost never are designed as bulk sensors even though they could be, at least for small analytes such as atrazine. Immunosensors for large analytes require the antibody to be immobilized on the surface of a support, usually as a nanometer thick coating or film. The situation is similar for DNA sensors where the size and diffusion of the analyte is critical. Whole-cell biosensors (in the majority of cases) have been used for low-molecular-weight analytes and, therefore, have been incorporated into analyte-permeable gels such as from alginates.

The surface of a biosensor layer is either covered with a polymer/enzyme matrix (like in most enzymatic biosensors) or directly with biorecognition elements such as antibodies or oligonucleotides. In this case, the surface needs to be made reactive first in order to allow immobilization of a biomolecule. Covalent attachment of a biomolecule to a support is much more commonly used than physical absorption. Numerous cross-linkers and spacers can be used.<sup>20,292,296</sup> Proteins such as bovine serum albumin often are also deposited on the surface, so to saturate remaining binding sites.

Immobilization of antibodies and oligonucleotides via the (noncovalent) biotin–avidin<sup>46,67,68,246,288,299</sup> or biotin–streptavidin<sup>47,354,355,371,374</sup> couple is widespread. A support modified with (strept)avidin can be used, in principle, for immobilization of any biotinylated molecule. Alternatively, biotinylated recognition elements can be immobilized via streptavidin onto a surface modified with biotin. Enzymes are often covalently immobilized onto preactivated transparent polyamide or poly(vinylidenedifluoride) membrane supports such as Immunodyne,<sup>73,90,140,163,227,228,230,232–234</sup> Biodyne,<sup>177,191,225</sup> and Immobilon.<sup>164,194,195</sup> Less common supports include eggshell membranes<sup>86,154</sup> and swim-bladder membranes<sup>88</sup> and were reported to be highly biocompatible.

Hydrophilic polymer matrixes are widely used for immobilization of biocomponents (such as enzymes and bioreceptors) and of optical indicators. Sol–gels (whose polarity can vary over a wide range by introducing organic groups to end up with ormosils)<sup>401,402</sup> have been often used for immobilization of enzymes,<sup>44,84,87,120,131,134,135,380,206,216</sup> bioreceptors,<sup>343</sup> and even whole cells.<sup>380,381</sup> One major reason for the popularity of sol–gels results from the fact that the activity of biocomponents is retained over a long time. Hydrogels have also become popular<sup>36,80,102,118,147,150,212,398</sup> because they do not require a modification of the biological component. Enzymes sometimes are cross-linked with glutaraldehyde and BSA to form a polymer network located on a support or directly in a hydrophilic polymer (e.g., PVA) layer.<sup>75,175,176,188,215,217,387</sup>

Koncki et al.<sup>97</sup> have designed optical biosensors based on the use of thin films of Prussian Blue incorporated into polypyrrole. Other semiconducting organic materials may be used as well. The composite film is deposited on a nonconducting support and used as an optical transducer for flow-through biosensors based on hydrolases and oxidases. Immobilization of glucose oxidase resulted in a glucose biosensor where the film responds to both pH and hydrogen peroxide by a change in its color. Millimolar concentrations can be determined. The biosensor is said to be quite stable owing to the presence of a poly(pyrrolylbenzoic acid) network in the composite material. This organic polymer plays a dual role as a binding agent for inorganic material

and as a functionalized support for strong covalent immobilization of enzyme molecules.

Polymer matrixes also can act as a support for the immobilization of indicators used in cellular or enzymatic sensors. Ruthenium(II) polypyridyl complexes are common when oxygen transducers are used (see Table 2). To achieve the desired oxygen sensitivity, they can be adsorbed onto silica beads that are dispersed in a layer of a highly oxygen-permeable silicone layer. Absorption-based and fluorescent pH indicators were employed in enzymatic biosensors using pH and NH<sub>3</sub> transducers. Permeability to protons is mandatory in these cases, and the indicators, therefore, often are contained in hydrogels. To prevent leaching of indicators to the sample media, they are sometimes absorbed onto the surface of microbeads.<sup>103,194</sup>

Dialysis (ultrafiltration) membranes are used in certain sensor types.<sup>41,42,48,49,221,222,224</sup> They allow small analytes to diffuse freely in and out of a chamber and interact there with a biorecognition element. The latter is either large enough itself or is conjugated with a large molecule in order to not leach out of the chamber.

In contrast to indicators, labels do not respond to substrates or reaction products but render a biomolecule detectable. Fluorescent labels are the most common ones. Fluoresceins, rhodamines, cyanine dyes, and numerous others are commercially available<sup>403</sup> and widely used (see Table 3). Ideally, a label should absorb in visible light to reduce background fluorescence, be bright, and be inert. Brightness (defined as the product of molar absorbance and quantum yield) is particularly significant and should exceed 30 000 M<sup>-1</sup>·cm<sup>-1</sup>). Since fluoresceins are viable pH indicators, thorough control of pH is essential for these labels. Luminescent colloidal semiconductor nanocrystals (quantum dots, QDs) also represent viable labels,<sup>44,55,56</sup> despite their cell toxicity and difficult surface chemistry, and can largely expand the range of useful fluorophores for biosensors.

The group of Seeger have found<sup>404</sup> that biotin-functionalized cellulose monolayers can act as a new kind of support and have used it for the fluorescent detection of single molecules via laser-induced confocal single-molecule spectroscopy in glass-bottom microplates. Gold nanobeads can be used to increase the brightness of fluorescent biosensors.<sup>37,272,345,405</sup>

## 9. Outlook

Optical biosensing has experienced a substantial growth despite the usual critical comments of certain “experts” that expect new technologies to make a breakthrough (mainly in commercial terms) within a few years and despite the overoptimistic presentations of certain researchers, which often does more harm to a new technology than supporting it. Optical biosensor technology is not a matter of spectroscopy only, or of material sciences, or any other single discipline, but rather requires various kinds of scientists to cooperate in order to end up with a viable biosensor scheme and, ideally, commercial products. Optical biosensors have numerous applications, and not each scheme will be applicable to any given analyte. Moreover, methods that may work for a specific analyte in a certain matrix may not even work for the same analyte in another matrix. This fact is but one of the reasons why biosensors, in a commercial sense, are not as successful as was expected initially.

The trend toward multianalyte sensing and toward biosensor arrays is obvious, even though certain single sensor

spots in an array may not be needed in any conceivable application. DNA arrays are technically the most advanced, not the least because DNA is built from 4 nucleotides only, which makes synthetic and surface chemistry comparably more simply than in the case of protein arrays. Enzyme arrays are rather established and have found application in clinical analyzers for glucose, urea, cholesterol, and lactate. Protein arrays are most versatile but also can be most complex, and this has hampered their technical realization. Proteins not only come in a variety of sequences (of 20 different amino acids!) but also in a variety of tertiary and quaternary structures, which makes labeling and immobilization an experience in each single case. Unfortunately, the current terror hype has directed research in protein arrays away from health and environment into other areas, which implies a massive redirection of tax money and appears not to really represent a useful long-term investment.

## 10. List of Abbreviations and Acronyms

Abs.	absorption
AChE	acetylcholine esterase
ADH	alcohol dehydrogenase
AOx	alcohol oxidase
AMPT	2-(2-acetoxy-5-methylphenylazo)- <i>N</i> -methyl-1,3-thiazolium methosulfate
ASF	African swine fever
BL	bioluminescence
BSA	bovine serum albumine
BTB	bromothymol blue
BTP	benzo[ <i>a</i> ]pyrene tetraol
b. luciferase	bacterial luciferase
CCA	chlorendic capronic acid
ChOx	choline oxidase
CLum.	chemiluminescence
CF	5(and 6)-carboxyfluorescein
CFU	colony-forming units
CDNB	1-chloro-2,4-dinitrobenzene
Cy-5	carboxymethylindocyanine succinimidyl ester
2,4-D	2,4-dinitrophenoxyacetic acid
DDAO	7-hydroxy-9H-1,3-dichloro-9,9-dimethylacridin-2-one
DFP	diisopropyl phosphorofluoridate
f. luciferase	firefly luciferase
EDC	ethyl-3-[1-dimethylaminopropyl]carbodiimide
ELum.	electroluminescence
EuTc	europium(III) tetracycline
FITC	fluorescein isothiocyanate
FRET	fluorescence resonance energy transfer
GAH	glutaminase
GDH	glucose dehydrogenase
GFOR	glucose-fructose oxidoreductase
GLOx	glutamate oxidase
GIDH	glutamate dehydrogenase
GOx	glucose oxidase
GPT	glutamic-pyruvic transaminase
GSH	glutathione
GST	glutathione- <i>S</i> -transferase
hCG	chorionic gonadotrophin
HPOx	horseradish peroxidase
HPTS	8-hydroxypyrene-1,3,6-trisulfonate
IgG	immunoglobulin
I.	intensity
LDH	lactate dehydrogenase
LOx	lactate oxidase
Lum.	luminescence
LyOx	lysine oxidase
NHS	<i>N</i> -hydroxysuccinimide
OPH	organophosphate hydrolase



OR	oxidoreductase
ORP	organophosphorous pesticides
PEG	poly(ethylene glycol)
PMMA	polymethylmethacrylate
POx	peroxidase
PSA	prostate-specific antigen
PtOEP	platinum(II) octaethylporphyrin
RDX	hexaxydro-1,3,5-trinitro-1,3,5-triazine
Refl.	reflectance
Ru-bipy	ruthenium(II) trisbipyridyl
Ru-phen	ruthenium(II) tris(1,10-phenanthroline)
Ru-dpp	ruthenium(II) tris(4,7-diphenyl-1,10-phenanthroline)
SEB	staphylococcal Enterotoxin B
SNARF	seminaphthofluorescein
TCPB	2,4,6-trichlorophenoxybutyrate
Ti(IV) reagent	titanium(IV) + 24(5-bromopyridyl)azo-5-( <i>N</i> -propyl- <i>N</i> -sulfopropylamino)phenol
TMR	tetramethylrhodamine
TNB	trinitrobenzene
TNT	trinitrotoluene
TRITC	tetramethylrhodamine-5-isothiocyanate
triazine derivative	4-chloro-6-(isopropylamine)-1,3,5-triazine-2-(6-aminohexane carboxylic acid)
TSH	thyroid stimulating hormone
XOx	xanthine oxidase

## 11. References

- Turner, A. P. F.; Karube, I.; Wilson, G. S., Eds. *Biosensors: Fundamentals and Applications*; Oxford University Press: Oxford, U.K., 1987.
- Edmonds, T. E., Ed. *Chemical Sensors*; Blackie and Son, Ltd.: London, U.K., 1988.
- Blum, L. J.; Coulet, P. R. *Biosensor Principles and Applications*; Marcel Dekker Inc.: New York, 1991.
- Wolfbeis, O. S., Ed. *Fiber Optic Chemical Sensors and Biosensors*; CRC Press: Boca Raton, FL, 1991; Vol. 1 and 2.
- Hall, E. A. H. *Biosensors*; Open University Press: Buckingham, U.K., 1990.
- Valcárel, M.; Luque de Castro, M. D. *Flow-Through (Bio)Chemical Sensors*; Elsevier: Amsterdam, The Netherlands, 1994.
- Taylor, R. F.; Schultz, J. S., Eds. *Handbook of Chemical and Biological Sensors*; Inst. Physics Publ.: Bristol, Philadelphia, PA, 1996.
- Vincenzini, P.; Dori, L., Eds. *Solid State Chemical and Biochemical Sensors*; Techna Publ.: Faenza, Italy, 1999.
- Ramsden, J. J. *J. Mol. Recognit.* **1997**, *10*, 109.
- Mehrvan, M.; Bis, C.; Scharer, J. M.; Moo-Young, M.; Luong, J. *Anal. Sci.* **2000**, *16*, 677.
- Kuswandi, B.; Andres, R.; Narayanaswamy, R. *Analyst* **2001**, *126*, 1469.
- Schobel, U.; Barzen, C.; Gauglitz, G. *Fresenius J. Anal. Chem.* **2000**, *366*, 646.
- Marazuela, M. D.; Moreno-Bondi, M. C. *Anal. Bioanal. Chem.* **2002**, *372*, 664.
- Monk, D. J.; Walt, D. R. *Anal. Bioanal. Chem.* **2004**, *379*, 931.
- Rogers, K. R.; Mulchandani, A. *Affinity Biosensors*; Humana Press: Totowa, NJ, 1998.
- Pickup, J. C.; Hussain, F.; Evans, N. D.; Rolinski, O. J.; Birch, D. J. S. *Biosens. Bioelectron.* **2005**, *20*, 2555.
- Marquette, C. A.; Blum, L. J. *Biosens. Bioelectron.* **2006**, *21*, 1424.
- Leca-Bouvier, B.; Blum, L. J. *Anal. Lett.* **2005**, *38*, 1491.
- Taitt, C. R.; Anderson, G. P.; Ligler, F. S. *Biosens. Bioelectron.* **2005**, *20*, 2470.
- Choi, M. M. F. *Microchim. Acta* **2004**, *148*, 107.
- Wolfbeis, O. S. *Anal. Chem.* **2004**, *76*, 3269.
- Wolfbeis, O. S. *Anal. Chem.* **2006**, *78*, 3859–3873.
- Brogan, K. L.; Walt, D. R. *Curr. Opin. Chem. Biol.* **2005**, *9*, 494.
- Nagl, S.; Schaeferling, M.; Wolfbeis, O. S. *Microchim. Acta* **2005**, *151*, 1.
- Walt, D. R. *Science* **2005**, *308*, 217.
- Walt, D. R. *BioTechniques* **2006**, *41*, 529.
- Wolfbeis, O. S. *Anal. Chem.* **2006**, *78*, 3859.
- Göpel, W.; Hesse, J.; Zemel, J. N., Eds. *Sensors: A Comprehensive Survey*; VCH Publishers: Weinheim, Germany, 1991; Vol. 2, Part 1, pp 1–27.
- Hulanicki, A.; Geab, S.; Ingman, F. *Pure Appl. Chem.* **1991**, *63*, 1247.
- Thevenot, D. R.; Toth, K.; Durst, R. A.; Wilson, G. S. *Biosens. Bioelectron.* **2001**, *16*, 121.
- Hilty, C.; Lowery, T. J.; Wemmer, D. E.; Pines, A. *Angew. Chem., Int. Ed.* **2005**, *45*, 70.
- Valcarcel, M.; Luque de Castro, M. D. *Flow-Through (Bio)Chemical Sensors*; Elsevier: Amsterdam, The Netherlands, 1994.
- Parker, C. A. *Photoluminescence of Solutions*; Elsevier: Amsterdam, The Netherlands, 1981.
- Yadavalli, V. K.; Koh, W. G.; Lazur, G. J.; Pishko, M. V. *Sens. Actuators, B* **2004**, *97*, 290.
- Xu, H.; Aylott, J. W.; Kopelman, R. *Analyst* **2002**, *127*, 1471.
- Russell, R. J.; Pishko, M. V.; Simonian, A. L.; Wild, J. R. *Anal. Chem.* **1999**, *71*, 4909.
- Simonian, A. L.; Good, T. A.; Wang, S. S.; Wild, J. R. *Anal. Chim. Acta* **2005**, *534*, 69.
- Viveros, L.; Paliwal, S.; McCrae, D.; Wild, J.; Simonian, A. L. *Sens. Actuators, B* **2006**, *115*, 150.
- Tsai, H. C.; Doong, R. A. *Anal. Biochem.* **2004**, *334*, 183.
- Ueberfeld, J.; Walt, D. R. *Anal. Chem.* **2004**, *76*, 947.
- Anderson, F. P.; Miller, W. G. *Clin. Chem.* **1988**, *34*, 1417.
- Hanbury, C. M.; Miller, W. G.; Harris, R. B. *Biosens. Bioelectron.* **1996**, *11*, 1129.
- Ko, S.; Grant, S. A. *Biosens. Bioelectron.* **2006**, *21*, 1283.
- Aoyagi, S.; Kudo, M. *Biosens. Bioelectron.* **2005**, *20*, 1680.
- Tyagi, S.; Kramer, F. R. *Nat. Biotechnol.* **1996**, *14*, 303.
- Fang, X.; Liu, X.; Schuster, S.; Tan, W. *J. Am. Chem. Soc.* **1999**, *121*, 2921.
- Liu, X.; Tan, W. *Anal. Chem.* **1999**, *71*, 5054.
- Meadows, D.; Schultz, J. S. *Talanta* **1988**, *35*, 145.
- Astles, J. R.; Miller, W. G. *Sens. Actuators, B* **1993**, *11*, 73.
- Song, X.; Swanson, B. I. *Anal. Chem.* **1999**, *71*, 2097.
- Thompson, R. B.; Ge, Z.; Patchan, M.; Huang, C. C.; Fierke, C. A. *Biosens. Bioelectron.* **1996**, *11*, 557.
- Thompson, R. B.; Patchan, M. W. *Anal. Biochem.* **1995**, *227*, 123.
- Ye, K.; Schultz, J. S. *Anal. Chem.* **2003**, *75*, 3451.
- Chinnayelka, S.; McShane, M. J. *Anal. Chem.* **2005**, *77*, 5501.
- Medintz, I. L.; Clapp, A. R.; Mattoussim, H.; Goldman, E. R.; Fisher, B.; Mauro, J. M. *Nat. Mater.* **2003**, *2*, 630.
- Sandros, M. G.; Gao, D.; Benson, D. E. *J. Am. Chem. Soc.* **2005**, *127*, 12198.
- Zeng, H. H.; Thompson, R. B.; Maliway, B. P.; Fones, G. R.; Moffett, J. W.; Fierke, C. A. *Anal. Chem.* **2003**, *75*, 6807.
- Papkovsky, D. B. *Sens. Actuators, B* **1993**, *11*, 293.
- Papkovsky, D. B.; Olah, J.; Kurochkin, I. N. *Sens. Actuators, B* **1993**, *11*, 525.
- Papkovsky, D. B.; O'Riordan, T. C.; Guilbault, G. G. *Anal. Chem.* **1999**, *71*, 1568.
- Schaeferling, M.; Wu, M.; Wolfbeis, O. S. *J. Fluoresc.* **2004**, *14*, 561.
- D'Auria, S.; Gryczynski, Z.; Gryczynski, I.; Rossi, M.; Lakowicz, J. R. *Anal. Biochem.* **2000**, *283*, 83.
- Dattelbaum, J. D.; Lakowicz, J. R. *Anal. Biochem.* **2001**, *291*, 89.
- Sanz-Vicente, I.; Castillo, J. R.; Galban, J. *Talanta* **2005**, *65*, 946.
- Hoefelschweiger, B. K.; Pfeifer, L.; Wolfbeis, O. S. *J. Biomol. Screening* **2005**, *10*, 685.
- Heideman, R. G.; Kooyman, R. P. H.; Greve, J. *Sens. Actuators, B* **1991**, *4*, 297.
- Stamm, Ch.; Lukosz, W. *Sens. Actuators, B* **1996**, *31*, 203.
- Clerc, D.; Lukosz, W. *Sens. Actuators, B* **1997**, *40*, 53.
- Brecht, A.; Piehler, J.; Lang, G.; Gauglitz, G. *Anal. Chim. Acta* **1995**, *311*, 289.
- Szekacs, A.; Trummer, N.; Adanyi, N.; Varadi, M.; Szendro, I. *Anal. Chim. Acta* **2003**, *487*, 31.
- Ruckstuhl, T.; Rankl, M.; Seeger, S. *Biosens. Bioelectron.* **2003**, *18*, 1193.
- Zourob, M.; Hawkes, J. J.; Coakley, W. T.; Brown, B. J. T.; Fielden, P. R.; McDonnell, M. B.; Goddard, N. J. *Anal. Chem.* **2005**, *77*, 6163.
- Trettnak, W.; Leiner, M. J.; Wolfbeis, O. S. *Analyst* **1988**, *113*, 1519.
- Dremel, B. A.; Schaffar, B. P.; Schmid, R. D. *Anal. Chim. Acta* **1989**, *225*, 293.
- Schaffar, B. P.; Wolfbeis, O. S. *Biosens. Bioelectron.* **1990**, *5*, 137.
- Moreno-Bondi, M. C.; Wolfbeis, O. S.; Leiner, M. J.; Schaffar, B. P. *Anal. Chem.* **1990**, *62*, 2377.
- Dremel, B. A.; Li, S. Y.; Schmid, R. D. *Biosens. Bioelectron.* **1992**, *7*, 133.
- Andres, K. D.; Wehnert, G.; Thordsen, O.; Scheper, T. *Sens. Actuators, B* **1993**, *11*, 395.
- Valencia-Gonzalez, M. J.; Liu, Y. M.; Diaz-Garcia, M. E.; Sanz-Medel, A. *Anal. Chim. Acta* **1993**, *283*, 439.
- Li, L.; Walt, D. R. *Anal. Chem.* **1995**, *67*, 3746.
- Neubauer, A.; Pum, D.; Sleytr, U. B.; Klimant, I.; Wolfbeis, O. S. *Biosens. Bioelectron.* **1996**, *11*, 317.
- Rosenzweig, Z.; Kopelman, R. *Anal. Chem.* **1996**, *68*, 1408.

- (83) Rosenzweig, Z.; Kopelman, R. *Sens. Actuators, B* **1996**, *35–36*, 475.
- (84) Wu, X.; Choi, M. M. F.; Xiao, D. *Analyst* **2000**, *125*, 157.
- (85) Wolfbeis, O. S.; Oehme, I.; Papkovskaya, N.; Klimant, I. *Biosens. Bioelectron.* **2000**, *15*, 69.
- (86) Choi, M. M. F.; Wilfred, S. *Analyst* **2001**, *126*, 1558.
- (87) Wu, X. J.; Choi, M. M. F. *Anal. Chim. Acta* **2004**, *514*, 219.
- (88) Zhou, Z.; Qiao, L.; Zhang, P.; Xiao, D.; Choi, M. M. F. *Anal. Bioanal. Chem.* **2005**, *383*, 673.
- (89) Matsubara, C.; Kudo, K.; Kawashita, T.; Takamura, K. *Anal. Chem.* **1985**, *57*, 1107.
- (90) Abdel-Latif, M. S.; Guilbault, G. G. *Anal. Chim. Acta* **1989**, *221*, 11.
- (91) Blum, L. J. *Enzyme Microb. Technol.* **1993**, *15*, 407.
- (92) Kremeskoetter, J.; Wilson, R.; Schiffrin, D. J.; Luff, B. J.; Wilkinson, J. S. *Meas. Sci. Technol.* **1995**, *6*, 1325.
- (93) Zhou, X.; Arnold, M. A. *Anal. Chim. Acta* **1995**, *304*, 147.
- (94) Marquette, C. A.; Blum, L. J. *Anal. Chim. Acta* **1999**, *381*, 1.
- (95) Harms, D.; Meyer, J.; Westerheide, L.; Krebs, B.; Karst, U. *Anal. Chim. Acta* **1999**, *401*, 83.
- (96) Marquette, C. A.; Leca, B. D.; Blum, L. J. *Luminescence* **2001**, *16*, 159.
- (97) Koncki, R.; Lenarczuk, T.; Radomska, A.; Glab, S. *Analyst* **2001**, *126*, 1080.
- (98) Lenarczuk, T.; Wencel, D.; Glab, S.; Koncki, R. *Anal. Chim. Acta* **2001**, *447*, 23.
- (99) Zhu, L.; Li, Y.; Zhu, G. *Sens. Actuators, B* **2002**, *86*, 209.
- (100) Zhu, L.; Li, Y.; Tian, F.; Xu, B.; Zhu, G. *Sens. Actuators, B* **2002**, *84*, 265.
- (101) Wolfbeis, O. S.; Schaeferling, M.; Duerkop, A. *Microchim. Acta* **2003**, *143*, 221.
- (102) Heo, J.; Crooks, R. M. *Anal. Chem.* **2005**, *77*, 6843.
- (103) Trettnak, W.; Leiner, M. J.; Wolfbeis, O. S. *Biosens.* **1988**, *4*, 15.
- (104) McCurley, M. F. *Biosens. Bioelectron.* **1994**, *9*, 527.
- (105) Piletsky, S. A.; Panasyuk, T. L.; Piletskaya, E. V.; Sergeeva, T. A.; El'skaya, A. V.; Pringsheim, E.; Wolfbeis, O. S. *Fresenius J. Anal. Chem.* **2000**, *366*, 807.
- (106) Voelkl, K. P.; Opitz, N.; Luebbbers, D. W. *Adv. Exp. Med. Biol.* **1988**, *222*, 199.
- (107) Knobbe, E. T.; Dunn, B.; Gold, M. *Proc. SPIE* **1989**, *906*, 39.
- (108) Cox, J. A.; Hensley, P. M.; Loch, C. L. *Microchim. Acta* **2003**, *142*, 1.
- (109) Wolfbeis, O. S.; Leiner, M. J. P.; Posch, H. E. *Microchim. Acta* **1986**, *90*, 359.
- (110) Alford, P. C.; Cook, M. J.; Lewis, A. P.; McAuliffe, S. G.; Skarda, V.; Thomson, A. J. *J. Chem. Soc., Perkin Trans. II* **1985**, *5*, 705.
- (111) Suchomel, P.; Wolfbeis, O. S. Unpublished results, 2007.
- (112) Pasic, A.; Koehler, H.; Schaupp, L.; Pieber, T. R.; Klimant, I. *Anal. Bioanal. Chem.* **2006**, *386*, 1293.
- (113) Pasic, A.; Koehler, H.; Klimant, I.; Schaupp, L. *Sens. Actuators, B* **2007**, *122*, 60.
- (114) Liebsch, G.; Klimant, I.; Wolfbeis, O. S. *Adv. Mater.* **1999**, *11*, 1296.
- (115) Mongey, K. F.; Vos, J. G.; MacCraith, B. D.; McDonagh, C. M.; Coates, C.; McGarvey, J. J. *J. Mater. Chem.* **1997**, *7*, 1473.
- (116) Borisov, S. M.; Wolfbeis, O. S. *Anal. Chem.* **2006**, *78*, 5094.
- (117) Borisov, S. M.; Vasylevska, A. S.; Krause, Ch.; Wolfbeis, O. S. *Adv. Funct. Mater.* **2006**, *16*, 1536.
- (118) Freeman, T. M.; Seitz, W. R. *Anal. Chem.* **1978**, *50*, 1243.
- (119) Preuschoff, F.; Spohn, U.; Janasek, D.; Weber, E. *Biosens. Bioelectron.* **1994**, *9*, 543.
- (120) Navas Diaz, A.; Ramos Peinado, M. C.; Torijas Minduez, M. C. *Anal. Chim. Acta* **1998**, *363*, 221.
- (121) Ramos, M. C.; Troijas, M. C.; Navas Diaz, A. *Sens. Actuators, B* **2001**, *73*, 71.
- (122) Schubert, F.; Wang, F.; Rinneberg, H. *Microchim. Acta* **1995**, *121*, 237.
- (123) Kim, S. H.; Kim, B.; Yadavalli, V. K.; Pishko, M. V. *Anal. Chem.* **2005**, *77*, 6828.
- (124) Pastor, I.; Esquembre, R.; Micol, V.; Mallavia, R.; Mateo, C. R. *Anal. Biochem.* **2004**, *334*, 335.
- (125) Wolfbeis, O. S.; Duerkop, A.; Wu, M.; Lin, Z. *Angew. Chem., Int. Ed.* **2002**, *41*, 4495.
- (126) Trettnak, W.; Wolfbeis, O. S. *Anal. Chim. Acta* **1989**, *221*, 195.
- (127) Trettnak, W.; Wolfbeis, O. S. *Fresenius J. Anal. Chem.* **1989**, *334*, 427.
- (128) Chudobova, I.; Vrbova, E.; Kodicek, M.; Janovcova, J.; Kas, J. *Anal. Chim. Acta* **1996**, *319*, 103.
- (129) Sierra, J. F.; Galban, J.; Castillo, J. R. *Anal. Chem.* **1997**, *69*, 1471.
- (130) De Marcos, S.; Sanz, V.; Andreu, Y.; Galban, J. *Microchim. Acta* **2006**, *153*, 163.
- (131) De Marcos, S.; Galindo, J.; Sierra, J. F.; Galban, J.; Castillo, J. R. *Sens. Actuators, B* **1999**, *57*, 227.
- (132) Sanz, V.; Galban, J.; de Marcos, S.; Castillo, J. R. *Talanta* **2003**, *60*, 415.
- (133) Sanz, V.; de Marcos, S.; Galban, J. *Biosens. Bioelectron.* **2007**, *22*, 956.
- (134) Aylott, J. W.; Richardson, D. J.; Russell, D. A. *Analyst* **1997**, *122*, 77.
- (135) Ferretti, S.; Lee, S. K.; MacCraith, B. D.; Oliva, A. G.; Richardson, D. J.; Russell, D. A.; Sapsford, K. E.; Vidal, M. M. *Analyst* **2000**, *125*, 1993.
- (136) De Marcos, S.; Galban, J.; Albajez, R.; Castillo, J. R. *Anal. Chim. Acta* **1997**, *343*, 117.
- (137) De Marcos, S.; Galban, J.; Alonso, C.; Castillo, J. R. *Analyst* **1997**, *122*, 355.
- (138) Galban, J.; de Marcos, S.; Segura, P.; Castillo, J. R. *Anal. Chim. Acta* **1994**, *299*, 277.
- (139) Blankenstein, G.; Preuschoff, F.; Spohn, U.; Mohr, K. H.; Kula, M. R. *Anal. Chim. Acta* **1993**, *271*, 231.
- (140) Spohn, U.; Preuschoff, F.; Blankenstein, G.; Janasek, D.; Kula, M. R.; Hacker, A. *Anal. Chim. Acta* **1995**, *303*, 109.
- (141) Kar, S.; Arnold, M. A. *Anal. Chem.* **1992**, *64*, 2438.
- (142) Cattaneo, M. V.; Male, K. B.; Luong, J. H. *Biosens. Bioelectron.* **1992**, *7*, 569.
- (143) Cattaneo, M. V.; Luong, J. H. *Biotechnol. Bioeng.* **1993**, *41*, 659.
- (144) Dremel, B. A.; Yang, W.; Schmid, R. D. *Anal. Chim. Acta* **1990**, *234*, 107.
- (145) Wolfbeis, O. S.; Posch, H. E. *Fresenius J. Anal. Chem.* **1988**, *332*, 255.
- (146) Mitsubayashi, K.; Kon, T.; Hashimoto, Y. *Biosens. Bioelectron.* **2003**, *19*, 193.
- (147) Wu, X. J.; Choi, M. M. F. *Anal. Chem.* **2004**, *76*, 4279.
- (148) Trettnak, W.; Wolfbeis, O. S. *Anal. Biochem.* **1990**, *184*, 124.
- (149) Marazuela, M. D.; Cuesta, B.; Moreno-Bondi, M. C.; Quejido, A. *Biosens. Bioelectron.* **1997**, *12*, 233.
- (150) Wu, X. J.; Choi, M. M. F. *Anal. Chem.* **2003**, *75*, 4019.
- (151) Xie, X.; Shakhsher, Z.; Suleiman, A. A.; Guilbault, G. G. *Talanta* **1994**, *41*, 317.
- (152) Li, X.; Rosenzweig, Z. *Anal. Chim. Acta* **1997**, *353*, 263.
- (153) Wu, X. J.; Choi, M. M. F.; Wu, X. M. *Analyst* **2004**, *129*, 1143.
- (154) Xiao, D.; Choi, M. M. F. *Anal. Chem.* **2002**, *74*, 863.
- (155) Opitz, N.; Luebbbers, D. W. *Talanta* **1988**, *35*, 123.
- (156) Marazuela, M. D.; Moreno-Bondi, M. C. *Anal. Chim. Acta* **1998**, *374*, 19.
- (157) Kotsira, V. P.; Clonis, Y. D. *J. Agric. Food Chem.* **1998**, *46*, 3389.
- (158) Trettnak, W.; Wolfbeis, O. S. *Anal. Lett.* **1989**, *22*, 2191.
- (159) Blum, L. J.; Gautier, S. M.; Berger, A.; Michel, P. E.; Coulet, P. R. *Sens. Actuators, B* **1995**, *29*, 1.
- (160) Xie, X.; Suleiman, A. A.; Guilbault, G. G.; Yang, Z.; Sun, Z. *Anal. Chim. Acta* **1992**, *266*, 325.
- (161) Tsafack, V. C.; Marquette, C. A.; Pizzolato, F.; Blum, L. J. *Biosens. Bioelectron.* **2000**, *15*, 125.
- (162) Preuschoff, F.; Spohn, U.; Weber, E.; Unverhau, K.; Mohr, K. H. *Anal. Chim. Acta* **1993**, *280*, 185.
- (163) Hlavay, J.; Guilbault, G. G. *Anal. Chim. Acta* **1994**, *299*, 91.
- (164) Hlavay, J.; Haemmerli, S. D.; Guilbault, G. G. *Biosens. Bioelectron.* **1994**, *9*, 189.
- (165) Rauch, P.; Ferri, E. N.; Girotti, S.; Rauchova, H.; Carrea, G.; Bovara, R.; Fini, F.; Roda, A. A. *Anal. Biochem.* **1997**, *245*, 133.
- (166) Tsafack, V. C.; Marquette, C. A.; Leca, B.; Blum, L. J. *Analyst* **2000**, *125*, 151.
- (167) Gong, Z.; Zhang, Z. *Anal. Lett.* **1996**, *29*, 695.
- (168) ZhuJun, Z.; Zhilong, G.; Wangbai, M. *Microchem. J.* **1995**, *52*, 131.
- (169) Marquette, C. A.; Degiuli, A.; Blum, L. J. *Biosens. Bioelectron.* **2003**, *19*, 433.
- (170) Marquette, C. A.; Thomas, D.; Degiuli, A.; Blum, L. J. *Anal. Bioanal. Chem.* **2003**, *377*, 922.
- (171) Corgier, B. P.; Marquette, C. A.; Blum, L. J. *Anal. Chim. Acta* **2005**, *538*, 1.
- (172) Goldfinch, M. J.; Lowe, C. R. *Anal. Biochem.* **1984**, *138*, 430.
- (173) Yerian, T. D.; Christian, G. D.; Ruzicka, J. *Anal. Chem.* **1988**, *60*, 1250.
- (174) Busch, M.; Hoebel, W.; Polster, J. *J. Biotechnol.* **1993**, *31*, 327.
- (175) Kulp, T. J.; Camins, I.; Angel, S. M.; Munkholm, C.; Walt, D. R. *Anal. Chem.* **1987**, *59*, 2849.
- (176) Fuh, M. R. S.; Burgess, L. W.; Christian, G. D. *Anal. Chem.* **1988**, *60*, 433.
- (177) Xie, X.; Suleiman, A. A.; Guilbault, G. G. *Biotechnol. Bioeng.* **1992**, *39*, 1147.
- (178) Hoebel, W.; Papperger, A.; Polster, J. *Biosens. Bioelectron.* **1992**, *7*, 549.
- (179) Healey, B. G.; Walt, D. R. *Anal. Chem.* **1995**, *67*, 4471.
- (180) Yerian, T. D.; Christian, G. D.; Ruzicka, J. *Analyst* **1986**, *111*, 865.
- (181) Gauglitz, G.; Reichert, M. *Sens. Actuators, B* **1992**, *6*, 83.
- (182) Scheper, Th.; Brandes, W.; Maschke, H.; Ploez, F.; Mueller, C. J. *Biotechnol.* **1993**, *31*, 345.



- (183) Busch, M.; Gutberlet, F.; Hoebel, W.; Polster, J.; Schmidt, H. L.; Schwenk, M. *Sens. Actuators, B* **1993**, *11*, 407.
- (184) de Marcos, S.; Hortigüela, R.; Galban, J.; Castillo, J. R.; Wolfbeis, O. S. *Microchim. Acta* **1999**, *130*, 267.
- (185) Koncki, R.; Wolfbeis, O. S. *Biosens. Bioelectron.* **1999**, *14*, 87.
- (186) Brennan, J. D.; Brown, R. S.; Manna, A. D.; Kallury, K. M.; Piuanno, P. P.; Krull, U. J. *Sens. Actuators, B* **1993**, *11*, 109.
- (187) Schalkhammer, Th.; Lobmaier, Ch.; Pittner, F.; Leitner, A.; Brunner, H.; Aussenegg, F. R. *Sens. Actuators, B* **1995**, *24–25*, 166.
- (188) Rhines, T. D.; Arnold, M. A. *Anal. Chim. Acta* **1989**, *227*, 387.
- (189) Xie, X.; Suleiman, A. A.; Guilbault, G. G. *Anal. Lett.* **1990**, *23*, 2143.
- (190) Xie, X.; Suleiman, A. A.; Guilbault, G. G. *Talanta* **1991**, *38*, 1197.
- (191) Wolfbeis, O. S.; Li, H. *Biosens. Bioelectron.* **1993**, *8*, 161.
- (192) Kawabata, Y.; Sugamoto, H.; Imasaka, T. *Anal. Chim. Acta* **1993**, *283*, 689.
- (193) Stamm, Ch.; Seiler, K.; Simon, W. *Anal. Chim. Acta* **1993**, *282*, 229.
- (194) Sansubrin, A.; Mascini, M. *Biosens. Bioelectron.* **1994**, *9*, 207.
- (195) Mascini, M. *Sens. Actuators, B* **1995**, *29*, 121.
- (196) Chen, H.; Wang, E. *Anal. Lett.* **2000**, *33*, 997.
- (197) Arnold, M. A. *Anal. Chem.* **1985**, *57*, 565.
- (198) Freeman, T. M.; Bachas, L. G. *Biosens. Bioelectron.* **1992**, *7*, 49.
- (199) Trettnak, W.; Reiningner, F.; Zinterl, E.; Wolfbeis, O. S. *Sens. Actuators, B* **1993**, *11*, 87.
- (200) Navas Diaz, A.; Ramos Peinado, M. C. *Sens. Actuators, B* **1997**, *38–39*, 426.
- (201) Choi, J. W.; Kim, Y. K.; Lee, I. H.; Min, J.; Lee, W. H. *Biosens. Bioelectron.* **2001**, *16*, 937.
- (202) Choi, J. W.; Kim, Y. K.; Song, S. Y.; Lee, I. H.; Lee, W. H. *Biosens. Bioelectron.* **2003**, *18*, 1461.
- (203) Choi, J. W.; Kim, Y. K.; Oh, B. K.; Song, S. Y.; Lee, H. L. *Biosens. Bioelectron.* **2003**, *18*, 591.
- (204) Xavier, M. P.; Vallejo, B.; Marazuela, M. D.; Moreno-Bondi, M. C.; Baldini, F.; Falai, A. *Biosens. Bioelectron.* **2000**, *14*, 895.
- (205) Andreou, V. G.; Clonis, Y. D. *Biosens. Bioelectron.* **2002**, *17*, 61.
- (206) Doong, R. A.; Tsai, H. C. *Anal. Chim. Acta* **2001**, *434*, 239.
- (207) Tsai, H. C.; Doong, R. A. *Biosens. Bioelectron.* **2005**, *20*, 1796.
- (208) Vamvakaki, V.; Fournier, D.; Chaniotakis, N. A. *Biosens. Bioelectron.* **2005**, *21*, 384.
- (209) Mulchandani, A.; Pan, S.; Chen, W. *Biotechnol. Prog.* **1999**, *15*, 130.
- (210) Preiningner, C. *Microchim. Acta* **1999**, *130*, 209.
- (211) Kuswandi, B. A. *Bioanal. Chem.* **2003**, *376*, 1104.
- (212) Walker, J. P.; Asher, S. A. *Anal. Chem.* **2005**, *77*, 1596.
- (213) Narayanaswamy, R.; Sevilla, F. *Anal. Lett.* **1988**, *21*, 1165.
- (214) Wangsa, J.; Arnold, M. A. *Anal. Chem.* **1988**, *60*, 1080.
- (215) Zhang, W.; Chang, H.; Rechnitz, G. A. *Anal. Chim. Acta* **1997**, *350*, 59.
- (216) Li, C. I.; Lin, Y. H.; Shin, C. L.; Tsaui, J. P.; Chau, L. K. *Biosens. Bioelectron.* **2002**, *17*, 323.
- (217) Wang, A.-J.; Arnold, M. A. *Anal. Chem.* **1992**, *64*, 1051.
- (218) Cordek, J.; Wang, X.; Tan, W. *Anal. Chem.* **1999**, *71*, 1529.
- (219) Walters, B. S.; Nielsen, T. J.; Arnold, M. A. *Talanta* **1988**, *35*, 151.
- (220) Williams, A. K.; Hupp, J. T. *J. Am. Chem. Soc.* **1998**, *120*, 4366.
- (221) Scheper, T.; Buckmann, A. F. *Biosens. Bioelectron.* **1990**, *5*, 125.
- (222) Schelp, C.; Scheper, T.; Buckmann, A. F.; Reardon, K. F. *Anal. Chim. Acta* **1991**, *225*, 223.
- (223) Lee, S. J.; Scheper, T.; Buckmann, A. F. *Biosens. Bioelectron.* **1994**, *9*, 29.
- (224) Lee, S. J.; Saleemuddin, M.; Scheper, T.; Loos, H.; Sahn, H. J. *Biotechnol.* **1994**, *36*, 39.
- (225) Gautier, S. M.; Blum, L. J.; Coulet, P. R. *Biosens.* **1989**, *4*, 181.
- (226) Blum, L. J.; Gautier, S. M.; Coulet, P. R. *Anal. Lett.* **1988**, *21*, 717.
- (227) Blum, L. J.; Gautier, S. M.; Coulet, P. R. *Anal. Chim. Acta* **1989**, *222*, 331.
- (228) Gautier, S. M.; Blum, L. J.; Coulet, P. R. *Anal. Chim. Acta* **1990**, *235*, 243.
- (229) Gautier, S. M.; Blum, L. J.; Coulet, P. R. *Sens. Actuators, B* **1990**, *1*, 580.
- (230) Gautier, S. M.; Blum, L. J.; Coulet, P. R. *Anal. Chim. Acta* **1991**, *243*, 149.
- (231) Gautier, S. M.; Blum, L. J.; Coulet, P. R. *Anal. Chim. Acta* **1991**, *255*, 253.
- (232) Gautier, S. M.; Blum, L. J.; Coulet, P. R. *Anal. Chim. Acta* **1992**, *266*, 331.
- (233) Gautier, S. M.; Blum, L. J.; Coulet, P. R. *J. Biolumin. Chemilumin.* **1990**, *5*, 57.
- (234) Blum, L. J.; Gautier, S. M.; Coulet, P. R. *J. Biotechnol.* **1993**, *31*, 357.
- (235) Michael, P. E.; Gautier-Sauvigne, S. M.; Blum, L. J. *Talanta* **1998**, *47*, 169.
- (236) Schubert, F. *Sens. Actuators, B* **1993**, *11*, 531.
- (237) Schaeferling, M.; Wolfbeis, O. S. *Chem.—Eur. J.* **2007**, *13*, 4342.
- (238) Schrenkhammer, P.; Rosnizek, I. D.; Duerkop, A.; Wolfbeis, O. S.; Schaeferling, M. J. *Biomol. Screening* **2008**, in press.
- (239) Tromberg, B. J.; Sepaniak, M. J.; Alarie, J. P.; Vo-Dinh, T.; Santella, R. M. *Anal. Chem.* **1988**, *60*, 1901.
- (240) Alarie, J. P.; Bowyer, J. R.; Sepaniak, M. J.; Hoyt, A. M.; Vo-Dinh, T. *Anal. Chim. Acta* **1990**, *236*, 237.
- (241) Bright, F. V.; Betts, T. A.; Litwiler, K. S. *Anal. Chem.* **1990**, *62*, 1065.
- (242) Zhou, Y.; Magill, J. V.; De La Rue, R. M.; Laybourn, P. J. R. *Sens. Actuators, B* **1993**, *11*, 245.
- (243) McCormack, T.; O'Keefe, G.; MacCraith, B. D.; O'Kennedy, R. *Sens. Actuators, B* **1997**, *41*, 89.
- (244) Bowyer, J. R.; Alarie, J. P.; Sepaniak, M. J.; Vo-Dinh, T.; Thompson, R. Q. *Analyst* **1991**, *116*, 117.
- (245) Zhou, Y.; Laybourn, P. J. R.; Magill, J. V.; De La Rue, R. M. *Biosens. Bioelectron.* **1991**, *6*, 595.
- (246) Sapsford, K. E.; Charles, P. T.; Patterson, C. H.; Ligler, F. S. *Anal. Chem.* **2002**, *74*, 1061.
- (247) Daniels, P. B.; Fletcher, J. E.; O'Neil, P. M.; Stafford, C. G.; Bacarese-Hamilton, T.; Robinson, G. A. *Sens. Actuators, B* **1995**, *26–27*, 447.
- (248) Lepesheva, G. I.; Azeva, T. N.; Knyukshko, V. N.; Chashchin, V. L.; Usanov, S. A. *Sens. Actuators, B* **2000**, *68*, 27.
- (249) Engstroem, H. A.; Andersson, P. O.; Ohlson, S. *Anal. Biochem.* **2006**, *357*, 159.
- (250) Reck, B.; Himmelspach, K.; Opitz, N.; Lübbers, D. W. *Analyst* **1988**, *113*, 1423.
- (251) Barnard, S. M.; Walt, D. R. *Science* **1991**, *251*, 927.
- (252) Anis, N. A.; Eldefrawi, M. E. *J. Agric. Food Chem.* **1993**, *41*, 843.
- (253) Wong, R. B.; Anis, N. A.; Eldefrawi, M. E. *Anal. Chim. Acta* **1993**, *279*, 141.
- (254) Oroszlan, P.; Duvencek, G. L.; Ehrat, M.; Widmer, H. M. *Sens. Actuators, B* **1993**, *11*, 301.
- (255) Owaku, K.; Goto, M.; Ikariyama, Y.; Aizawa, M. *Anal. Chem.* **1995**, *67*, 1613.
- (256) Devine, P. J.; Anis, N. A.; Wright, J.; Kim, S.; Eldefrawi, A. T.; Eldefrawi, M. E. *Anal. Biochem.* **1995**, *227*, 216.
- (257) Shriver-Lake, L. C.; Breslin, K. A.; Charles, P. T.; Conrad, D. W.; Golden, J. P.; Ligler, F. S. *Anal. Chem.* **1995**, *67*, 2431.
- (258) Brummel, K. E.; Wright, J.; Eldefrawi, M. E. *J. Agric. Food Chem.* **1997**, *45*, 3292.
- (259) Bakaltcheva, I. B.; Ligler, F. S.; Patterson, C. H.; Shriver-Lake, L. C. *Anal. Chim. Acta* **1999**, *399*, 13.
- (260) Zhao, C. Q.; Anis, N. A.; Rogers, K. R.; Kline, R. H.; Wright, J.; Eldefrawi, A. T.; Eldefrawi, M. E. *J. Agric. Food Chem.* **1995**, *43*, 2308.
- (261) Schult, K.; Katerkamp, A.; Trau, D.; Grawe, F.; Cammann, K.; Meusel, M. *Anal. Chem.* **1999**, *71*, 5430.
- (262) Tromberg, B. J.; Sepaniak, M. J.; Vo-Dinh, T.; Griffin, G. D. *Anal. Chem.* **1987**, *59*, 1226.
- (263) Sloper, A. N.; Deacon, J. K.; Flanagan, M. T. *Sens. Actuators, B* **1990**, *1*, 589.
- (264) Shriver-Lake, L. C.; Ogert, R. A.; Ligler, F. S. *Sens. Actuators, B* **1993**, *11*, 239.
- (265) Ogert, R. A.; Brown, J. E.; Singh, B. R.; Shriver-Lake, L. C.; Ligler, F. S. *Anal. Biochem.* **1992**, *205*, 306.
- (266) Vidal, M. I.; Oliva, A. G. *Sens. Actuators, B* **1997**, *38–39*, 448.
- (267) Daneshvar, M. I.; Casay, G. A.; Patonay, G.; Lipowska, M.; Strekowski, L.; Ewans, L., III; Tarazi, L.; George, A. *J. Fluoresc.* **1996**, *6*, 69.
- (268) Zhou, C.; Pivarnik, P.; Auger, S.; Rand, A.; Letcher, S. *Sens. Actuators, B* **1997**, *42*, 169.
- (269) Narang, U.; Anderson, G. P.; Ligler, F. S.; Burans, J. *Biosens. Bioelectron.* **1997**, *12*, 937.
- (270) King, K. D.; Anderson, G. P.; Bullock, K. E.; Regina, M. J.; Saaski, E. W.; Ligler, F. S. *Biosens. Bioelectron.* **1999**, *14*, 163.
- (271) Ligler, F. S.; Breimer, M.; Golden, J. P.; Nivens, D. A.; Dodson, J. P.; Green, T. M.; Haders, D. P.; Sadik, O. A. *Anal. Chem.* **2002**, *74*, 713.
- (272) Hong, B.; Kang, K. A. *Biosens. Bioelectron.* **2006**, *21*, 1333.
- (273) Sheikh, S. H.; Mulchandani, A. *Biosens. Bioelectron.* **2001**, *16*, 647.
- (274) Bier, F. F.; Stocklein, W.; Bocher, M.; Bilitewski, U.; Schmid, R. D. *Sens. Actuators, B* **1992**, *7*, 509.
- (275) Bier, F. F.; Jockers, R.; Schmid, R. D. *Analyst* **1994**, *119*, 437.
- (276) Brecht, A.; Klotz, A.; Barzen, C.; Gauglitz, G.; Harris, R. D.; Quigley, G. R.; Wilkinson, J. S.; Sztajnbnok, P.; Abuknesha, R.; Gascon, J. *Anal. Chim. Acta* **1998**, *362*, 69.
- (277) Rodriguez-Mozaz, S.; Reeder, S.; Lopez de Alda, M.; Gauglitz, G.; Barcelo, D. *Biosens. Bioelectron.* **2004**, *19*, 633.
- (278) Cummins, C. M.; Koivunen, M. E.; Stephanian, A.; Gee, S. J.; Hammock, B. D.; Kennedy, I. M. *Biosens. Bioelectron.* **2006**, *21*, 1077.
- (279) Mosiello, L.; Nencini, L.; Serge, L.; Spano, M. *Sens. Actuators, B* **1997**, *38–39*, 353.



- (280) Barzen, C.; Brecht, A.; Gauglitz, G. *Biosens. Bioelectron.* **2002**, *17*, 289.
- (281) Mallyt, E.; Barzen, C.; Abuknesha, R.; Gauglitz, G.; Barcelo, D. *Anal. Chim. Acta* **2001**, *427*, 165.
- (282) Tschmelak, J.; Kumpf, M.; Käppel, N.; Proll, G.; Gauglitz, G. *Talanta* **2006**, *69*, 343.
- (283) Homola, J., Ed. *Surface Plasmon Resonance Biosensors*; Springer-Verlag: Berlin, 2006.
- (284) Wolfbeis, O. S. *Trends Anal. Chem.* **1996**, *15*, 225.
- (285) Weigl, B. H.; Wolfbeis, O. S. *Anal. Chem.* **1994**, *66*, 332.
- (286) Ruckstuhl, T.; Walser, A.; Verdes, D.; Seeger, S. *Biosens. Bioelectron.* **2005**, *20*, 1872.
- (287) Kuerner, J. M.; Wolfbeis, O. S.; Klimant, I. *Anal. Chem.* **2002**, *74*, 2151.
- (288) Luo, S.; Walt, D. R. *Anal. Chem.* **1989**, *61*, 1069.
- (289) Vermette, P.; Gengenbach, T.; Divisekera, U.; Kambouris, P. A.; Griesser, H. J.; Meagher, L. J. *Colloid Interface Sci.* **2003**, *259*, 13.
- (290) Sato, K.; Sawayanagi, M.; Hosokawa, K.; Maeda, M. *Anal. Sci.* **2004**, *20*, 893.
- (291) Johnson-White, B.; Lin, B.; Ligler, F. S. *Anal. Chem.* **2007**, *79*, 140.
- (292) Schriver-Lake, L. C.; Donner, B.; Edelstein, R.; Breslin, K.; Bhatia, S. K.; Ligler, F. S. *Biosens. Bioelectron.* **1997**, *12*, 1101.
- (293) Preininger, C.; Mencaglia, A.; Baldini, F. *Anal. Chim. Acta* **2000**, *403*, 67.
- (294) Liu, X.; Wang, H.; Herron, J. N.; Prestwich, G. D. *Bioconjugate Chem.* **2000**, *11*, 755.
- (295) Akkoyun, A.; Bilitewski, U. *Biosens. Bioelectron.* **2002**, *17*, 655.
- (296) Tedeschi, L.; Domenici, C.; Ahluwalia, A.; Baldini, F.; Mencaglia, A. *Biosens. Bioelectron.* **2003**, *19*, 85.
- (297) Anderson, G. P.; Jacoby, M. A.; Ligler, F. S.; King, K. D. *Biosens. Bioelectron.* **1997**, *12*, 329.
- (298) Kim, J.; Singh, N.; Lyon, L. A. *Angew. Chem., Int. Ed.* **2006**, *45*, 1446.
- (299) Konry, T.; Novoa, A.; Cosnier, S.; Marks, R. S. *Anal. Chem.* **2003**, *75*, 2633.
- (300) Leshem, B.; Sarfati, G.; Novoa, A.; Breslav, I.; Marks, R. S. *Luminescence* **2004**, *19*, 69.
- (301) Herrmann, S.; Leshem, B.; Landes, S.; Rager-Zisman, B.; Marks, R. S. *Talanta* **2005**, *66*, 6.
- (302) Kulagina, N. V.; Lassman, M. E.; Ligler, F. S.; Taitt, C. R. *Anal. Chem.* **2005**, *77*, 6504.
- (303) Kulagina, N. V.; Schaffer, K. M.; Anderson, G. P.; Ligler, F. S.; Taitt, C. R. *Anal. Chim. Acta* **2006**, *575*, 9.
- (304) Martinez, J. S.; Grace, W. K.; Grace, K. M.; Hartman, N.; Swanson, B. I. *J. Mater. Chem.* **2005**, *15*, 4639.
- (305) Anderson, F. P.; King, K. D.; Gaffney, K. L.; Johnson, L. H. *Biosens. Bioelectron.* **2000**, *14*, 771.
- (306) Petrou, P. S.; Kakabakos, S. E.; Christofidis, I.; Argitis, P.; Misiakos, K. *Biosens. Bioelectron.* **2002**, *17*, 261.
- (307) Feldstein, M. J.; Golden, J. P.; Rowe, C. A.; MacCraith, B. D.; Ligler, F. S. *J. Biomed. Microdev.* **1999**, *1*, 139.
- (308) Moreno-Bondí, M. C.; Taitt, C. R.; Shriver-Lake, L. C.; Ligler, F. S. *Biosens. Bioelectron.* **2006**, *21*, 1880.
- (309) Ngundi, M. M.; Qadri, S. A.; Wallace, E. V.; Moore, M. H.; Lassman, M. E.; Shriver-Lake, L. C.; Ligler, F. S.; Taitt, C. R. *Environ. Sci. Technol.* **2006**, *40*, 2352.
- (310) Sapsford, K. E.; Ngundi, M. M.; Moore, M. H.; Lassman, M. E.; Shriver-Lake, L. C.; Taitt, C. R.; Ligler, F. S. *Sens. Actuators, B* **2006**, *113*, 599.
- (311) Sapsford, K. E.; Taitt, C. R.; Loo, N.; Ligler, F. S. *Appl. Environ. Microbiol.* **2005**, *71*, 5590.
- (312) Ngundi, M. M.; Shriver-Lake, L. C.; Moore, M. H.; Lassman, M. E.; Ligler, F. S.; Taitt, C. R. *Anal. Chem.* **2005**, *77*, 148.
- (313) Taitt, C. R.; Shubin, Y. S.; Angel, R.; Ligler, F. S. *Appl. Environ. Microbiol.* **2004**, *70*, 152.
- (314) Shriver-Lake, L. C.; Turner, S.; Taitt, C. R. *Anal. Chim. Acta* **2007**, *584*, 66.
- (315) Sapsford, K. E.; Rasooly, A.; Taitt, C. R.; Ligler, F. S. *Anal. Chem.* **2004**, *76*, 433.
- (316) Taitt, C. R.; Anderson, G. P.; Lingerfelt, B. M.; Feldstein, M. J.; Ligler, F. S. *Anal. Chem.* **2002**, *74*, 6114.
- (317) Tschmelak, J.; Proll, G.; Gauglitz, G. *Biosens. Bioelectron.* **2004**, *20*, 743.
- (318) Tschmelak, J.; Proll, G.; Gauglitz, G. *Anal. Chim. Acta* **2004**, *519*, 143.
- (319) Tschmelak, J.; Kaepfel, N.; Gauglitz, G. *Anal. Bioanal. Chem.* **2005**, *382*, 1895.
- (320) Tschmelak, J.; Proll, G.; Gauglitz, G. *Anal. Bioanal. Chem.* **2004**, *379*, 1004.
- (321) Tschmelak, J.; Proll, G.; Gauglitz, G. *Talanta* **2005**, *65*, 313.
- (322) Rissin, D. M.; Walt, D. R. *Anal. Chim. Acta* **2006**, *564*, 34.
- (323) Schultz, J. S.; Mansouri, S.; Goldstein, I. J. *Diabetes Care* **1982**, *5*, 245.
- (324) Mansouri, S.; Schultz, J. S. *Bio/Technology* **1984**, *2*, 885.
- (325) Srinivasan, K. R.; Mansouri, S.; Schultz, J. S. *Biotechnol. Bioeng.* **1986**, *28*, 233.
- (326) Meadows, D.; Schultz, J. S. *Anal. Chim. Acta* **1993**, *280*, 21.
- (327) Russell, R. J.; Pishko, M. V.; Gefrides, C. C.; McShane, M. J.; Cote, G. L. *Anal. Chem.* **1999**, *71*, 3126.
- (328) Ballerstadt, R.; Schultz, J. S. *Anal. Chem.* **2000**, *72*, 4185.
- (329) Ballerstadt, R.; Polak, A.; Beuhler, A.; Frye, J. *Biosens. Bioelectron.* **2004**, *19*, 905.
- (330) Ge, X.; Tolosa, L.; Simpson, J.; Rao, G. *Biotechnol. Bioeng.* **2003**, *846*, 723.
- (331) Marvin, J. S.; Hellinga, H. W. *J. Am. Chem. Soc.* **1998**, *120*, 7.
- (332) Gilardl, G.; Zhou, L. Q.; Hibbert, L.; Cass, A. E. G. *Anal. Chem.* **1994**, *66*, 3840.
- (333) Ge, X.; Tolosa, L.; Rao, G. *Anal. Chem.* **2004**, *76*, 1403.
- (334) Ogasawa, F. K.; Wang, Y.; Bobbitt, D. R. *Anal. Chem.* **1992**, *64*, 1637.
- (335) Sanz, V.; De Marcos, S.; Galban, J. *Analyst* **2007**, *132*, 59.
- (336) Thompson, R. B.; Jones, E. R. *Anal. Chem.* **1993**, *65*, 730.
- (337) Lundgren, J. S.; Salins, L. L. E.; Kaneva, I.; Daunert, S. *Anal. Chem.* **1999**, *71*, 589.
- (338) Okoh, M. P.; Hunter, J. L.; Corrie, J. E. T.; Webb, M. R. *Biochemistry* **2006**, *45*, 14764.
- (339) Shrestha, S.; Salins, L. L. E.; Ensor, C. M.; Daunert, S. *Biotechnol. Bioeng.* **2002**, *78*, 517.
- (340) Sumner, J. P.; Westerberg, N. M.; Stoddard, A. K.; Hurst, T. K.; Cramer, M.; Thompson, R. B.; Fierke, C. A.; Kopelman, R. *Biosens. Bioelectron.* **2006**, *21*, 1302.
- (341) Sumner, J. P.; Westerberg, N. M.; Stoddard, A. K.; Fierke, C. A.; Kopelman, R. *Sens. Actuators, B* **2006**, *113*, 760.
- (342) Blyth, D. J.; Aylott, J. W.; Richardson, D. J.; Russell, D. A. *Analyst* **1995**, *120*, 2725.
- (343) Aylott, J. W.; Richardson, D. J.; Russell, D. A. *Chem. Mater.* **1997**, *9*, 2261.
- (344) Barker, S. L. R.; Kopelman, R.; Meyer, T. E.; Cusanovich, M. A. *Anal. Chem.* **1998**, *70*, 971.
- (345) Barker, S. L. R.; Clark, H. A.; Swallen, S. F.; Kopelman, R. *Anal. Chem.* **1999**, *71*, 1767.
- (346) Blyth, D. J.; Aylott, J. W.; Moir, J. W. B.; Richardson, D. J.; Russell, D. A. *Analyst* **1999**, *124*, 129.
- (347) Barker, S. L. R.; Zhao, Y.; Marletta, M. A.; Kopelman, R. *Anal. Chem.* **1999**, *71*, 2071.
- (348) ZhuJun, Z.; Seitz, W. R. *Anal. Chem.* **1986**, *58*, 220.
- (349) Rogers, K. R.; Valdes, J. J.; Eldefrawi, M. E. *Anal. Biochem.* **1989**, *182*, 353.
- (350) Ngundi, M. M.; Taitt, C. R.; McMurphy, S. A.; Kahne, D.; Ligler, F. S. *Biosens. Bioelectron.* **2006**, *21*, 1195.
- (351) Graham, C. R.; Leslie, D.; Squirrell, D. J. *Biosens. Bioelectron.* **1992**, *7*, 487.
- (352) Piuanno, P. A.; Krull, U. J.; Hudson, R. H.; Damha, M. J.; Cohen, H. *Anal. Chim. Acta* **1994**, *288*, 205.
- (353) Piuanno, P. A.; Krull, U. J.; Hudson, R. H.; Damha, M. J.; Cohen, H. *Anal. Chem.* **1995**, *67*, 2635.
- (354) Watts, H. J.; Yeung, D.; Parkes, H. *Anal. Chem.* **1995**, *67*, 4283.
- (355) Abel, A. P.; Weller, M. G.; Duveneck, G. L.; Ehrat, M.; Widmer, H. M. *Anal. Chem.* **1996**, *68*, 2905.
- (356) Pilevar, S.; Davis, C. C.; Portugal, F. *Anal. Chem.* **1998**, *70*, 2031.
- (357) Kleinjung, F.; Klusmann, S.; Erdmann, V. A.; Scheller, F. W.; Furste, L. P.; Bier, F. F. *Anal. Chem.* **1998**, *70*, 328.
- (358) Bagby, D. H.; Piuanno, P. A.; Wust, C. C.; Krull, U. J. *Anal. Chim. Acta* **2000**, *411*, 19.
- (359) Dhadwal, H. S.; Kemp, P.; Aller, J.; Dantzer, M. M. *Anal. Chim. Acta* **2004**, *501*, 205.
- (360) Ferguson, J. A.; Boles, T. C.; Adams, C. P.; Walt, D. R. *Nat. Biotechnol.* **1996**, *14*, 1681.
- (361) Epstein, J. R.; Lee, M.; Walt, D. R. *Anal. Chem.* **2002**, *74*, 1836.
- (362) Michael, K. L.; Taylor, L. C.; Schultz, S. L.; Walt, D. R. *Anal. Chem.* **1998**, *70*, 1242.
- (363) Ferguson, J. A.; Steemers, F. J.; Walt, D. R. *Anal. Chem.* **2000**, *72*, 5618.
- (364) Song, L.; Ahn, S.; Walt, D. R. *Anal. Chem.* **2006**, *78*, 1023.
- (365) Bowden, M.; Song, L.; Walt, D. R. *Anal. Chem.* **2005**, *77*, 5583.
- (366) Ahn, S.; Kulis, D. M.; Erdner, D. L.; Anderson, D. M.; Walt, D. R. *Appl. Environ. Microbiol.* **2006**, *72*, 5742.
- (367) Ahn, S.; Walt, D. R. *Anal. Chem.* **2005**, *77*, 5041.
- (368) Swanson, P.; Gelbart, R.; Atlas, E.; Yang, L.; Grogan, T.; Butler, W. F.; Ackley, D. E.; Sheldon, E. *Sens. Actuators, B* **2000**, *64*, 22.
- (369) Yang, J. M.; Bell, J.; Huang, Y.; Tirado, M.; Thomas, D.; Forster, A. H.; Haigns, R. W.; Swanson, P. D.; Wallace, R. B.; Martinsons, B.; Krihak, M. *Biosens. Bioelectron.* **2002**, *17*, 605.
- (370) Rissin, D. M.; Walt, D. R. *J. Am. Chem. Soc.* **2006**, *128*, 6286.
- (371) Li, J.; Tan, W.; Wang, K.; Xiao, D.; Yang, X.; He, X.; Tang, Z. *Anal. Sci.* **2001**, *17*, 1149.

- (372) Du, H.; Disney, M. D.; Miller, B. L.; Krauss, T. D. *J. Am. Chem. Soc.* **2003**, *125*, 4012.
- (373) Du, H.; Strohsahl, C. M.; Camera, J.; Miller, B. L.; Krauss, T. D. *J. Am. Chem. Soc.* **2005**, *127*, 7932.
- (374) Hartley, H. A.; Baeumner, A. J. *Anal. Bioanal. Chem.* **2003**, 376, 319.
- (375) Baeumner, A. J.; Jones, C.; Wong, C. Y.; Price, A. *Anal. Bioanal. Chem.* **2004**, *378*, 1587.
- (376) Baemner, A. J.; Schleisinger, N. A.; Slutzki, N. S.; Romano, J.; Lee, E. M.; Montagna, R. A. *Anal. Chem.* **2002**, *74*, 1442.
- (377) Lee, M.; Walt, D. R. *Anal. Biochem.* **2000**, 282, 142.
- (378) Rupcich, N.; Nutiu, R.; Li, Y.; Brennan, J. D. *Anal. Chem.* **2005**, *77*, 4300.
- (379) Preininger, C.; Klimant, I.; Wolfbeis, O. S. *Anal. Chem.* **1994**, *66*, 1841.
- (380) Kwok, N.-Y.; Dong, S.; Lo, W.; Wong, K.-Y. *Sens. Actuators, B* **2005**, *110*, 289.
- (381) Lin, L.; Xiao, L.-L.; Huang, S.; Zhao, L.; Cui, J.-S.; Wang, X.-H.; Chen, X. *Biosens. Bioelectron.* **2006**, *21*, 1703.
- (382) Kumar, J.; Kumar Jha, S.; D'Souza, S. F. D. *Biosens. Bioelectron.* **2006**, *21*, 2100.
- (383) Mulchandani, A.; Kaneva, I.; Chen, W. *Anal. Chem.* **1998**, *70*, 5042.
- (384) Bains, W. *Biosens. Bioelectron.* **1994**, *9*, 111.
- (385) Frense, D.; Müller, A.; Beckmann, D. *Sens. Actuators, B* **1998**, *51*, 256.
- (386) Naessens, M.; Leclerc, J. C.; Tran-Minh, C. *Ecotoxicol. Environ. Saf.* **2000**, *46*, 181.
- (387) Giardi, M. T.; Guzzella, L.; Euzet, P.; Rouillon, R.; Esposito, D. *Environ. Sci. Technol.* **2005**, *39*, 5378.
- (388) Virta, M.; Lampinen, J.; Karp, M. *Anal. Chem.* **1995**, *67*, 667.
- (389) Biran, I.; Rissin, D. M.; Ron, E. Z.; Walt, D. R. *Anal. Biochem.* **2003**, *315*, 106.
- (390) Leth, S.; Maltoni, S.; Simkus, R.; Mattiasson, B.; Corbisier, P.; Klimant, I.; Wolfbeis, O. S.; Csoregi, E. *Electroanalysis* **2002**, *14*, 35.
- (391) Heitzer, A.; Malachowsky, K.; Thonnard, J. E.; Beinkowski, P. R.; White, D. C.; Sayer, G. S. *Appl. Environ. Microbiol.* **1994**, *60*, 1487.
- (392) Ikariyama, Y.; Nishiguchi, S.; Koyama, T.; Kobatake, E.; Aizawa, M.; Tsuda, M.; Nakazawa, T. *Anal. Chem.* **1997**, *69*, 2600.
- (393) Gil, G. C.; Mitchell, R. J.; Chang, S. T.; Gu, M. B. *Biosens. Bioelectron.* **2000**, *15*, 23.
- (394) Gil, G. C.; Kim, Y. L.; Gu, M. B. *Biosens. Bioelectron.* **2002**, *17*, 427.
- (395) Choi, S. H.; Gu, M. B. *Biosens. Bioelectron.* **2002**, *17*, 433.
- (396) Shetty, R. S.; Ramanathan, S.; Badr, I. H.; Wolford, J. L.; Daunert, S. *Anal. Chem.* **1999**, *71*, 763.
- (397) Michelini, E.; Leskinen, P.; Virta, M.; Karp, M.; Roda, A. *Biosens. Bioelectron.* **2005**, *20*, 2261.
- (398) Fine, T.; Leskinen, P.; Isobe, T.; Shiraiishi, H.; Morita, M.; Marks, R. S.; Virta, M. *Biosens. Bioelectron.* **2006**, *21*, 2263.
- (399) Ignatov, S. G.; Ferguson, J. A.; Walt, D. R. *Biosens. Bioelectron.* **2001**, *16*, 109.
- (400) Lundstrom, I.; Gustafsson, A.; Odman, S.; Karlsson, J. O.; Andersson, R. G.; Grundstrom, N.; Sundgren, H.; Elwing, H. *Sens. Actuators, B* **1990**, *1*, 533.
- (401) Rantanen, T.; Paekkilae, H.; Jaemsen, L.; Kuningas, K.; Ukonaho, T.; Loevgren, T.; Soukka, T. *Anal. Chem.* **2007**, *79*, 6312.
- (402) Wang, L.; Yan, R.; Huo, Z.; Wang, L.; Zeng, J.; Bao, J.; Wang, X.; Peng, Q.; Li, Y. *Angew. Chem., Int. Ed.* **2005**, *44*, 6054.
- (403) Wang, L.; Li, Y. *Chem. Commun.* **2006**, 2557.
- (404) Abrams, W. R.; Barber, C. A.; McCann, K.; Tong, G.; Chen, Z.; Mauk, M. G.; Wang, J.; Volkov, A.; Bourdelle, P.; Corstjens, P. L. A. M.; Zuiderwijk, M.; Kardos, K.; Li, S.; Tanke, H. J.; Niedbala, R. S.; Malamud, D.; Bau, H. *Ann. N. Y. Acad. Sci.* **2007**, *1098*, 375.
- (405) Wolfbeis, O. S.; Reisfeld, R.; Oehme, I. In *Structure and Bonding*; Springer: Berlin, 1996; Vol. 85, p 51.
- (406) MacCraith, B. D.; McDonagh, C. J. *Fluoresc.* **2002**, *12*, 333.
- (407) See, for example, the following: [www.probes.com](http://www.probes.com); [www.sigmaaldrich.com](http://www.sigmaaldrich.com); [www.luxcell.com](http://www.luxcell.com); [www.attotec.de](http://www.attotec.de); [www.chromeon.com](http://www.chromeon.com).
- (408) Jung, S.; Angerer, B.; Loescher, F.; Niehren, S.; Winkle, J.; Seeger, S. *ChemBioChem* **2006**, *7*, 900.
- (409) Thanh, N. T. K.; Vernhet, A.; Rosenzweig, Z. In *Springer Series on Chemical Sensors and Biosensors*; Orellana, G., Moreno-Bondi, M., Eds.; Springer Publishing: New York, 2005; Vol. 3, p 261.
- (410) Arain, S.; John, G. T.; Kranse, C.; Gerlach, J.; Wolfbeis, O. S.; Klimant, I. *Sens. Actuators, B* **2006**, *113*, 639.

CR068105T